

JAERI-M

6 5 0 8

FREQUENCY CHARACTERISTICS OF THE HORIZONTAL  
MOTION OF A JT-60 PLASMA COLUMN

April 1976

Yuichiro KAMBAYASHI

日 本 原 子 力 研 究 所  
Japan Atomic Energy Research Institute

この報告書は、日本原子力研究所が JAERI-M レポートとして、不定期に刊行している研究報告書です。入手、複製などのお問い合わせは、日本原子力研究所技術情報部（茨城県那珂郡東海村）あて、お申しこしください。

JAERI-M reports, issued irregularly, describe the results of research works carried out in JAERI. Inquiries about the availability of reports and their reproduction should be addressed to Division of Technical Information, Japan Atomic Energy Research Institute, Tokai-mura, Naka-gun, Ibaraki-ken, Japan.

Frequency Characteristics of the Horizontal  
Motion of a JT-60 Plasma Column

Yuichiro KAMBAYASHI

Division of Reactor Engineering, Tokai, JAERI

(Received March 15, 1976 )

After briefing the kinetics model for the horizontal displacement of a toroidal plasma column in the Tokamak device, frequency characteristics of the horizontal motion of a JT-60 plasma column are described, especially, influence of the uncertainty of parameters on the characteristics.

JAERI-M 6508

JT-60に関するプラズマ柱の水平方向変位周波数特性

日本原子力研究所東海研究所原子炉工学部

上 林 有一郎

(1976年3月15日受理)

トカマク型プラズマ閉じ込め装置におけるプラズマ柱の水平方向変位に関する動特性モデルについて述べ、このモデルにもとづき、JT-60のプラズマ柱の水平方向変位に関する周波数特性を求め、コイル時定数等の相異によりもたらされる特性の相違に検討を加えた。

## CONTENTS

Introduction	1
1. A kinetics Model for the Horizontal Displacement of a Toroidal Plasma Column .....	2
1-1 Description of a plasma confining device .....	2
1-2 Equation of the motion of a toroidal plasma column .....	2
1-3 Circuit equations .....	6
1-4 Vertical field supplied by conductor currents ...	8
1-5 A set of equations for the horizontal displacement of a toroidal plasma column .....	9
2. Frequency Characteristics of the Horizontal Displacement of a Plasma Column .....	11
2-1 Values of parameters .....	11
2-2 Influence of $\Gamma_0$ and G on frequency characteristics of the plasma column displacement to vertical field change and on that to terminal voltage change of the conductor v ...	12
2-2-1 Influence of $\Gamma_0$ and G on frequency characteristics of the plasma column displacement to vertical field change .....	12
2-2-2 Influence of $\Gamma_0$ and G on frequency characteristics of the plasma column displacement to terminal voltage change of the conductor v .....	13
2-3 Influence of the intrinsic time constants, $\tau_i$ , $\tau_v$ and $\tau_t$ , on frequency characteristics of the plasma column displacement to vertical field change .....	15
2-3-1 Influence of the intrinsic time constant, $\tau_t$ , on frequency characteristics of the plasma column displacement to vertical field change.	15
2-3-2 Influence of the intrinsic time constant, $\tau_v$ , on frequency characteristics of the plasma column displacement to vertical field change.	16

2-3-3	Influence of the intrinsic time constant, $\tau_\ell$ , on frequency characteristics of the plasma column displacement to vertical field change .....	17
2-4	Influence of the intrinsic time constants, $\tau_\ell$ , $\tau_v$ and $\tau_t$ , on frequency characteristics of the plasma column displacement to terminal voltage change of the conductor v .....	18
2-4-1	Influence of the intrinsic time constant, $\tau_t$ , on frequency characteristics of the plasma column displacement to terminal voltage change of the conductor v .....	19
2-4-2	Influence of the intrinsic time constant, $\tau_v$ , on frequency characteristics of the plasma column displacement to terminal voltage change of the conductor v .....	20
2-4-3	Influence of the intrinsic time constant, $\tau_\ell$ , on frequency characteristics of the plasma column displacement to terminal voltage change of the conductor v .....	21
3.	Summary and Conclusion .....	23
	References .....	24

## INTRODUCTION

For the purpose of realizing the thermo-nuclear fusion, it is essential to have a long-lived confined plasma which may be obtained by employing the positional control of a plasma column. The positional equilibrium of a plasma column is considered as a balance between the expansive force due to the kinetic energy of plasma particles and the magnetic energy of the plasma current, on one hand, the inward force appearing as a result of the interaction of the plasma current with the vertical field, on the other. If the force balance were lost, the plasma column would go into movement. For maintaining the plasma column at a desired equilibrium position, any displacement of the column should be suppressed and, if it occurs, the column should be put back where it has been. To achieve this requirement, the position of the column must be detected and its motion be controlled. The extension of confining time of the plasma may depend largely on functions provided for the control system, and so the system should be skillfully designed and its development can not be done without knowledge of the characteristics proper to the concerned apparatus.

The author reported a kinetics model representing the horizontal displacement of a toroidal plasma column in JAERI-M-6292, in which he gave a numerical code "FLIC" which calculates the frequency characteristics and a analogue simulator which analyses the time response. And now, after a description of the model, he will apply the model to Japan Torus 60, and give frequency characteristics of the plasma column displacement to vertical field change and to terminal voltage change of one of the conductors. And also investigated influence of the uncertainty of design parameters on these characteristics.

## 1. A KINETICS MODEL FOR THE HORIZONTAL DISPLACEMENT OF A TOROIDAL PLASMA COLUMN

A set of equations is given which represents the horizontal displacement of a toroidal plasma column in the Tokamak device. The conditions of equilibrium for a plasma column may be defined by a force-balance equation over the minor radius of the plasma column, which assumes the model to be satisfied, and also by the force-balance equation over the major radius. These equations may depend on the shape of the column cross-section and on the density profile of the plasma current and on the shape the plasma pressure over the column cross-section. It may be assumed that the plasma column has a circular cross-section and the current is distributed homogeneously over the column cross-section and that the asymmetry of distribution of the plasma pressure resulting from toroidality is small. The last assumption may be admitted under the condition that the ratio of the minor radius  $a$  to the major radius  $R$  of the plasma column is small ( $a/R \ll 1$ ). On these assumptions we will derive the equations simulating the horizontal displacement of a toroidal plasma column.

### 1-1 Description of a plasma confining device

A plasma confining device, of which the layout is shown on Fig. 1, is now considered. A plasma column of minor radius  $a$  and major radius  $R$  is confined in a conducting casing of radius  $R_c$ ; on a circle of radius  $r_v$  are located the conductors  $v$ , of which the current has a cosinusoidal density profile on the cross-section and supplies the vertical magnetic field; and, the toroidal coil is assumed to have the form of an axisymmetric toroidal shell with minor radius  $r_t$ . It is also assumed that each of the conductors has a circular cross-section of which the centre is found on the torus axis. Subscripts  $l$ ,  $v$  and  $t$  are used in the model for variables and constants, in conductor  $l$ ,  $v$  and  $t$  respectively;  $p$ , in the plasma column, and  $0$  in the initial equilibrium state.

### 1-2 Equation of the motion of a toroidal plasma column



A plasma column is maintained in equilibrium with the aid of an approximately homogeneous magnetic field transverse to the plane of the torus which is given as below: (1), (2)

$$B_{z0} = \frac{\mu_0 I_p}{4\pi R} \Gamma \quad (1)$$

where  $\Gamma = \ln \frac{8R}{a} + \beta_0 + \frac{\ell_1 - 3}{2}$  (2)

and  $\mu_0 \ell_1 / 4\pi$  is the internal inductance of the plasma column per unit length, and  $I_p$  is the plasma current. Motion of the plasma column depends on the total radial force,  $f$ , acting on the plasma column which may be written as follows under an accidental change of the vertical field from  $B_{z0}$ , required for the equilibrium, to  $B_z$ .

$$f = 2\pi R I_p (B_{z0} - B_z) \quad (3)$$

With  $B_z$  less than  $B_{z0}$ ,  $f$  has a positive value and the major radius of the plasma column increases. In the vicinity of the equilibrium, equation of the motion of the plasma column may be written as

$$M \frac{d^2 R}{dt^2} = \frac{\mu_0}{2} I_p^2 \Gamma - 2\pi R I_p B_z \quad (4)$$

where  $M$  is total mass of the plasma column.

It is seen that the first term on the right hand side of Eq. (4) is the expansive force due to the magnetic energy of the plasma current and the kinetic energy of the plasma particles, and the second term is the inward force caused by the interaction between the plasma current and the vertical field. The vertical field  $B_z$  is composed of the vertical fields  $B_i$  ( $i=1, v, t$ ) produced by the conductor currents  $I_i$  ( $i=1, v, t$ ) and the so-called disturbance  $B_d$ .

$$B_z = \sum_{i=1, v, t, d} B_i \quad (5)$$

where  $B_i$  ( $i=1, t, d$ ) are assumed to be homogeneous at the plasma column position but  $B_v$  to have a positional gradient given

below:

$$B_v = B_{vc} \left( 1 + m \frac{\delta R}{R_0} \right) \quad (6)$$

where  $R$  is a small displacement of the plasma column from the torus axis,  $B_{vc}$  is the vertical field produced by the conductor current  $I_v$  at the torus axis, and  $m$  is a constant characterizing the positional gradient of vertical field  $B_v$ .

The stability conditions relative to the horizontal displacement of the plasma column may be written as satisfying the formula. (4)

$$-\frac{3}{2} < m < 0 \quad (7)$$

The minor radius of the plasma column may be assumed to vary with displacement of the plasma column as follows.

$$a = a_0 \left( 1 + \alpha \frac{\delta R}{R_0} \right) \quad (8)$$

The value of  $\alpha$ , which characterizes the positional gradient of the minor radius of the plasma column, results in  $1/2$  with the assumption that the plasma column conserves the toroidal flux despite the displacement of the plasma column and in 0 with the assumption that the minor radius of the plasma column remains unchanged, and so the value of  $\alpha$  may be found within the range bounded by these two values.

$$0 < \alpha < \frac{1}{2} \quad (9)$$

The plasma current  $I_p$  varies with displacement of the plasma column as

$$I_p = I_{p0} \left( 1 + n \frac{\delta R}{R_0} \right) \quad (10)$$

$I_{p0}$  refers to initial equilibrium value of the plasma current at the centre of the torus cross-section. The value of  $n$ , which characterizes the positional gradient of the plasma current, results in 0 with the assumption that the plasma current remains unchanged despite the displacement of the plasma column

and in-1 with the assumption that the plasma column conserves the poloidal flux, but the plasma current does not vary with displacement of the plasma column under influence of the large inductance in series with the plasma. So the value of n may be found within the range given below.

$$-1 < n < 0 \tag{11}$$

The large inductance in series with the plasma implies that the internal inductance  $i$  and the poloidal beta remain unchanged, admitting redistribution of the plasma current. <sup>(3)</sup>

Rewriting each term of Eq. (4) as the sum of the steady equilibrium term and the time-varying one, the equation of motion of the plasma column (4) may be reduced to a linear one in the vicinity of a steady equilibrium state.

$$B_i = B_{i0} + \delta B \quad (i=z, \ell, v, t, d) \quad B_{i0} = 0 \quad (i= \ell, t, d)$$

$$\delta B_v = B_{vco} m \frac{\delta R}{R_0} + \delta B_{vc} \tag{12}$$

$$M \frac{d^2}{dt^2} \frac{\delta R}{R_0} = \frac{\mu_0}{2} \Gamma_0 I_{po}^2 \left[ G \frac{\delta R}{R_0} - \sum_{i=\ell, vc, t, d} \frac{\delta B_i}{B_{vco}} \right] \tag{13}$$

where

$$\Gamma_0 = \ell n \frac{\delta R_0}{a_0} + \beta_0 + \frac{\ell i - 3}{2} \tag{14}$$

$$G = \frac{1-\alpha}{\Gamma_0} - 1 + n - m \tag{15}$$

$$B_{vco} = \frac{\mu_0 \Gamma_0 I_{po}}{4\pi R_0} \tag{16}$$

Eq. (13) has the form of the so-called wave-equation with a frequency

$$\left[ \frac{\mu_0 \Gamma_0 I_{po}^2}{2M} G \right]^{1/2} \tag{17}$$

which is found around  $10^6$  c/s for the plasma.

On the other hand, the plasma has the mutual magnetic coupling with each of the conductors which carries a lower cut-off frequency in the system, and this implies that the left hand side of Eq. (13) can be omitted. So, the equation of motion of the toroidal plasma column is written as

$$G \frac{\delta R}{R_0} = \sum_{i=\ell, v, t, d} \frac{\delta B_i}{B_{vco}} \quad (18)$$

### 1-3 Circuit equations

Motion of the plasma column induces a certain amount of current in each of the conductors and results in appearance of the vertical field to prevent its own motion. Moreover, the conductor currents are mutually affected through magnetic couplings. So, the equation of motion of the plasma column (18) must be solved simultaneously with the equations concerning the conductor currents and the circuit equations must be set up, beginning with self and mutual inductances.

Now, the assumptions are made. (1) Each of the conductors has a circular cross-section coaxial with the plasma column; (2) each of the conductor currents has a cosinusoidal density profile on the cross-section of the conductor, and, (3) the plasma current has a homogeneous density profile on the cross-section of the plasma column.

In obtaining inductances of the plasma column, by assumption (3) the displacement of the plasma column is replaced by a dipole current having a cosinusoidal density profile in the periphery of the cross-section of the plasma column, and self (L) and mutual (M) inductances will be written as

$$\begin{cases} L_i = \frac{\pi^2}{4} \mu_0 R_0 N_i^2 & (i = \ell, v, t) \\ M_{pi} = -\frac{\pi \mu_0}{2r_i} R_0 N_i \delta R & (i = \ell, v, t) \\ M_{ij} = \frac{\pi^2 r_i}{4r_j} \mu_0 R_0 N_i N_j & (i=\ell, v, j=v, t, i \neq j) \end{cases} \quad (19)$$

where N is the number of turns of a conductor concerned with the vertical field, and r is the minor radius of the conductor.

With the inductances, circuit equations may be set up as

$$\begin{cases} 0 = R_\ell I_\ell + L_\ell \frac{dI_\ell}{dt} + \frac{dM_{p\ell}}{dt} \cdot I_p + M_{p\ell} \frac{dI_p}{dt} + M_{\ell v} \frac{dI_v}{dt} + M_{\ell t} \frac{dI_t}{dt} \\ V = R_v I_v + L_v \frac{dI_v}{dt} + \frac{dM_{pv}}{dt} \cdot I_p + M_{pv} \frac{dI_p}{dt} + M_{v\ell} \frac{dI_\ell}{dt} + M_{vt} \frac{dI_t}{dt} \\ 0 = R_t I_t + L_t \frac{dI_t}{dt} + \frac{dM_{pt}}{dt} \cdot I_p + M_{pt} \frac{dI_p}{dt} + M_{t\ell} \frac{dI_\ell}{dt} + M_{tv} \frac{dI_v}{dt} \end{cases} \quad (20)$$

where  $V$  is the voltage applied to the terminals of conductor (the conductors 1 and  $t$  have no terminals concerned with the virtual field),  $R_i$  ( $i=1, v, t$ ) are resistances of the conductors, and  $I_i$  ( $i=1, v, t$ ) are the conductor currents supplying the virtual field.

With Eqs. (10), (11) and (19), the following relation is given.

$$\frac{M_{pi} \cdot \frac{dI_p}{dt}}{\frac{dM_{pi}}{dt} \cdot I_p} = \frac{n\delta R}{R_0} \ll 1 \quad (21)$$

Eq. (21) indicated that the value of  $M_{pi} \cdot dI_p/dt$  is small compared with that of  $dM_{pi}/dt \cdot I_p$ , and the term  $M_{pi} \cdot dI_p/dt$  ( $i=1, v, t$ ) will be omitted. The intrinsic time constants ( $\tau_i$ ;  $i=1, v, t$ ) of conductors are now defined as

$$\tau_i = \frac{L_i}{R_i} \quad (i = 1, v, t) \quad (22)$$

And, the variables  $V$  and  $I_i$  ( $i=1, v, t, p$ ) are both rewritten as the sum of the steady equilibrium term (denoted by the subscript  $o$ ) and the time-varying one (denoted by  $\delta$ )

$$\left\{ \begin{array}{l} V = V_o + \delta V \\ I_i = I_{io} + \delta I_i \quad (i=1, v, t) \\ I_{io} = 0 \quad (i=1, t) \\ I_p = I_{po} + \delta I_p \\ \quad = I_{po} \left( 1 + n \frac{\delta R}{R_c} \right) \quad (\text{used Eq. (10)}) \end{array} \right. \quad (23)$$

$I_{1o}$  and  $I_{to}$  can be set at zero because the conductors 1 and  $t$  have no current source in the steady equilibrium state, and  $I_{vo}$ , motivated by  $V_o$ , supplies the virtual field required for an initial equilibrium of the plasma column. Using the initial

equilibrium vertical field  $B_{vco}$ , it can be written as

$$I_{vo} = \frac{4r_v}{\mu_0 N_v} B_{vco} \quad (24)$$

where  $B_{vco} = \frac{\mu_0 \Gamma_0 I_{po}}{4\pi R_0}$  (given by Eq. (16))

and  $\Gamma_0 = \ln \frac{\delta R_0}{a_0} + \beta_\theta + \frac{\ell_i - 3}{2}$  (given by Eq. (14))

Eq. (20) is rewritten with Eqs. (21) (24), and a set of circuit equations is obtained.

$$0 = \frac{1}{\tau_\ell} \frac{\delta I_\ell}{I_{po}} + \frac{d}{dt} \left( \frac{\delta I_\ell}{I_{po}} \right) - \frac{2R_0}{\pi r_\ell} \frac{d}{dt} \left( \frac{\delta R}{R_0} \right) + \frac{r_\ell N_v}{r_v} \frac{d}{dt} \left( \frac{\delta I_v}{I_{po}} \right) + \frac{r_\ell}{r_t} \frac{d}{dt} \left( \frac{\delta I_t}{I_{po}} \right)$$

$$\frac{r_v \Gamma_0}{\pi r_v R_0 N_v} \frac{\delta V}{V_0} = \frac{1}{\tau_v} \frac{\delta I_v}{I_{po}} + \frac{d}{dt} \left( \frac{\delta I_v}{I_{po}} \right) - \frac{2R_0}{\pi r_v N_v} \frac{d}{dt} \left( \frac{\delta R}{R_0} \right) + \frac{r_\ell}{r_v N_v} \frac{d}{dt} \left( \frac{\delta I_\ell}{I_{po}} \right) + \frac{r_v}{r_t N_v} \frac{d}{dt} \left( \frac{\delta I_t}{I_{po}} \right) \quad (25)$$

$$0 = \frac{1}{\tau_t} \frac{\delta I_t}{I_{po}} + \frac{d}{dt} \left( \frac{\delta I_t}{I_{po}} \right) - \frac{2R_0}{\pi r_t} \frac{d}{dt} \left( \frac{\delta R}{R_0} \right) + \frac{r_\ell}{r_t} \frac{d}{dt} \left( \frac{\delta I_\ell}{I_{po}} \right) + \frac{r_v N_v}{r_t} \frac{d}{dt} \left( \frac{\delta I_v}{I_{po}} \right)$$

#### 1-4 Vertical field supplied by the conductor currents

The vertical field supplied by the conductor currents will be considered. As described already, concerning the circuit equations, horizontal motion of the plasma column with a homogeneous current density profile may induce in each of the conductors a certain amount of current with a cosinusoidal density profile on the cross-section. Each of these conductor currents with a cosinusoidal density profile will produce at the plasma column a homogeneous vertical field of which the intensity may be given as

$$B_i = \frac{\mu_0 N_i I_i}{4r_i} \quad (i = \ell, v, t) \quad (26)$$

Of the vertical field,  $B_v$  has the positional gradient defined by Eq. (6) to stabilize motion of the plasma column, and symbol  $B_{vc}$  is used for  $B_v$  to show clearly that  $B_v$ , given Eq. (26), is the field on the torus axis.

Each of the vertical fields  $B_i$  ( $i=1, v, t$ ) is composed of two terms — a steady equilibrium one (shown by the subscript o) and a time-varying one (by  $\delta$ )

$$\begin{aligned}
 B_i &= B_{i0} + \delta B_i \\
 &= \delta B_i \quad (i=1, t)
 \end{aligned} \tag{27}$$

$$B_{vc} = B_{vco} + \delta B_{vc}$$

$$B_{vco} = \frac{\mu_0 \Gamma_0 I_{po}}{4\pi R_0} \quad (\text{given by Eq. (16)})$$

$B_{i0}$  ( $i=1, t$ ) can be set as zero in Eq. (27) because  $I_{i0}$  ( $=1, t$ ) are zero. Using Eqs. (23) and (27), Eq. (26) is rewritten as follows:

$$\frac{\delta B_i}{B_{vco}} = \frac{\pi R_0 N_i}{r_i \Gamma_0} \frac{\delta I_i}{I_{po}} \quad (i = \ell, v, t) \tag{28}$$

Using Eq. (24), the conductor currents are normalized by the steady equilibrium value of the plasma current,  $I_{po}$ , and the virtical fields by that of the virtical field,  $B_{vco}$ . Eq. (28) gives the virtical fields produced by the conductor currents.

1-5 A set of equations for the horizontal displacement of a toroidal plasma column

The equations representing horizontal displacement of a plasma column is introduced, which is summarized as below:

$$\left\{ \begin{aligned}
 G \frac{\delta R}{R_0} &= \sum_{i=\ell, vc, t, d} \frac{\delta B_i}{B_{vco}} \\
 0 &= \frac{1}{r_\ell} \frac{\delta I_\ell}{I_{po}} + \frac{d}{dt} \left( \frac{\delta I_\ell}{I_{po}} \right) - \frac{2R_0}{\pi r_\ell} \frac{d}{dt} \left( \frac{\delta R}{R_0} \right) + \frac{r_\ell N_v}{r_v} \frac{d}{dt} \left( \frac{\delta I_v}{I_{po}} \right) + \frac{r_\ell}{r_t} \frac{d}{dt} \left( \frac{\delta I_t}{I_{po}} \right) \\
 \frac{r_v \Gamma_0}{\pi r_v R_0 N_v} \frac{\delta V}{V_0} &= \frac{1}{r_v} \frac{\delta I_v}{I_{po}} + \frac{d}{dt} \left( \frac{\delta I_v}{I_{po}} \right) - \frac{2R_0}{\pi r_v N_v} \frac{d}{dt} \left( \frac{\delta R}{R_0} \right) + \frac{r_\ell}{r_v N_v} \frac{d}{dt} \left( \frac{\delta I_\ell}{I_{po}} \right) + \frac{r_v}{r_t N_v} \frac{d}{dt} \left( \frac{\delta I_t}{I_{po}} \right) \\
 0 &= \frac{1}{r_t} \frac{\delta I_t}{I_{po}} + \frac{d}{dt} \left( \frac{\delta I_t}{I_{po}} \right) - \frac{2R_0}{\pi r_t} \frac{d}{dt} \left( \frac{\delta R}{R_0} \right) + \frac{r_\ell}{r_t} \frac{d}{dt} \left( \frac{\delta I_\ell}{I_{po}} \right) + \frac{r_v N_v}{r_t} \frac{d}{dt} \left( \frac{\delta I_v}{I_{po}} \right) \\
 \frac{\delta B_i}{B_{vco}} &= \frac{\pi R_0 N_i}{r_i \Gamma_0} \frac{\delta I_i}{I_{po}} \quad (i = \ell, vc, t) \\
 \Gamma_0 &= \ell n \frac{8R_0}{a_0} + \beta_\theta + \frac{\ell i - 3}{2} \\
 G &= \frac{1-\alpha}{\Gamma_0} - 1 + n - m
 \end{aligned} \right. \tag{29}$$

$$-\frac{3}{2} < m < 0$$

$$0 < \alpha < \frac{1}{2}$$

$$-1 < n < 0$$



## 2. FREQUENCY CHARACTERISTICS OF THE HORIZONTAL DISPLACEMENT OF A PLASMA COLUMN

The model for horizontal displacement of a plasma column has been given in the preceding section. And it will be applied to a plasma confining device Japan Torus 60 and its frequency characteristics are investigated, especially the influence of intrinsic time constants on the characteristics. Calculations were carried out with a numerical code FLIC which is based on the said model and given in JAERI-M-6292.

The present chapter contains — (1) Values of parameters, (2) Influence of  $\sqrt{c'}$  and G on the frequency characteristics of plasma column displacement to virtual field change and on that to terminal voltage change of the conductor v, (3) Influence of intrinsic time constants on that to virtual field change, and (4) Influence of intrinsic time constants on that to terminal voltage change of the conductor v.

### 2-1 Values of parameters

Parameters required for analyzing the displacement of a plasma column are listed in Table 1, where the values concern Japan Torus 60. Major radius,  $R_0$ , and minor radius,  $a_0$ , of the plasma column and minor radii,  $r_i$  ( $i=1, v, t$ ), and equivalent numbers of turns,  $N_i$  ( $i=1, v, t$ ), of conductors, may be known from dimensions of the device. Value of beta,  $\beta_0$ , may be expected to be 0.1 but reach to 1.0. The internal inductance of the plasma column,  $l_i$ , is expected to be 0.9 but may be found in the range between 0.5 and 1.5. Speaking of the boundary values of  $l_i$ , 0.5 will be given with a parabolic density profile of the plasma current and 1.5 with a homogeneous one. As described already,  $m$ ,  $\alpha$  and  $n$ , which characterize positional gradients of the virtual field, minor radius of the plasma column and plasma current, respectively, are found in the ranges below:

$$\left\{ \begin{array}{l} -\frac{3}{2} < m < 0 \\ 0 < \alpha < \frac{1}{2} \\ -1 < n < 0 \end{array} \right. \quad (30)$$

$\bar{\Gamma}_0$ , defined by Eq. (2), depends on  $\beta_e$  and  $l_i$ , of which the values are shown in Table 2, with  $\beta_e$  in the vertical column and  $l_i$  in the horizontal.  $\bar{\Gamma}_0$  may be set at 2.23 which concerns the expected value of  $\beta_e$  and that of  $l_i$ , and its influence on the characteristics will be investigated setting  $\bar{\Gamma}_0$  at one of three values, 2.0, 2.2 and 2.4, successively. These values of  $\bar{\Gamma}_0$  cover the region enclosed by a thick line in Table 2.  $G$ , defined by Eq. (15), depends on  $m, \alpha, n$  and  $\bar{\Gamma}_0$ , of which the values are shown in Table 4 with  $\bar{\Gamma}_0$  in the vertical column,  $(n-m)$  in Table 3 in the horizontal, being used as a parameter. The values of  $G$  are found in a wide range between 0.14 with  $\alpha(0), n-m(0.65)$  and  $\bar{\Gamma}_0(2.03)$ , and -1.60 with  $\alpha(0.5), n-m(-0.75)$  and  $\bar{\Gamma}_0(3.43)$ .  $G$  may be set at -0.8, which is a simple average value, with knowledge of the influence of  $G$  on the characteristics. The influence will be investigated setting  $G$  at one of three values, -0.6, -0.8 and -1.0, successively. The obtained results state adequacy of going with these  $G$ 's which cover the region enclosed with a thick line in Table 4.

Finally the intrinsic time constants of conductors,  $\tau_i$  ( $i=1, v, t$ ), will be considered. Maximum values of the constants may be expected as  $\tau_l(0.03)$ ,  $\tau_v(1.0)$  and  $\tau_t(10.0)$ . But, the influence of the uncertainty of the values on the dynamics of the plasma column have not been investigated. We will see the influence, setting successively each of these constants at one of their three values —  $\tau_l(0.01, 0.02, 0.03)$ ,  $\tau_v(0.2, 0.5, 1.0)$  and  $\tau_t(2.0, 5.0, 10.0)$ .

- 2-2 Influence of  $\bar{\Gamma}_0$  and  $G$  on frequency characteristics of the plasma column displacement to vertical field change and on that to terminal voltage change of the conductor  $v$
- 2-2-1 Influence of  $\bar{\Gamma}_0$  and  $G$  on frequency characteristics of the plasma column displacement to vertical field change

Influence of  $\bar{\Gamma}_0$  and  $G$  on frequency characteristics of the plasma column displacement to vertical field change will be investigated. The characteristics are shown in Figs. 2-1 ~ 2-6, where the intrinsic time constants are set at  $\tau_l(0.03)$ ,  $\tau_v(0.5)$  and  $\tau_t(5.0)$  which are reasonable values.

The influence of  $G$  on the characteristics can be investigated with Figs. 2-1 ~ 2-3 where  $\sqrt{C_0}$  is set at 2.0, 2.2 and 2.4, respectively. Each of the three curves in each figure concerns one of the three  $G$ s, -0.6, -0.8 and -1.0. It is seen in the figures that three curves show similar appearance, without variation of the value of  $\sqrt{C_0}$ , on gain diagrams and on phase ones, respectively, and lie within narrow limits of which the width increases slightly with increase of  $\sqrt{C_0}$  but that of the gain characteristics does not exceed 1 db nor that of the phase ones 3 deg. The discrepancy among the gain curves and also that among the phase ones, tracing to different values of  $G$ , decrease with increase of the frequency and in the high frequency range the former reduces to 0.8 db and the latter disappears. And it is thus possible to say that the uncertainty of  $G$  does not much influence the characteristics in the whole frequency range.

The influence of  $\sqrt{C_0}$  on the characteristics can be investigated with Figs. 2-4 ~ 2-6 where  $G$  are set at -0.6, -0.8 and -1.0, respectively. Each of the three curves in each figure concerns one of  $\sqrt{C_0}$ s, 2.0, 2.2 and 2.4. It is seen in the figures that three curves show, without variation of the value of  $G$ , similar appearances on gain diagrams and on phase ones, respectively, and lie within narrow limits of which the width of the gain characteristics does not exceed 1.4 db, nor that of the phase ones 0.5 deg in the low frequency range, and disappears with increase of the frequency. And so it is possible to say that the uncertainty of  $\sqrt{C_0}$  does not much influence the characteristics in the whole frequency range.

After consideration mentioned above, it may be said that the uncertainty of  $\sqrt{C_0}$  or  $G$ , or of both, does not much influence the characteristics in the whole frequency range, so that the horizontal displacement of a plasma column to vertical field change may be analyzed with reasonable values of  $\sqrt{C_0}$  and  $G$ .

2-2-2 Influence of  $\sqrt{C_0}$  and  $G$  on frequency characteristics of the plasma column displacement to terminal voltage change of the conductor  $v$

Influence of  $\sqrt{C_0}$  and  $G$  on frequency characteristics of the

plasma column displacement to terminal voltage change of the conductor  $v$  will be investigated. The characteristics are shown in Figs. 3-1 ~ 3-6 where the intrinsic time constants are set at  $\tau_p$  (0.03),  $\tau_v$  (0.5) and  $\tau_t$  (5.0) which are the same values as in the preceding section.

The influence of  $G$  on the characteristics can be investigated with Figs. 3-1 ~ 3-3 where  $\sqrt{\sigma}$  are set at 2.0, 2.2 and 2.4, respectively. Each of the three curves in each figure concerns one of three  $G$ s, -0.6, -0.8 and -1.0. It is seen in the figures that three curves agree with each other, without variation of the value of  $\sqrt{\sigma}$ , on gain diagrams and on phase ones, respectively. In the low frequency range, however, the curves lie within narrow limits of which the width of the gain characteristics is about 1 db and that of the phase 3 deg. And so it is possible to say that the uncertainty of  $G$  does not much influence the characteristics in the whole frequency range.

The influence of  $\sqrt{\sigma}$  on the characteristics can be investigated with Figs. 3-4 ~ 3-6 where  $G$  are set at -0.6, -0.8 and -1.0, respectively. Each of the three curves in each figure concerns one of three  $\sqrt{\sigma}$ s, 2.0, 2.2 and 2.4. It is seen in the figures that, without variation of the value of  $G$ , three gain curves show similar appearances and lie within narrow limits of which the width does not exceed 1.5 db, and three phase curves agree with each other in the whole frequency range. And it is possible to say that the uncertainty of  $\sqrt{\sigma}$  does not much influence the characteristics in the whole frequency range.

After consideration mentioned above, it may be said that the uncertainty of  $\sqrt{\sigma}$  or  $G$ , or of both, does not much influence the characteristics in the whole frequency range, so that the horizontal displacement of a plasma column to terminal voltage change of the conductor  $v$  may be analyzed with reasonable values of  $\sqrt{\sigma}$  and  $G$ .

It is concluded that the uncertainty of  $\sqrt{\sigma}$  or  $G$ , or of both, does not so much influence the frequency characteristics of the plasma column displacement to vertical field change nor that to terminal voltage change of the conductor  $v$ , so that these characteristics can be analyzed with reasonable values of  $\sqrt{\sigma}$  and  $G$ . Influence of the intrinsic time constants on the

characteristics will be investigated in the next section, giving 2.2 to  $\Gamma_0$  and -0.8 to G

2-3 Influence of the intrinsic time constants,  $\tau_l$ , and  $\tau_t$  on the frequency characteristics of the plasma column displacement to vertical field change

Influence of the intrinsic time constants of conductors,  $\tau_l$ ,  $\tau_v$  and  $\tau_t$ , on frequency characteristics of the plasma column displacement to vertical field change will be investigated. The characteristics are shown in Figs. 4-1 ~ 4-27 where  $\Gamma_0$  is set at 2.2 and G at -0.8 as described already, and  $\tau_l$  is set at one of the three  $\tau_l$  s (0.03, 0.02, 0.01),  $\tau_v$  at one of the three  $\tau_v$  s (1.0, 0.5, 0.2) and  $\tau_t$  at one of the three  $\tau_t$  s (10.0, 5.0, 2.0). These values of the intrinsic time constants are found around the expected values. The influence of  $\tau_t$  on the characteristics will be investigated with Figs. 4-1 ~ 4-9, that of  $\tau_v$  with Figs. 4-10 ~ 4-18 and that of  $\tau_l$  with Figs. 4-19 ~ 4-27.

2-3-1 Influence of the intrinsic time constant,  $\tau_t$ , on frequency characteristics of the plasma column displacement to vertical field change

Influence of the intrinsic time constant of the conductor  $\tau_t$ , on frequency characteristics of the plasma column displacement to vertical field change will be investigated. The characteristics are shown in Figs. 4-1 ~ 4-9.  $\tau_l$  is set at 0.03 in Figs. 4-1, 4-2 and 4-3, at 0.02 in Figs. 4-4, 4-5 and 4-6, and at 0.01 in Figs. 4-7, 4-8 and 4-9.  $\tau_v$  is set at 1.0 in Figs. 4-1, 4-4 and 4-7, at 0.5 in Figs. 4-2, 4-5 and 4-8 and 0.2 in Figs. 4-3, 4-6 and 4-9. Each of the three curves in the figures concerns one of the three  $\tau_t$  s, 10.0, 5.0 and 2.0.

It is seen in the figures that three gain curves, and also three phase ones, agree with each other in the frequency range beyond 0.5 c/s, especially so at higher than 1.0 c/s, regardless of the values of  $\tau_l$ ,  $\tau_v$ . The discrepancy among the gain curves, which is about 0.6 db at 0.2 c/s, ceases to appear at 1 c/s and no longer appears in the frequency range beyond 1 c/s. The dis-

crepancy among the phase ones, which is about 14 deg. at 0.2 c/s, reduces to 4 deg. at 0.5 c/s, disappears at 1 c/s, and no longer appears in the range beyond 1 c/s. On the other hand, in the range below 0.5 c/s, the characteristics are affected by  $\tau_t$ , and the discrepancies, among the gain ones and the phase ones, become larger with decrease of the frequency.

In the cases of the same  $\tau_t$  value, the discrepancies among gain curves and also phase ones increase as the  $\tau_v$  value decreases, in the range of 0.5 c/s to 1 c/s, but the absolute values are small. And therefore the values of  $\tau_v$  do not much influence mutual arrangement of the three gain curves nor the three phase ones in the whole frequency range. In the cases of the same  $\tau_v$  value, the values of  $\tau_t$  do not influence mutual arrangement of the three gain curves nor the three phase ones in the whole frequency range.

It is thus possible to say by investigation that the uncertainty of  $\tau_t$  has no much influence the characteristics of the plasma column displacement to vertical field change in the frequency range beyond 0.5 c/s. In the frequency range below it, however, the characteristics are affected by the uncertainty of  $\tau_t$ .

### 2-3-2 Influence of the intrinsic time constant, $\tau_v$ , on frequency characteristics of the plasma column displacement to vertical field change

Influence of the intrinsic time constant of the conductor  $v$ ,  $\tau_v$ , on frequency characteristics of the plasma column displacement to vertical field change will be investigated.

The characteristics are shown in Figs. 4-10 ~ 4-18.  $\tau_t$  is set at 10.0 in Figs. 4-10, 4-11 and 4-12, at 5.0 in Figs. 4-13, 4-14 and 4-15 and at 2.0 in Figs. 4-16, 4-17 and 4-18.  $\tau_\ell$  is set at 0.03 in Figs. 4-10, 4-13 and 4-16, at 0.02 in Figs. 4-11, 4-14 and 4-17 and at 0.01 in Figs. 4-12, 4-15 and 4-18. Each of the three curves in each figure concerns one of the three  $\tau_v$ s, 1.0, 0.5 and 0.2.

It is seen in the figures that, regardless of the value of  $\tau_t$  or  $\tau_\ell$ , or of both, each of the three gain curves and also

each of the three phase ones, show different appearance from each other in the frequency range below 5.0 c/s. But on the gain diagrams and also on the phase ones, the three curves agree with each other in the range beyond 5.0 c/s, and in the lowest range they come again to agree with each other. Moreover the disagreement among the curves may not be so fatal because they lie in narrow limites of which the width of the gain characteristics does not exceed 2 db nor that of the phase 8 deg.

In the cases of the same  $\tau_t$  value, the agreement among the three gain curves and also that among the phase ones may be weakend with decrease of  $\tau_l$  in the range beyond 5 c/s, but deteriorated so little that the values of  $\tau_l$  does not affect significantly mutual arrangement of the three gain curves nor that of the phase ones in the whole frequency range. In the cases of the same  $\tau_l$  value, the discrepancy among the three gain curves may grow as the  $\tau_t$  value decreases in the lowest frequency range, but the absolute value is small. Therefore, the values of  $\tau_t$  does not much influence mutual arrangement of the three gain curves in the whole frequency range.

It is thus possible to say by investigation that the uncertainty of  $\tau_v$  affects the characteristics of the plasma column displacement to vertical field change in the frequency range below 5 c/s, but the discrepancies among the characteristic curves are not so large that the influence of  $\tau_v$  may not be so much.

### 2-3-3 Influence of the intrinsic time constant, $\tau_l$ , on frequency characteristics of the plasma column displacement to vertical field change

Influence of the intrinsic time constant of the conductor 1,  $\tau_l$ , on frequency characteristics of the plasma column displacement to vertical field change will be investigated. The characteristics are shown in Figs. 4-19~4-27.  $\tau_v$  is set at 1.0 in Figs. 4-19, 4-20 and 4-21, at 0.5 in Figs. 4-22, 4-23 and 4-24 and at 0.2 in Figs. 4-25, 4-26 and 4-27.  $\tau_t$  is set at 10.0 in Figs. 4-19, 4-22 and 4-25, at 0.5 in Figs. 4-20,

4-23 and 4-26 and at 2.0 in Figs. 4-21, 4-24 and 4-27. Each of the three curves in each figure concerns one of the three  $\tau_\ell$  s, 0.03, 0.02 and 0.01.

It is seen in the figures that the three curves lie, regardless of the value of  $\tau_v$  or  $\tau_t$ , or of both, in narrow limits of which the width of the gain characteristics is about 1.1 db at 50.0 c/s and reduces to 0.4 db at 5.0 c/s, and that of the phase ones is about 3 deg. in the frequency range beyond 5.0 c/s. Moreover the discrepancy among the gain curves and also that among the phase ones decrease with decrease of the frequency and cease to appear in the low frequency range.

In the cases of the same  $\tau_v$  value, the discrepancy among the gain curves and also that among the phase ones rest unchanged regardless of the values of  $\tau_t$  and so the values of  $\tau_t$  may not affect mutual arrangement of the three gain curves nor that of the phase ones in the whole frequency range. In the cases of the same  $\tau_t$  value, the agreement among the three gain curves and also that among the phase ones might be weakened with decrease of the  $\tau_v$  value, but so little that the values of  $\tau_v$  may not affect significantly mutual arrangement of the three gain curves in the whole frequency range.

It is thus possible to say by investigation that the uncertainty of  $\tau_\ell$  does not influence so much the characteristics of the plasma column position to vertical field change in the whole frequency range.

2-4 Influence of the intrinsic time constants,  $\tau_\ell$ ,  $\tau_v$  and  $\tau_t$ , on frequency characteristics of the plasma column displacement to terminal voltage change of the conductor v

Influence of the intrinsic time constants of conductors,  $\tau_\ell$ ,  $\tau_v$  and  $\tau_t$ , on frequency characteristics of the plasma column displacement to terminal voltage change of the conductor v will be investigated. The characteristics are shown in Figs. 5-1~5-27 where  $\sqrt{\sigma}$  is set at 2.2 and G at -0.8 in accordance with the obtained results in the preceding section, and  $\tau_\ell$  is set at one of the three  $\tau_\ell$  s (0.03, 0.02, 0.01),  $\tau_v$  at one of the three  $\tau_v$  s (1.0, 0.5, 0.2) and  $\tau_t$  at one of the three  $\tau_t$  s



(10.0, 5.0, 2.0). The values of the intrinsic time constants are found around the expected values. The influence of  $\tau_t$  on the characteristics will be investigated with Figs. 5-1 ~ 5-9, that of  $\tau_v$  with Figs. 5-10 ~ 5-18 and that of  $\tau_l$  with Figs. 5-19 ~ 5-27.

2-4-1 Influence of the intrinsic time constant,  $\tau_t$ , on frequency characteristics of the plasma column displacement to terminal voltage change of the conductor v

Influence of the intrinsic time constant of the conductor t,  $\tau_t$ , on frequency characteristics of the plasma column displacement to terminal voltage change of the conductor v will be investigated. The characteristics are shown in Figs. 5-1 ~ 5-9.  $\tau_l$  is set at 0.03 in Figs. 5-1, 5-2 and 5-3, at 0.02 in Figs. 5-4, 5-5 and 5-6 and at 0.01 in Figs. 5-7, 5-8 and 5-9.  $\tau_v$  is set at 1.0 in Figs. 5-1, 5-4 and 5-7, at 0.5 in Figs. 5-2, 5-5 and 5-8 and 0.2 in Figs. 5-3, 5-6 and 5-9. Each of the three curves in each figure concerns one of the three  $\tau_t$ s, 10.0, 5.0 and 2.0.

It is seen in the figures that three curves agree with each other in the frequency range beyond 0.3 c/s. The discrepancy among them is about 2 db at 0.2 c/s, reduces to 1 db at 0.3 c/s and disappears in the range beyond 0.4 c/s. But in the range below 0.3 c/s, the characteristics are affected by the  $\tau_t$  values and the discrepancy increase with decrease of the frequency to 9 db at 0.05 c/s. Three phase curves agree with each other in the frequency range beyond 1 c/s. The discrepancy among them is about 6 deg. at 0.8 c/s, reduces to 4 deg. at 1 c/s and ceases to appear in the range beyond 2 c/s. But in the range below 1 c/s, the characteristics are affected by the  $\tau_t$  values, and the discrepancy increases with decrease of the frequency to 34 deg. at 0.1 c/s, but in the range below 0.1 c/s the discrepancy is likely to decrease and reduces to 23 deg. at 0.05 c/s.

In the cases of the same  $\tau_l$  value, the agreement among the gain curves and also that among the phase ones may be slightly weakened with decrease of the  $\tau_v$  value, but deteriorated so small that the values of  $\tau_v$  may not affect mutual arrangement

of the three gain curves nor that of the phase ones in the whole frequency range. In the cases of the same  $\tau_v$  value, the values of  $\tau_l$  may not influence mutual arrangement among the three gain curves nor that of the phase ones in the whole frequency range.

It is thus possible to say by investigation that the uncertainty of  $\tau_l$  does not influence significantly the characteristics of the plasma column displacement to terminal voltage change of the conductor  $v$  in the frequency range beyond 0.6 c/s. But in the frequency range below 0.6 c/s, the characteristics are affected by the uncertainty of  $\tau_t$ .

#### 2-4-2 Influence of the intrinsic time constant, $\tau_v$ , on frequency characteristics of the plasma column displacement to terminal voltage change of the conductor $v$

Influence of the intrinsic time constant of the conductor  $v$ ,  $\tau_v$ , on frequency characteristics of the plasma column displacement to terminal voltage change of the conductor  $v$  will be investigated. The characteristics are shown in Figs. 5-10 ~ 5-18.  $\tau_t$  is set at 10.0 in Figs. 5-10, 5-11 and 5-12, at 5.0 in Figs. 5-13, 5-14 and 5-15 and at 2.0 in Figs. 5-16, 5-17 and 5-18.  $\tau_l$  is set at 0.03 in Figs. 5-10, 5-13 and 5-16, at 0.02 in Figs. 5-11, 5-14 and 5-17 and at 0.01 in Figs. 5-12, 5-15 and 5-18. Each of the three curves in each figure concerns one of the three  $\tau_v$ s, 1.0, 0.5 and 0.2.

It is seen in the figures that, regardless of the value of  $\tau_t$  or  $\tau_l$ , or of both, the characteristics are affected noticeably by  $\tau_v$  and each of the three curves shows its different appearance from each other in the whole frequency range. The discrepancy among the three gain curves is about 14 db in the range beyond 2 c/s but decreases with decrease of the frequency and reduces to 4 db at 0.2 c/s. The discrepancy among the three phase curves, which is less than 10 deg. in the range below 0.1 c/s, increases to 38 deg. at 0.5 c/s but in the range beyond 0.5 c/s decreases with increase of the frequency. The discrepancy reduces to 10 deg. at 5 c/s, to 8 deg. at 10 c/s and to 3 deg. at 50 c/s.

In the cases of the same  $\tau_t$  value, the values of  $\tau_l$  may not affect mutual arrangement of the three gain curves nor that of the three phase ones in the whole frequency range. The discrepancy among the three phase curves may be reduced with decrease of the  $\tau_l$  value but too little to be mentioned any more. In the cases of the same  $\tau_t$  value, the discrepancy among the three gain curves may be reduced with increase of the  $\tau_t$  value but too little to be mentioned, and it may be said that the value of  $\tau_t$  does not affect significantly mutual arrangement of the three gain curves nor that of the three phase ones in the whole frequency range.

It is possible to say by investigation that the uncertainty of  $\tau_v$  influences the characteristics of the plasma column displacement to terminal voltage change of the conductor v in the whole frequency range.

#### 2-4-3 Influence of the intrinsic time constant, $\tau_l$ , on frequency characteristics of the plasma column displacement to terminal voltage change of the conductor v

Influence of the intrinsic time constant of the conductor 1,  $\tau_l$ , on frequency characteristics of the plasma column displacement to terminal voltage change of the conductor v will be investigated. The characteristics are shown in Figs. 5-19 ~ 5-27.  $\tau_v$  is set at 1.0 in Figs. 5-19, 5-20 and 5-21, at 0.5 in Figs. 5-22, 5-23 and 5-24 and at 0.2 in Figs. 5-25, 5-26 and 6-27.  $\tau_t$  is set at 10.0 in Figs. 5-19, 5-22 and 5-25, at 0.5 in Figs. 5-20, 5-23 and 5-26 and at 2.0 in Figs. 5-21, 5-24 and 5-27. Each of the three curves in each figure concerns one of the three  $\tau_l$ s, 0.03, 0.02 and 0.01.

It is seen in the figures that three gain curves agree with each other, regardless of  $\tau_v$  or  $\tau_t$ , or of both, in the frequency range below 5 c/s. The discrepancy among them, which is about 1.5 db at 5 c/s, decreases with decrease of the frequency and ceases to appear in the frequency range below 1 c/s. But the discrepancy increases, with increase of the

frequency, to 2 db at 10 c/s and to 7 db at 50 c/s. Three phase curves, among which the agreement is weaker than that among the gain ones, lies in narrow limits in the frequency range below 0.5 c/s, of which the width does not exceed 3 deg. at 0.5 c/s. But in the frequency range beyond 0.5 c/s, the discrepancy increases, with increase of the frequency, to 10 deg. at 4 c/s, 12 deg. at 5 c/s and 24 deg. at 50 c/s.

In the cases of the same  $\tau_v$  value, the discrepancy among the three gain curves and also that among the phase ones rest unchanged regardless of the values of  $\tau_t$  and so the values of  $\tau_t$  may not affect mutual arrangement of the three curves in the whole frequency range. In the cases of the same  $\tau_t$  value, the agreement among the gain curves and also that among the phase ones is weakened with decrease of the  $\tau_v$  value, but so little that the value of  $\tau_v$  does not affect mutual arrangement of the three curves in the whole frequency range.

It is possible to say by investigation that the uncertainty of  $\tau_l$  does not influence significantly the characteristics of the plasma column displacement to terminal voltage change of the conductor  $v$  in the frequency range below 4 c/s, but in the range beyond 4 c/s, the uncertainty of  $\tau_l$  may influence the characteristics.

## 3. SUMMARY AND CONCLUSION

Frequency characteristics of the horizontal motion of a JT-60 plasma column have been described, especially influence of the uncertainty in parameters on the characteristics investigated.

Concerning the characteristics to vertical field change, the uncertainty of  $\sqrt{\sigma}$  or G, or of both, little influences the characteristics in the whole frequency range, and therefore, motion of the plasma column to a vertical field change may be analyzed with reasonable values of  $\sqrt{\sigma}$  and G. The uncertainty of  $\tau_x$  does not much influence the characteristics in the range beyond 0.5 c/s, but not so in the range below it. The uncertainty of  $\tau_v$  affects the characteristics in the range below 5 c/s, but not so much. The uncertainty of  $\tau_z$  does not almost influence the characteristics in the whole frequency range.

Concerning the characteristics to terminal voltage change of the conductor v, the uncertainty of  $\sqrt{\sigma}$  or G, or of both, little influences the characteristics in the whole frequency range, and therefore, motion of the plasma column to a terminal voltage change of the conductor v may be analyzed with reasonable values of  $\sqrt{\sigma}$  and G. The uncertainty of  $\tau_x$  does not much influence the characteristics in the range beyond 0.6 c/s, but not so in the range below it. The uncertainty of  $\tau_v$  does affect the characteristics in the whole frequency range. The uncertainty of  $\tau_z$  does not influence the characteristics in the range below 4 c/s, but affects them a little in the range beyond it.

A knowledge of the influence of parameters on characteristics of the plasma column is essential in analyzing motion of the plasma column and developing the control method for the control column motion. Control performance of the JT-60 plasma column will be described in a later report.

## REFERENCES

- 1) MUKHOVATOV, V.S., SHAFRANOV, V.D., Plasma Equilibrium in a TOKAMAK, Nuclear Fusion 11 (1971)
- 2) LEONTOVICH, M.A., Reviews of Plasma Physics 2, Translated from Russian by HERBERT LASHINSKY, Consultants Bureau, New York (1966)
- 3) HUGILL, J., GIBSON, A., Servo Control of Plasma Position in CLEO-TOKAMAK, CLM-P 382 (1974)
- 4) KAMBAYASHI, Y., HARA, M., A Kinetics Model for the Horizontal Displacement of a Toroidal Plasma Column, JAERI-M 6292 (1975)

Table 1 List of parameters

Notation	Expected Value	Possible Value	Complement
$R_0$	3.0		Major radius of the plasma column
$a_0$	1.0		Minor radius of the plasma column
$r_l$	1.2		Minor radius of the conductor l
$r_v$	1.4		Minor radius of the conductor v
$r_t$	1.8		Minor radius of the conductor t
$N_l$	1		Equivalent number of turns of the conductor l
$N_v$	6.4		Equivalent number of turns of the conductor v
$N_t$	1		Equivalent number of turns of the conductor t
$\tau_l$	< 0.03		Intrinsic time constant of the conductor l
$\tau_v$	< 1.0		Intrinsic time constant of the conductor v
$\tau_t$	< 10.0		Intrinsic time constant of the conductor t
$\beta_0$	0.1		Value of poloidal beta
$l_i$	0.9		Internal inductance of the plasma column
$m$		$-1.5 < < 0$	Positional gradient of the vertical field
$\alpha$		$0 < < 0.5$	Positional gradient of the minor radius
$n$		$-1 < < 0$	Positional gradient of the plasma current
$\Gamma_0$			$\Gamma_0 = k_n \frac{\partial R_0}{\partial a_0} + \beta_0 + \frac{k_i - 3}{2}$
$G$			$G = \frac{1 - \alpha}{\Gamma_0} - 1 + n - m$

Table 2 Values of  $\bar{\rho}$

1.00	2.93	2.98	3.03	3.08	3.13	3.18	3.23	3.28	3.33	3.38	3.43
.90	2.83	2.88	2.93	2.98	3.03	3.08	3.13	3.18	3.23	3.28	3.33
.80	2.73	2.78	2.83	2.88	2.93	2.98	3.03	3.08	3.13	3.18	3.23
.70	2.63	2.68	2.73	2.78	2.83	2.88	2.93	2.98	3.03	3.08	3.13
.60	2.53	2.58	2.63	2.68	2.73	2.78	2.83	2.88	2.93	2.98	3.03
.50	2.43	2.48	2.53	2.58	2.63	2.68	2.73	2.78	2.83	2.88	2.93
.40	2.33	2.38	2.43	2.48	2.53	2.58	2.63	2.68	2.73	2.78	2.83
.30	2.23	2.28	2.33	2.38	2.43	2.48	2.53	2.58	2.63	2.68	2.73
.20	2.13	2.18	2.23	2.28	2.33	2.38	2.43	2.48	2.53	2.58	2.63
.10	2.03	2.08	2.13	2.18	2.23	2.28	2.33	2.38	2.43	2.48	2.53
$\rho_0 \backslash l_i$	.50	.60	.70	.80	.90	1.00	1.10	1.20	1.30	1.40	1.50

Table 3 Values of (n-m)

-.25	-.75	-.65	-.55	-.45	-.35	-.25	-.15	-.05	.05	.15	.25
-.35	-.65	-.55	-.45	-.35	-.25	-.15	-.05	.05	.15	.25	.35
-.45	-.55	-.45	-.35	-.25	-.15	-.05	.05	.15	.25	.35	.45
-.55	-.45	-.35	-.25	-.15	-.05	.05	.15	.25	.35	.45	.55
-.65	-.35	-.25	-.15	-.05	.05	.15	.25	.35	.45	.55	.65
$m \backslash n$	-1.00	-.90	-.80	-.70	-.60	-.50	-.40	-.30	-.20	-.10	.00



Table 4-1 Values of G (K=0.0)

3.43	-1.46	-1.36	-1.26	-1.15	-1.06	-.96	-.86	-.76	-.66	-.56	-.46	-.36	-.26	-.16	-.06
3.33	-1.45	-1.35	-1.25	-1.15	-1.05	-.95	-.85	-.75	-.65	-.55	-.45	-.35	-.25	-.15	-.05
3.23	-1.44	-1.34	-1.24	-1.14	-1.04	-.94	-.84	-.74	-.64	-.54	-.44	-.34	-.24	-.14	-.04
3.13	-1.43	-1.33	-1.23	-1.13	-1.03	-.93	-.83	-.73	-.63	-.53	-.43	-.33	-.23	-.13	-.03
3.03	-1.42	-1.32	-1.22	-1.12	-1.02	-.92	-.82	-.72	-.62	-.52	-.42	-.32	-.22	-.12	-.02
2.93	-1.41	-1.31	-1.21	-1.11	-1.01	-.91	-.81	-.71	-.61	-.51	-.41	-.31	-.21	-.11	-.01
2.83	-1.40	-1.30	-1.20	-1.10	-1.00	-.90	-.80	-.70	-.60	-.50	-.40	-.30	-.20	-.10	-.00
2.73	-1.38	-1.28	-1.18	-1.08	-.98	-.88	-.78	-.68	-.58	-.48	-.38	-.28	-.18	-.08	-.02
2.63	-1.37	-1.27	-1.17	-1.07	-.97	-.87	-.77	-.67	-.57	-.47	-.37	-.27	-.17	-.07	-.03
2.53	-1.35	-1.25	-1.15	-1.05	-.95	-.85	-.75	-.65	-.55	-.45	-.35	-.25	-.15	-.05	-.05
2.43	-1.34	-1.24	-1.14	-1.04	-.94	-.84	-.74	-.64	-.54	-.44	-.34	-.24	-.14	-.04	-.06
2.33	-1.32	-1.22	-1.12	-1.02	-.92	-.82	-.72	-.62	-.52	-.42	-.32	-.22	-.12	-.02	-.08
2.23	-1.30	-1.20	-1.10	-1.00	-.90	-.80	-.70	-.60	-.50	-.40	-.30	-.20	-.10	-.00	-.10
2.13	-1.28	-1.18	-1.08	-.98	-.88	-.78	-.68	-.58	-.48	-.38	-.28	-.18	-.08	-.02	-.12
2.03	-1.26	-1.15	-1.06	-.96	-.86	-.76	-.66	-.56	-.46	-.36	-.26	-.16	-.06	-.04	-.14
$\Gamma$	-.75	-.65	-.55	-.45	-.35	-.25	-.15	-.05	.05	.15	.25	.35	.45	.55	.65
$\eta$ -m															

Table 4-2 Values of G (K=0.1)

3.43	-1.49	-1.39	-1.29	-1.19	-1.09	-.99	-.89	-.79	-.69	-.59	-.49	-.39	-.29	-.19	-.09
3.33	-1.48	-1.38	-1.28	-1.18	-1.08	-.98	-.88	-.78	-.68	-.58	-.48	-.38	-.28	-.18	-.08
3.23	-1.47	-1.37	-1.27	-1.17	-1.07	-.97	-.87	-.77	-.67	-.57	-.47	-.37	-.27	-.17	-.07
3.13	-1.45	-1.36	-1.26	-1.16	-1.06	-.96	-.86	-.76	-.66	-.56	-.46	-.36	-.26	-.16	-.06
3.03	-1.44	-1.35	-1.25	-1.15	-1.05	-.95	-.85	-.75	-.65	-.55	-.45	-.35	-.25	-.15	-.05
2.93	-1.44	-1.34	-1.24	-1.14	-1.04	-.94	-.84	-.74	-.64	-.54	-.44	-.34	-.24	-.14	-.04
2.83	-1.43	-1.33	-1.23	-1.13	-1.03	-.93	-.83	-.73	-.63	-.53	-.43	-.33	-.23	-.13	-.03
2.73	-1.42	-1.32	-1.22	-1.12	-1.02	-.92	-.82	-.72	-.62	-.52	-.42	-.32	-.22	-.12	-.02
2.63	-1.41	-1.31	-1.21	-1.11	-1.01	-.91	-.81	-.71	-.61	-.51	-.41	-.31	-.21	-.11	-.01
2.53	-1.39	-1.29	-1.19	-1.09	-.99	-.89	-.79	-.69	-.59	-.49	-.39	-.29	-.19	-.09	-.01
2.43	-1.38	-1.28	-1.18	-1.08	-.98	-.88	-.78	-.68	-.58	-.48	-.38	-.28	-.18	-.08	-.02
2.33	-1.36	-1.26	-1.16	-1.06	-.96	-.86	-.76	-.66	-.56	-.46	-.36	-.26	-.16	-.06	-.04
2.23	-1.35	-1.25	-1.15	-1.05	-.95	-.85	-.75	-.65	-.55	-.45	-.35	-.25	-.15	-.05	-.05
2.13	-1.33	-1.23	-1.13	-1.03	-.93	-.83	-.73	-.63	-.53	-.43	-.33	-.23	-.13	-.03	-.07
2.03	-1.31	-1.21	-1.11	-1.01	-.91	-.81	-.71	-.61	-.51	-.41	-.31	-.21	-.11	-.01	-.09
$\Gamma$	-.75	-.65	-.55	-.45	-.35	-.25	-.15	-.05	.05	.15	.25	.35	.45	.55	.65
$\eta$ -m															

Table 4-3 Values of G ( $\alpha=0.2$ )

3.43	-1.52	-1.42	-1.32	-1.22	-1.12	-.92	-.72	-.52	-.32	-.22	-.12
3.33	-1.51	-1.41	-1.31	-1.21	-1.11	-.91	-.71	-.51	-.31	-.21	-.11
3.23	-1.50	-1.40	-1.30	-1.20	-1.10	-.90	-.70	-.50	-.30	-.20	-.10
3.13	-1.49	-1.39	-1.29	-1.19	-1.09	-.89	-.69	-.49	-.29	-.19	-.09
3.03	-1.48	-1.38	-1.28	-1.18	-1.08	-.88	-.68	-.48	-.28	-.18	-.08
2.93	-1.47	-1.37	-1.27	-1.17	-1.07	-.87	-.67	-.47	-.27	-.17	-.07
2.83	-1.46	-1.36	-1.26	-1.16	-1.06	-.86	-.66	-.46	-.26	-.16	-.06
2.73	-1.45	-1.35	-1.25	-1.15	-1.05	-.85	-.65	-.45	-.25	-.15	-.05
2.63	-1.43	-1.33	-1.23	-1.13	-1.03	-.83	-.63	-.43	-.23	-.13	-.03
2.53	-1.42	-1.32	-1.22	-1.12	-1.02	-.82	-.62	-.42	-.22	-.12	-.02
2.43	-1.41	-1.31	-1.21	-1.11	-1.01	-.81	-.61	-.41	-.21	-.11	-.01
2.33	-1.39	-1.29	-1.19	-1.09	-.99	-.79	-.59	-.39	-.19	-.09	-.01
2.23	-1.37	-1.27	-1.17	-1.07	-.97	-.77	-.57	-.37	-.17	-.07	-.03
2.13	-1.35	-1.25	-1.15	-1.05	-.95	-.75	-.55	-.35	-.15	-.05	-.04
$\Gamma$	-.75	-.65	-.55	-.45	-.35	-.25	-.15	-.05	.25	.45	.65

Table 4-4 Values of G ( $\alpha=0.3$ )

3.43	-1.55	-1.45	-1.35	-1.25	-1.15	-.95	-.75	-.55	-.35	-.25	-.15	-.05	.25	.45	.65
3.33	-1.54	-1.44	-1.34	-1.24	-1.14	-.94	-.74	-.54	-.34	-.24	-.14	-.04	.24	.44	.64
3.23	-1.53	-1.43	-1.33	-1.23	-1.13	-.93	-.73	-.53	-.33	-.23	-.13	-.03	.23	.43	.63
3.13	-1.52	-1.42	-1.32	-1.22	-1.12	-.92	-.72	-.52	-.32	-.22	-.12	-.02	.22	.42	.62
3.03	-1.51	-1.41	-1.31	-1.21	-1.11	-.91	-.71	-.51	-.31	-.21	-.11	-.01	.21	.41	.61
2.93	-1.50	-1.40	-1.30	-1.20	-1.10	-.90	-.70	-.50	-.30	-.20	-.10	-.00	.20	.40	.60
2.83	-1.49	-1.39	-1.29	-1.19	-1.09	-.89	-.69	-.49	-.29	-.19	-.09	-.00	.19	.39	.59
2.73	-1.48	-1.38	-1.28	-1.18	-1.08	-.88	-.68	-.48	-.28	-.18	-.08	-.00	.18	.38	.58
2.63	-1.47	-1.37	-1.27	-1.17	-1.07	-.87	-.67	-.47	-.27	-.17	-.07	-.00	.17	.37	.57
2.53	-1.46	-1.36	-1.26	-1.16	-1.06	-.86	-.66	-.46	-.26	-.16	-.06	-.00	.16	.36	.56
2.43	-1.45	-1.35	-1.25	-1.15	-1.05	-.85	-.65	-.45	-.25	-.15	-.05	-.00	.15	.35	.55
2.33	-1.44	-1.34	-1.24	-1.14	-1.04	-.84	-.64	-.44	-.24	-.14	-.04	-.00	.14	.34	.54
2.23	-1.42	-1.32	-1.22	-1.12	-1.02	-.82	-.62	-.42	-.22	-.12	-.02	-.00	.12	.32	.52
2.13	-1.40	-1.30	-1.20	-1.10	-1.00	-.80	-.60	-.40	-.20	-.10	-.00	-.00	.10	.30	.50
$\Gamma$	-.75	-.65	-.55	-.45	-.35	-.25	-.15	-.05	.25	.45	.65	.85	.05	.25	.45

Table 4-5 Values of G ( $\alpha=0.4$ )

3.43	-1.57	-1.67	-1.37	-1.27	-1.17	-1.07	-.97	-.87	-.77	-.67	-.57	-.47	-.37	-.27	-.17
3.33	-1.57	-1.47	-1.37	-1.27	-1.17	-1.07	-.97	-.87	-.77	-.67	-.57	-.47	-.37	-.27	-.17
3.23	-1.56	-1.46	-1.36	-1.26	-1.16	-1.06	-.96	-.86	-.76	-.66	-.56	-.46	-.36	-.26	-.16
3.13	-1.56	-1.46	-1.36	-1.26	-1.16	-1.06	-.96	-.86	-.76	-.66	-.56	-.46	-.36	-.26	-.16
3.03	-1.55	-1.45	-1.35	-1.25	-1.15	-1.05	-.95	-.85	-.75	-.65	-.55	-.45	-.35	-.25	-.15
2.93	-1.55	-1.45	-1.35	-1.25	-1.15	-1.05	-.95	-.85	-.75	-.65	-.55	-.45	-.35	-.25	-.15
2.83	-1.54	-1.44	-1.34	-1.24	-1.14	-1.04	-.94	-.84	-.74	-.64	-.54	-.44	-.34	-.24	-.14
2.73	-1.53	-1.43	-1.33	-1.23	-1.13	-1.03	-.93	-.83	-.73	-.63	-.53	-.43	-.33	-.23	-.13
2.63	-1.52	-1.42	-1.32	-1.22	-1.12	-1.02	-.92	-.82	-.72	-.62	-.52	-.42	-.32	-.22	-.12
2.53	-1.51	-1.41	-1.31	-1.21	-1.11	-1.01	-.91	-.81	-.71	-.61	-.51	-.41	-.31	-.21	-.11
2.43	-1.50	-1.40	-1.30	-1.20	-1.10	-1.00	-.90	-.80	-.70	-.60	-.50	-.40	-.30	-.20	-.10
2.33	-1.49	-1.39	-1.29	-1.19	-1.09	-.99	-.89	-.79	-.69	-.59	-.49	-.39	-.29	-.19	-.09
2.23	-1.48	-1.38	-1.28	-1.18	-1.08	-.98	-.88	-.78	-.68	-.58	-.48	-.38	-.28	-.18	-.08
2.13	-1.47	-1.37	-1.27	-1.17	-1.07	-.97	-.87	-.77	-.67	-.57	-.47	-.37	-.27	-.17	-.07
2.03	-1.45	-1.35	-1.25	-1.15	-1.05	-.95	-.85	-.75	-.65	-.55	-.45	-.35	-.25	-.15	-.05
$\sqrt{1-\pi}$	-.75	-.65	-.55	-.45	-.35	-.25	-.15	-.05	.05	.15	.25	.35	.45	.55	.65

Table 4-6 Values of G ( $\alpha=0.5$ )

3.43	-1.60	-1.50	-1.40	-1.30	-1.20	-1.10	-1.00	-.90	-.80	-.70	-.60	-.50	-.40	-.30	-.20
3.33	-1.60	-1.50	-1.40	-1.30	-1.20	-1.10	-1.00	-.90	-.80	-.70	-.60	-.50	-.40	-.30	-.20
3.23	-1.60	-1.49	-1.39	-1.29	-1.19	-1.09	-.99	-.89	-.79	-.69	-.59	-.49	-.39	-.29	-.19
3.13	-1.59	-1.48	-1.38	-1.28	-1.18	-1.08	-.98	-.88	-.78	-.68	-.58	-.48	-.38	-.28	-.18
3.03	-1.58	-1.48	-1.38	-1.28	-1.18	-1.08	-.98	-.88	-.78	-.68	-.58	-.48	-.38	-.28	-.18
2.93	-1.57	-1.47	-1.37	-1.27	-1.17	-1.07	-.97	-.87	-.77	-.67	-.57	-.47	-.37	-.27	-.17
2.83	-1.57	-1.47	-1.37	-1.27	-1.17	-1.07	-.97	-.87	-.77	-.67	-.57	-.47	-.37	-.27	-.17
2.73	-1.56	-1.46	-1.36	-1.26	-1.16	-1.06	-.96	-.86	-.76	-.66	-.56	-.46	-.36	-.26	-.16
2.63	-1.55	-1.45	-1.35	-1.25	-1.15	-1.05	-.95	-.85	-.75	-.65	-.55	-.45	-.35	-.25	-.15
2.53	-1.54	-1.44	-1.34	-1.24	-1.14	-1.04	-.94	-.84	-.74	-.64	-.54	-.44	-.34	-.24	-.14
2.43	-1.54	-1.44	-1.34	-1.24	-1.14	-1.04	-.94	-.84	-.74	-.64	-.54	-.44	-.34	-.24	-.14
2.33	-1.53	-1.43	-1.33	-1.23	-1.13	-1.03	-.93	-.83	-.73	-.63	-.53	-.43	-.33	-.23	-.13
2.23	-1.52	-1.42	-1.32	-1.22	-1.12	-1.02	-.92	-.82	-.72	-.62	-.52	-.42	-.32	-.22	-.12
2.13	-1.52	-1.42	-1.32	-1.22	-1.12	-1.02	-.92	-.82	-.72	-.62	-.52	-.42	-.32	-.22	-.12
2.03	-1.52	-1.42	-1.32	-1.22	-1.12	-1.02	-.92	-.82	-.72	-.62	-.52	-.42	-.32	-.22	-.12
$\sqrt{1-\pi}$	-.75	-.65	-.55	-.45	-.35	-.25	-.15	-.05	.05	.15	.25	.35	.45	.55	.65

Table 5-1 List of figures

Fig.2- Fig.3-	$\Gamma_0 = \ln \frac{8R_0}{\alpha_0} + \beta_0 + \frac{l_i - 3}{2}$			$\frac{1-\alpha}{\Gamma_0} - i + n - m$		
	2.0	2.2	2.4	-0.6	-0.8	-1.0
1	○			⊗	○	⊗
2		○		⊗	○	⊗
3			○	⊗	○	⊗
4	⊗	○	⊗	○		
5	⊗	○	⊗		○	
6	⊗	○	⊗			○

$\tau_l$	$\tau_v$	$\tau_t$
0.03	0.5	5.0

Table 5-2 List of figures

$\Gamma_0 = \ln \frac{8R_0}{\alpha_0} + \beta_0 + \frac{l_i - 3}{2}$	$\frac{1-\alpha}{\Gamma_0} - i + n - m$
2.2	-0.8

Fig.4- Fig.5-	$\tau_l$			$\tau_v$			$\tau_t$		
	0.03	0.02	0.01	1.0	0.5	0.2	10.0	5.0	2.0
1	○			○			⊗	○	⊗
2	○				○		⊗	○	⊗
3	○					○	⊗	○	⊗
4		○		○			⊗	○	⊗
5		○			○		⊗	○	⊗
6		○				○	⊗	○	⊗
7			○	○			⊗	○	⊗
8			○		○		⊗	○	⊗
9			○			○	⊗	○	⊗
10	○			⊗	○	⊗	○		
11		○		⊗	○	⊗	○		
12			○	⊗	○	⊗	○		
13	○			⊗	○	⊗		○	
14		○		⊗	○	⊗		○	
15			○	⊗	○	⊗		○	
16	○			⊗	○	⊗			○
17		○		⊗	○	⊗			○
18			○	○	○	○			○
19	⊗	○	⊗	○			○		
20	⊗	○	⊗	○				○	
21	⊗	○	⊗	○					○
22	⊗	○	⊗		○		○		
23	⊗	○	⊗		○			○	
24	⊗	○	⊗		○				○
25	⊗	○	⊗			○	○		
26	⊗	○	⊗			○		○	
27	⊗	○	⊗			○			○

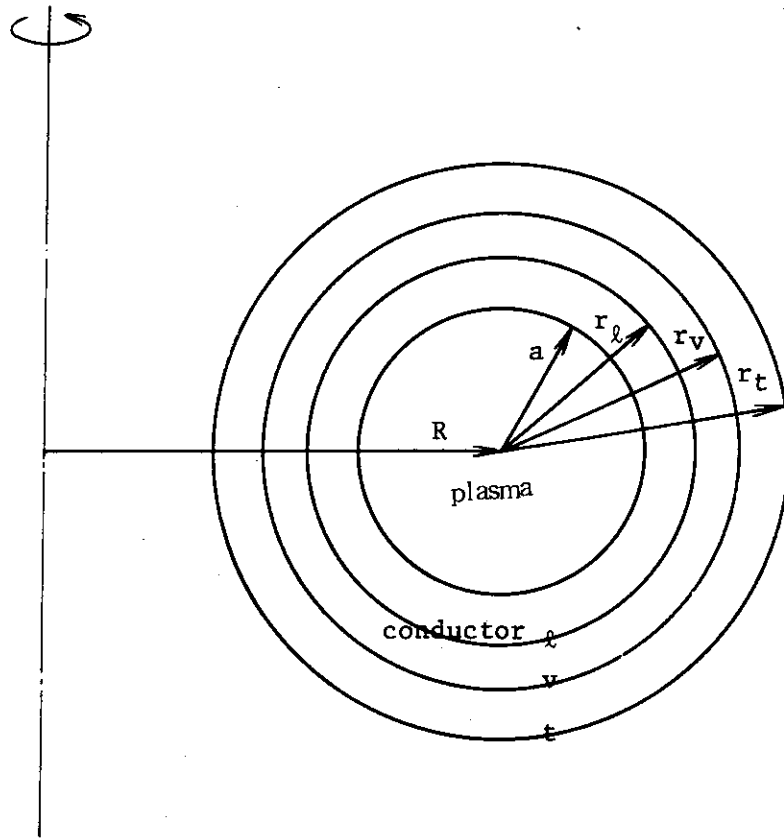
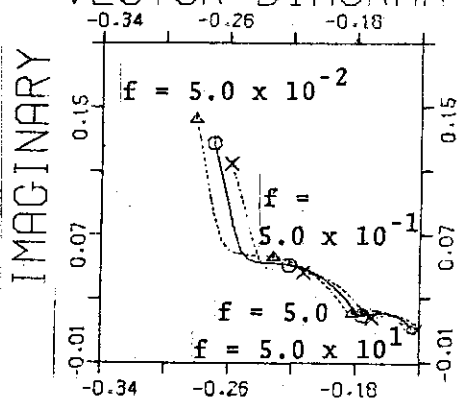


Fig.1 Layout of the device considered

Fig. 2-1  
 Frequency Characteristics  
 Disturbance ( $\delta B_d/B_{vco}$ )  
 → Plasma Position ( $\delta R/R_0$ )

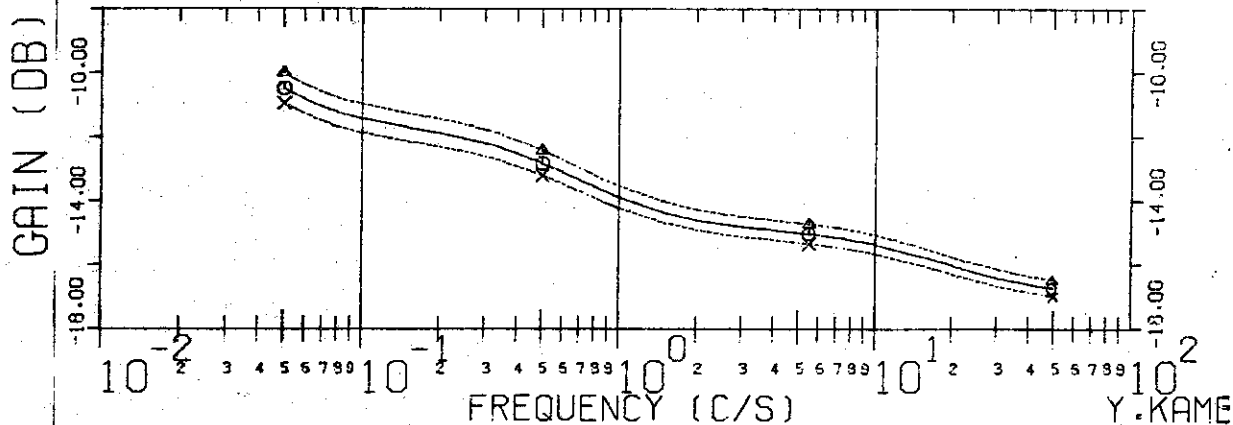
$\Gamma_0 = 2.0$   
 $G = -0.6$  ---  $\Delta$  ---  
 $-0.8$  ---  $\circ$  ---  
 $-1.0$  ---  $\times$  ---  
 $\tau_L = 0.03$   
 $\tau_V = 0.5$   
 $\tau_t = 5.0$

FIG. 2-1-C  
 VECTOR DIAGRAM



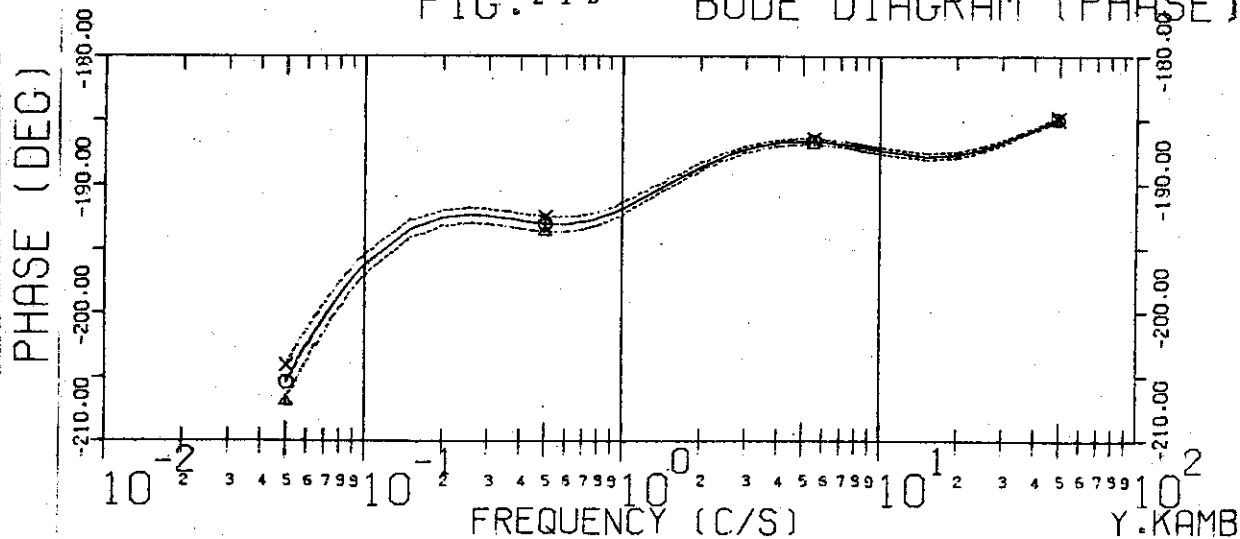
REAL Y.KAMB

FIG. 2-1-A BODE DIAGRAM (GAIN)



Y.KAME

FIG. 2-1-B BODE DIAGRAM (PHASE)



Y.KAMB

Fig.2-2  
 Frequency Characteristics  
 Disturbance ( $\delta B_d/B_{vco}$ )  
 → Plasma Position ( $\delta R/R_0$ )

$\Gamma_0 = 2.2$   
 $G = -0.6$  ---  $\Delta$  ---  
 $-0.8$  ---  $\circ$  ---  
 $-1.0$  ---  $\times$  ---  
 $\tau_f = 0.03$   
 $\tau_v = 0.5$   
 $\tau_t = 5.0$

FIG. 2-2-C  
 VECTOR DIAGRAM

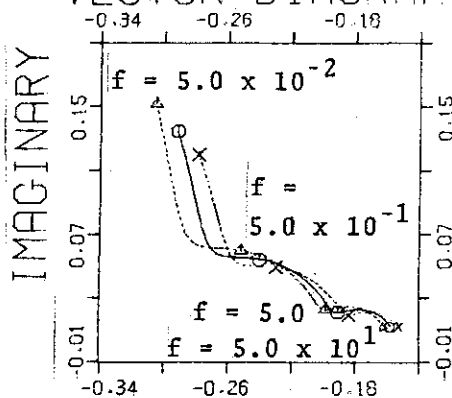


FIG. 2-2-A

BODE DIAGRAM (GAIN)

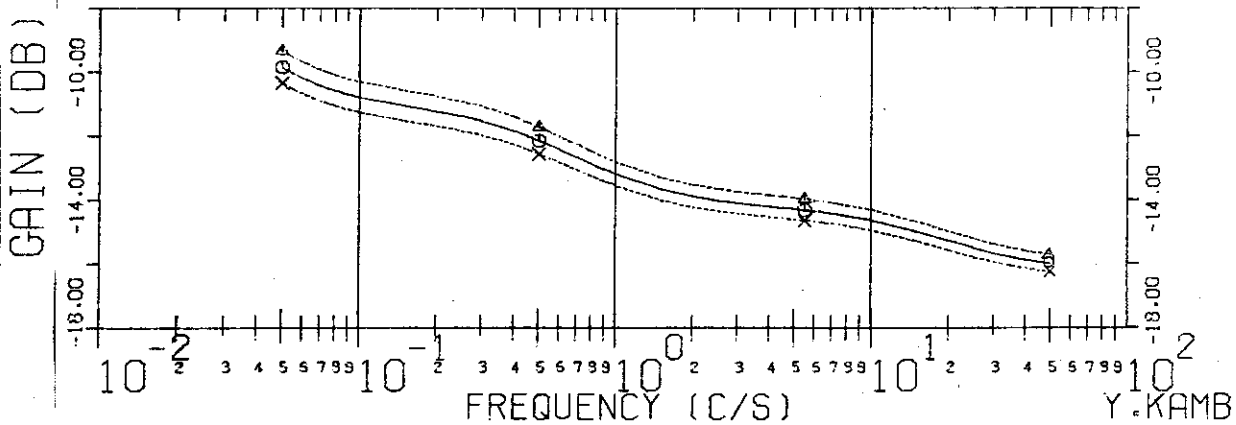


FIG. 2-2-B

BODE DIAGRAM (PHASE)

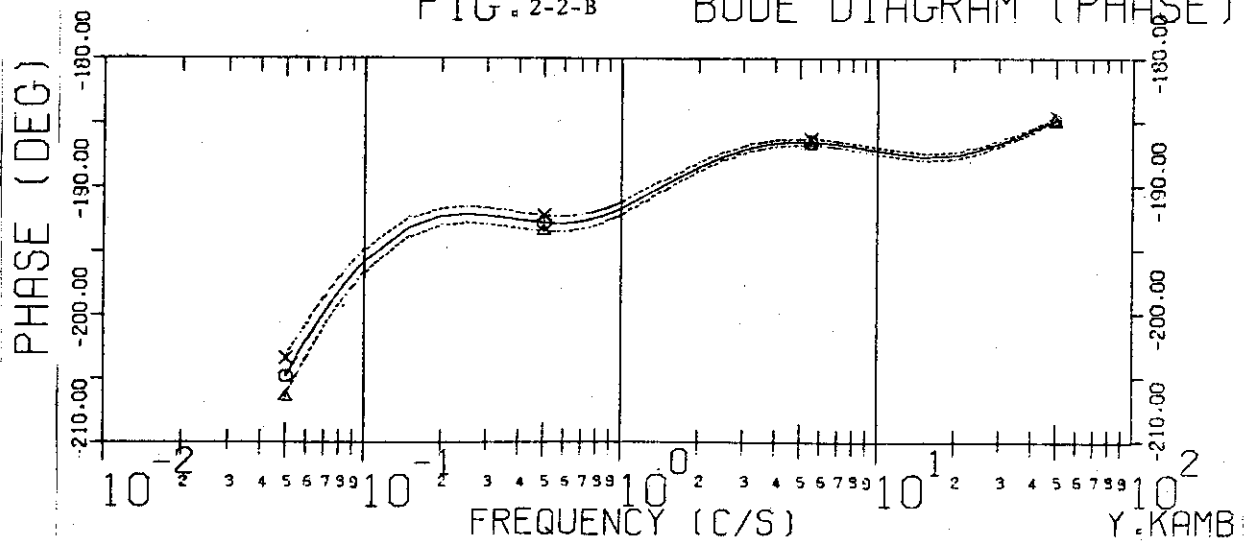


Fig. 2-3  
 Frequency Characteristics  
 Disturbance ( $\delta B_d/B_{VCO}$ )  
 —→ Plasma Position ( $\delta R/R_0$ )

$\Gamma_0 = 2.4$   
 $G = -0.6$  —  $\Delta$  — —  
 $-0.8$  —  $\circ$  — —  
 $-1.0$  —  $\times$  — —  
 $\tau_p = 0.03$   
 $\tau_v = 0.5$   
 $\tau_t = 5.0$

FIG. 2-3-C  
 VECTOR DIAGRAM

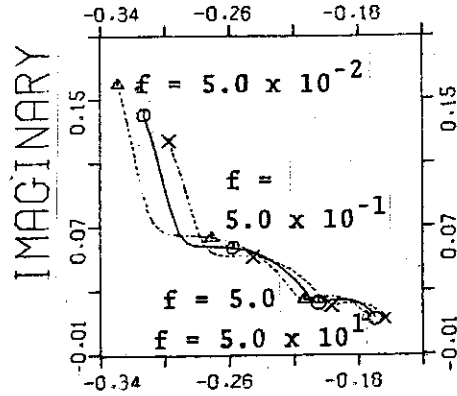


FIG. 2-3-A

BODE DIAGRAM (GAIN)  
 Y.KAMB

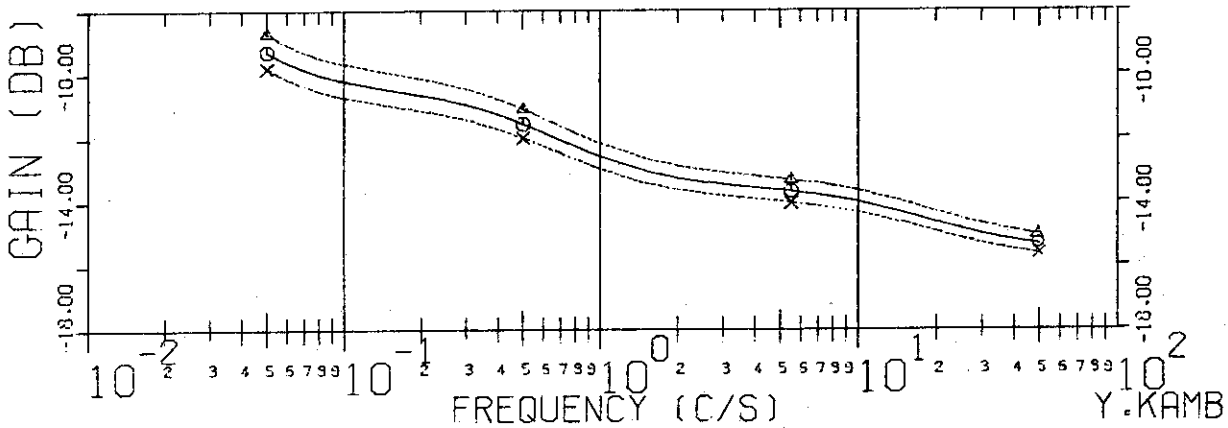


FIG. 2-3-B

BODE DIAGRAM (PHASE)  
 Y.KAMB

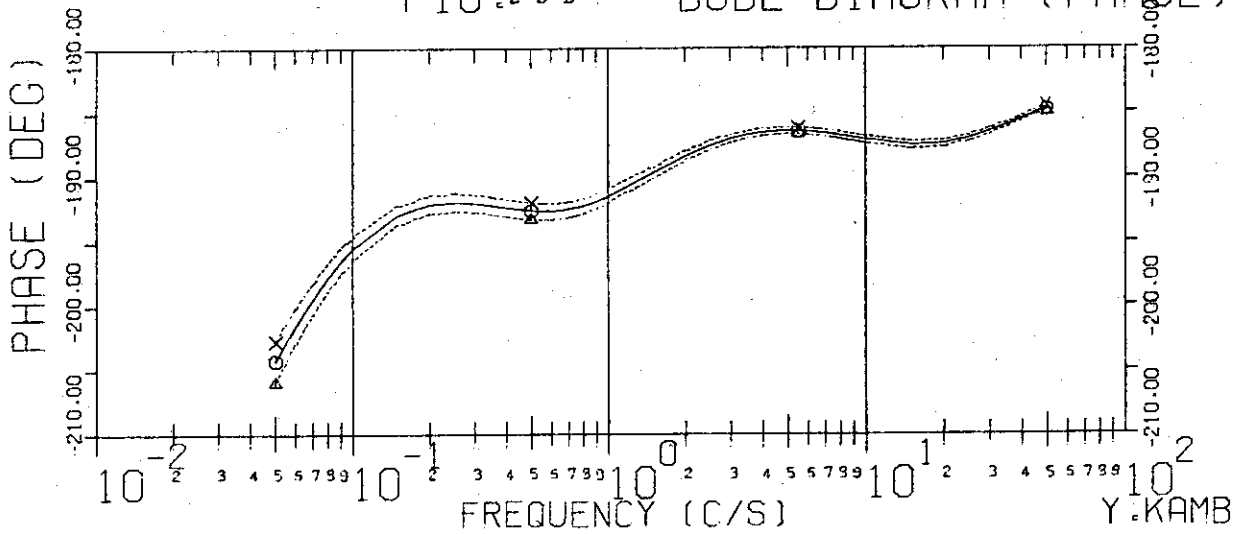




Fig.2-4  
 Frequency Characteristics  
 Disturbance ( $\delta B_d/B_{vco}$ )  
 $\rightarrow$  Plasma Position ( $\delta R/R_0$ )

$\Gamma_0 = 2.0$  ---  $\Delta$  ---  
 $2.2$  ---  $\circ$  ---  
 $2.4$  ---  $\times$  ---  
 $G = -0.6$   
 $\tau_\lambda = 0.03$   
 $\tau_v = 0.5$   
 $\tau_t = 5.0$

FIG. 2-4-C  
 VECTOR DIAGRAM

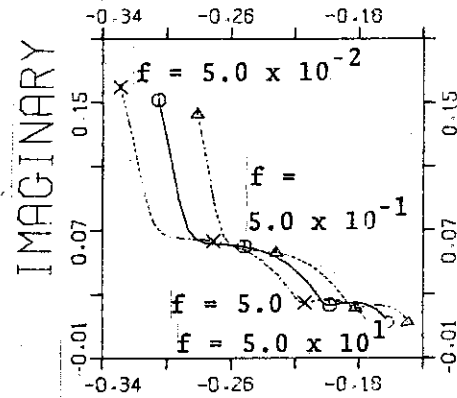


FIG. 2-4-A

BODE DIAGRAM (GAIN)  
 Y.KAMB

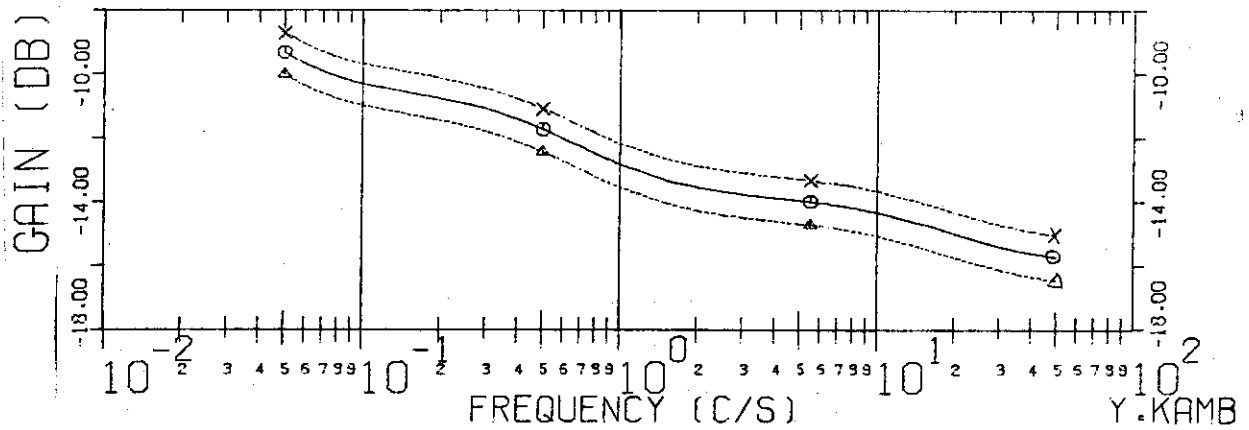


FIG. 2-4-B

BODE DIAGRAM (PHASE)  
 Y.KAMB

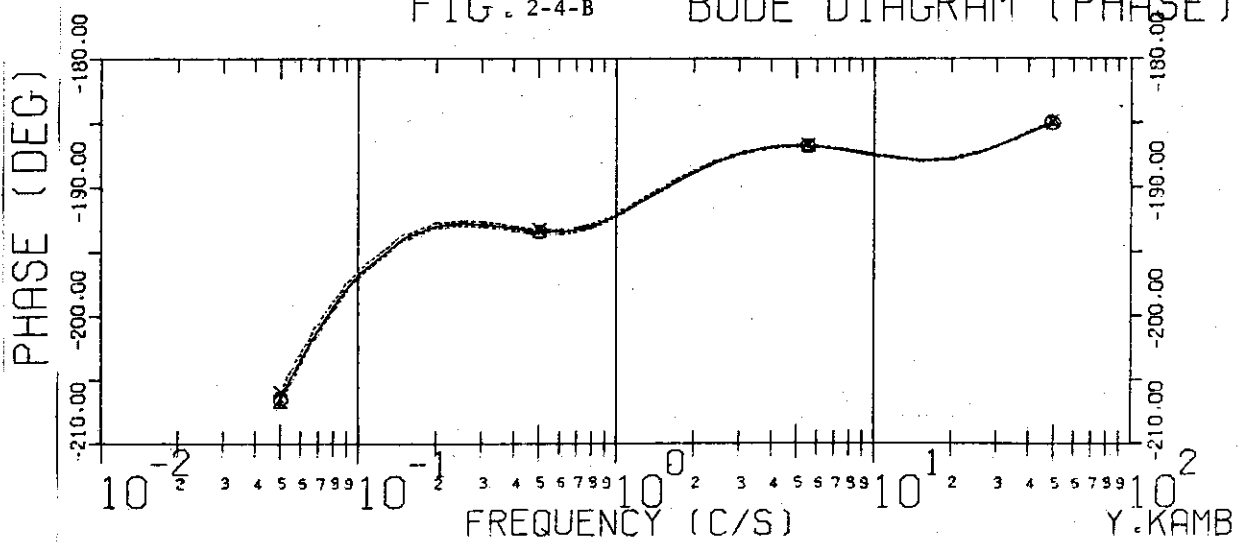


Fig. 2-5  
 Frequency Characteristics  
 Disturbance ( $\delta B_d/B_{vco}$ )  
 → Plasma Position ( $\delta R/R_0$ )

$\Gamma_0 = 2.0$  ---  $\Delta$  ---  
 $2.2$  ---  $\circ$  ---  
 $2.4$  ---  $\times$  ---  
 $G = -0.8$   
 $\tau_f = 0.03$   
 $\tau_v = 0.5$   
 $\tau_t = 5.0$

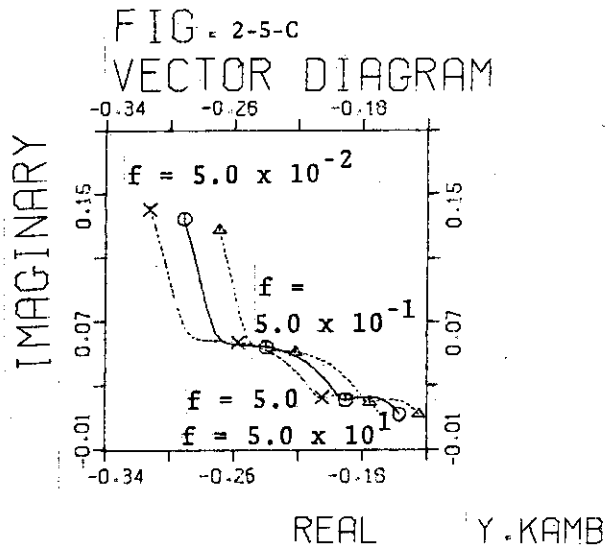


FIG. 2-5-A BODE DIAGRAM (GAIN)

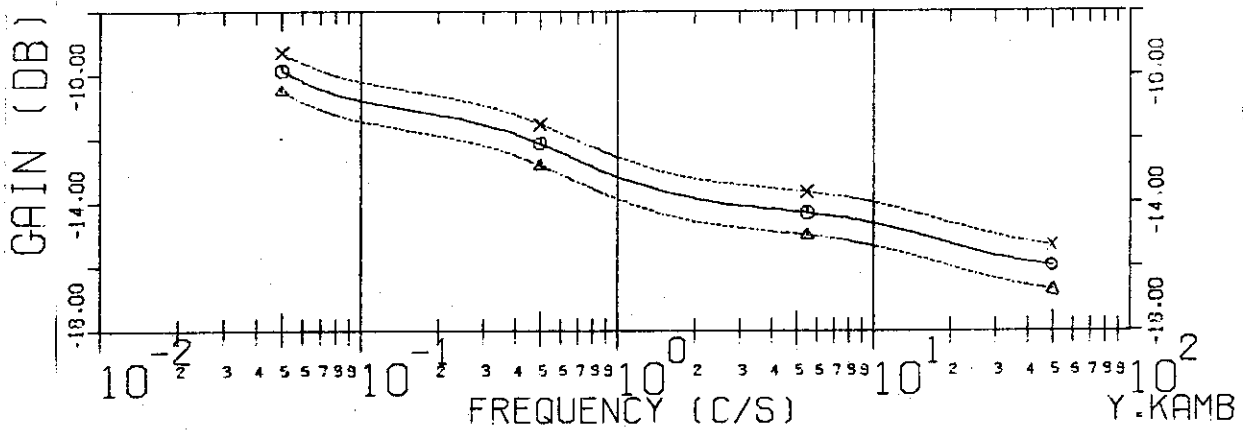


FIG. 2-5-B BODE DIAGRAM (PHASE)

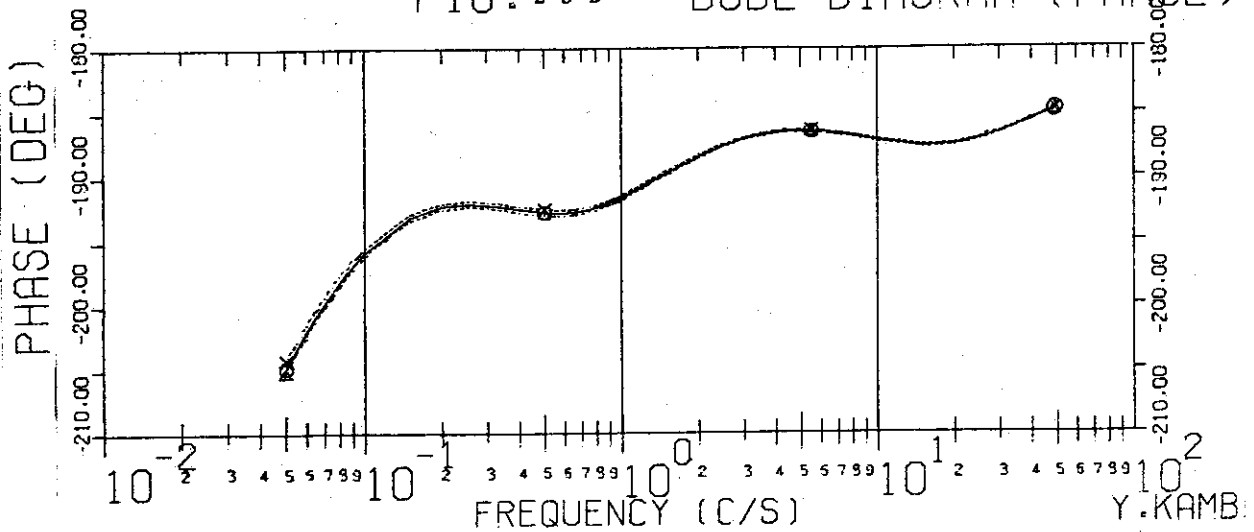


Fig.2-6  
 Frequency Characteristics  
 Disturbance ( $\delta B_d/B_{vco}$ )  
 → Plasma Position ( $\delta R/R_0$ )

$\Gamma_0 = 2.0$  ---  $\Delta$  ---  
 $2.2$  ---  $\circ$  ---  
 $2.4$  ---  $\times$  ---  
 $G = -1.0$   
 $\tau_l = 0.03$   
 $\tau_v = 0.5$   
 $\tau_t = 5.0$

FIG. 2-6-C  
 VECTOR DIAGRAM

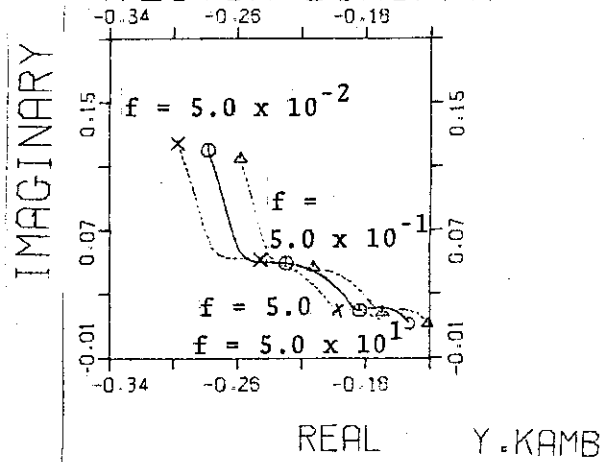


FIG. 2-6-A

BODE DIAGRAM (GAIN)

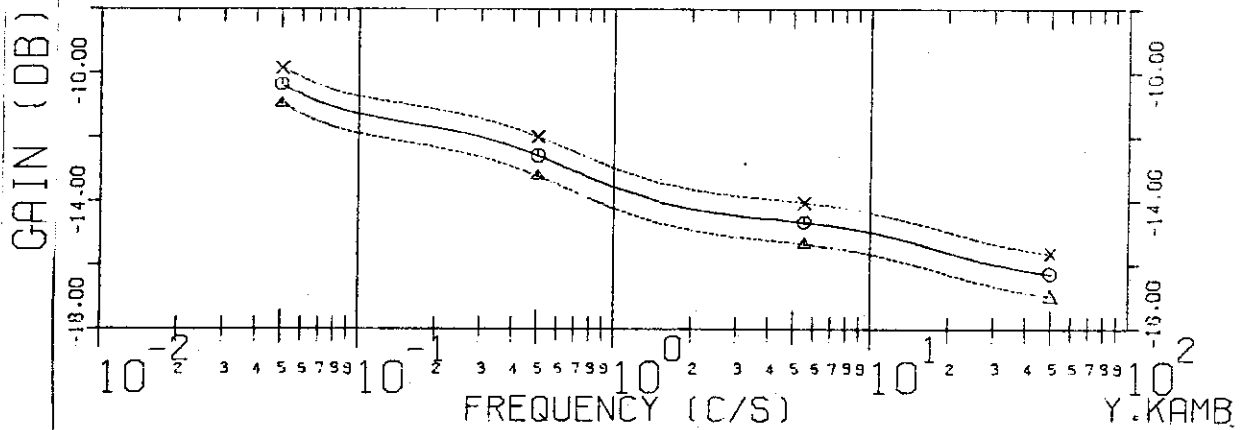


FIG. 2-6-B

BODE DIAGRAM (PHASE)

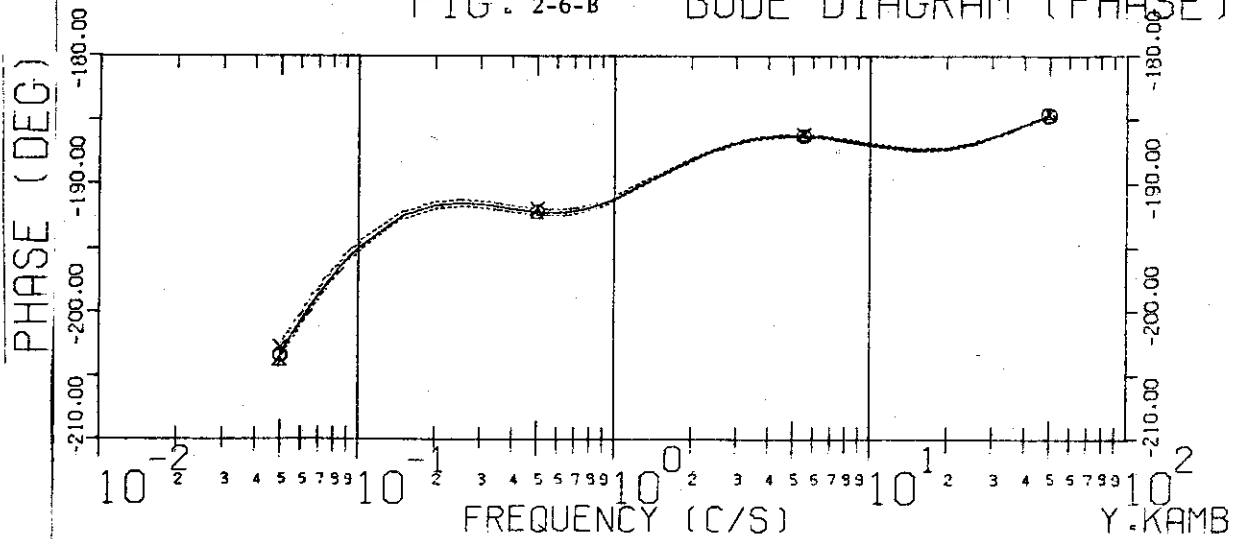


Fig. 3-1 Frequency Characteristics  
 Terminal Voltage ( $\delta V/V_0$ ) --- Plasma Position ( $\delta R/R_0$ )

$\Gamma_0 = 2.0$                        $\tau_f = 0.03$   
 $G = -0.6$  ---  $\triangle$  ---             $\tau_v = 0.5$   
           - 0.8 ---  $\circ$  ---             $\tau_t = 5.0$   
           - 1.0 --- X ---

FIG. 3-1-A BODE DIAGRAM (GAIN)

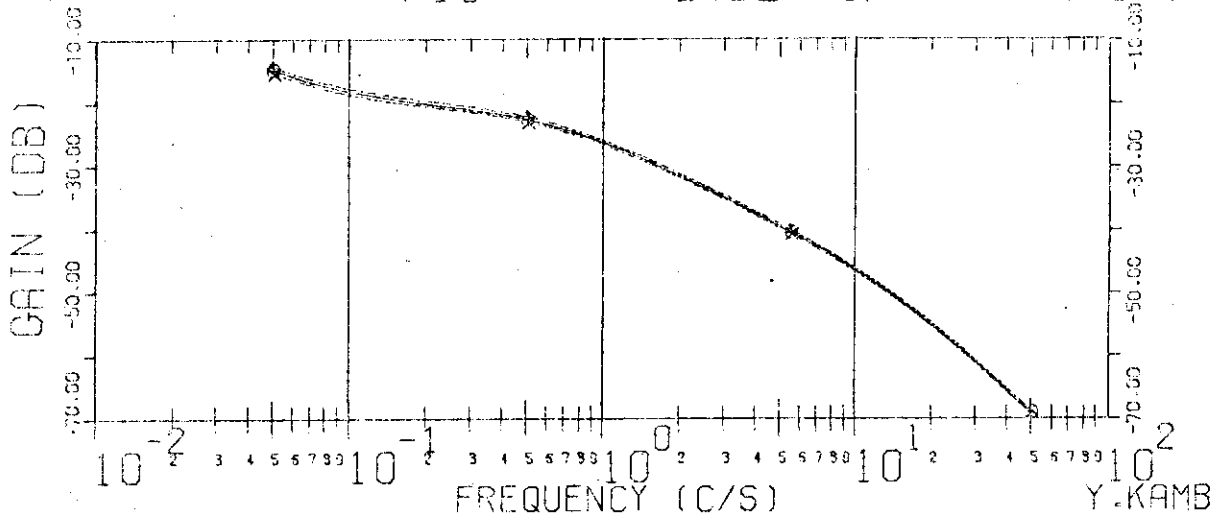


FIG. 3-1-B BODE DIAGRAM (PHASE)

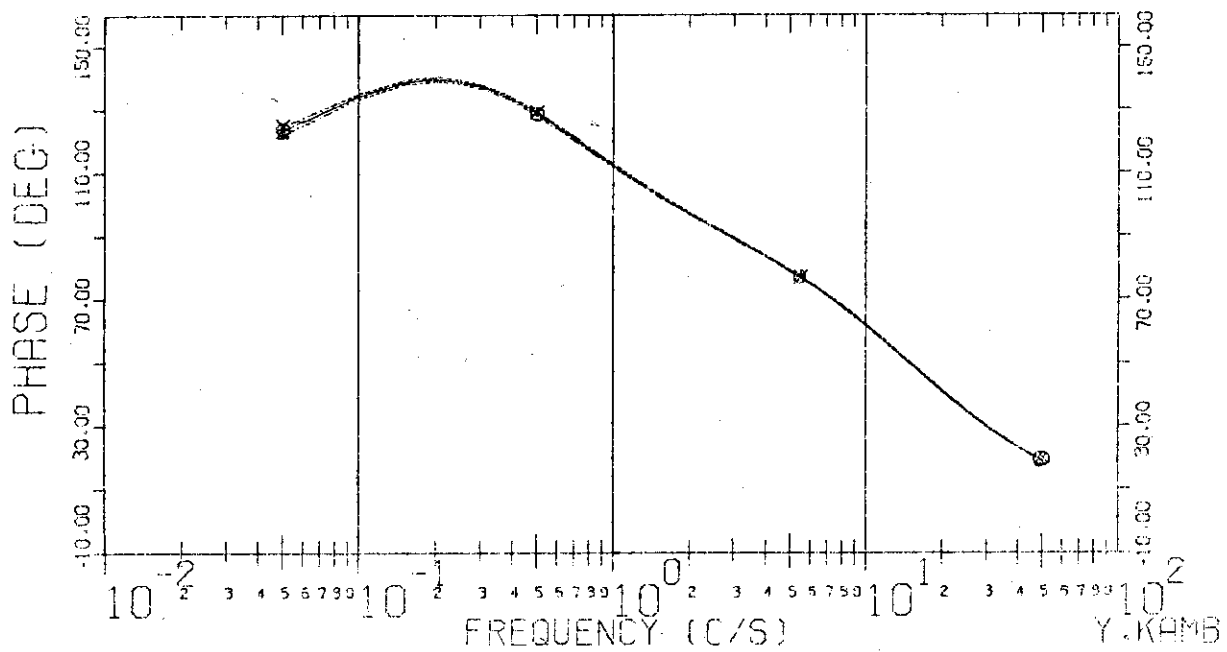


Fig.3-2 Frequency Characteristics  
Terminal Voltage ( $\delta V/V_0$ )  $\rightarrow$  Plasma Position ( $\delta R/R_0$ )

$\Gamma_0 = 2.2$		$\tau_l = 0.03$
$G = -0.6$ --- $\Delta$ ---		$\tau_v = 0.5$
- 0.8 --- $\ominus$ ---		$\tau_t = 5.0$
- 1.0 --- $\times$ ---		

FIG. 3-2-A BODE DIAGRAM (GAIN)

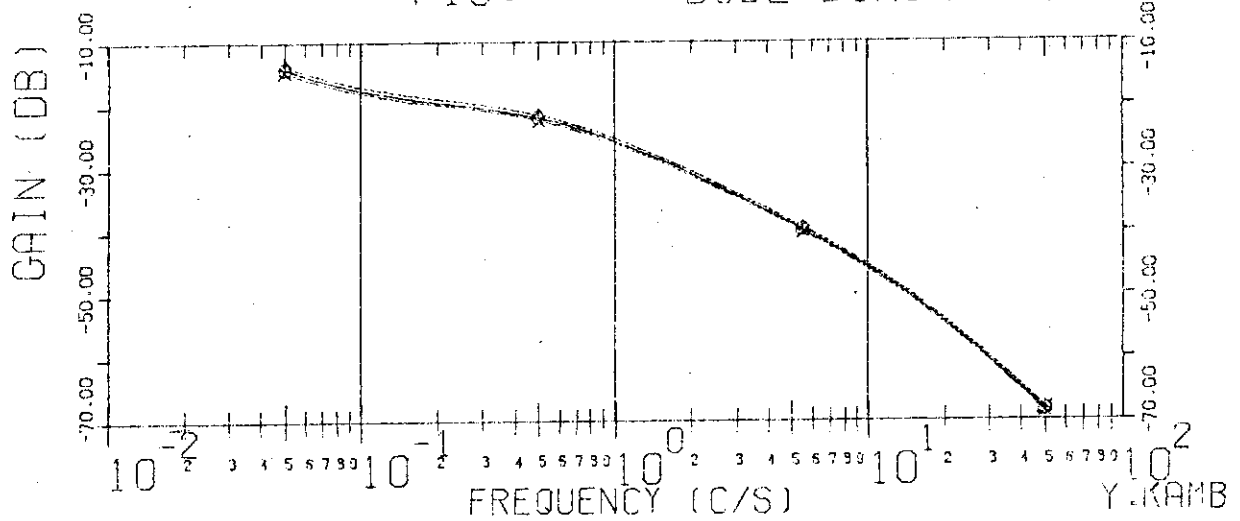
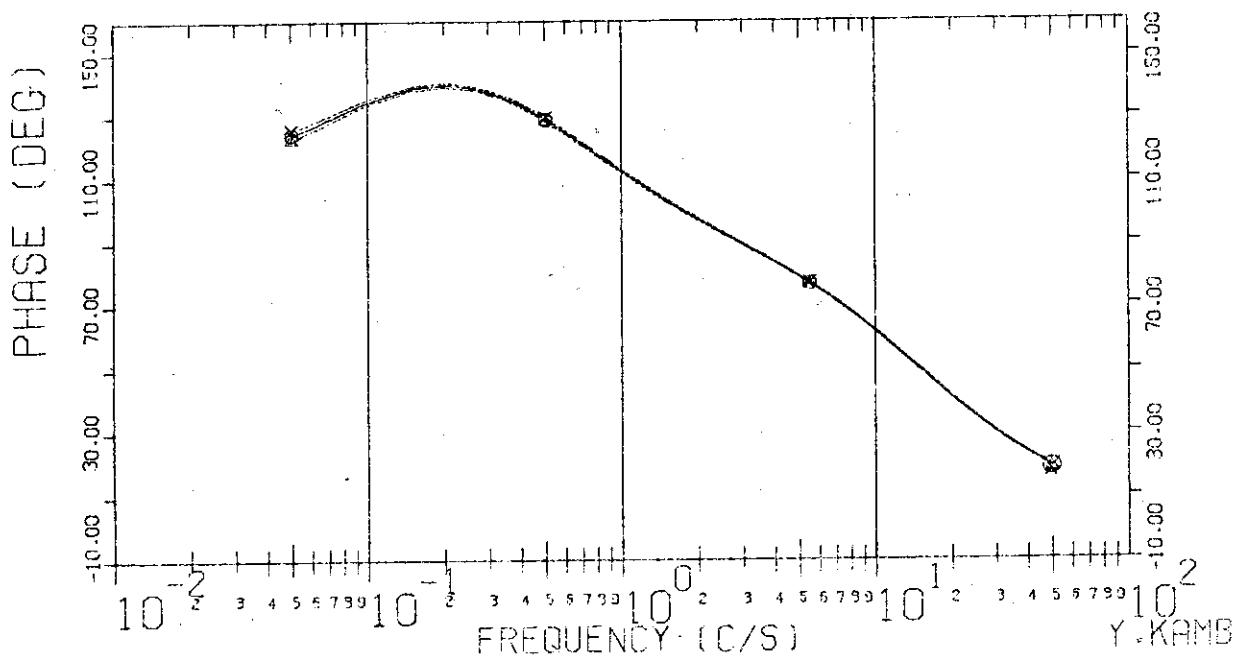


FIG. 3-2-B BODE DIAGRAM (PHASE)



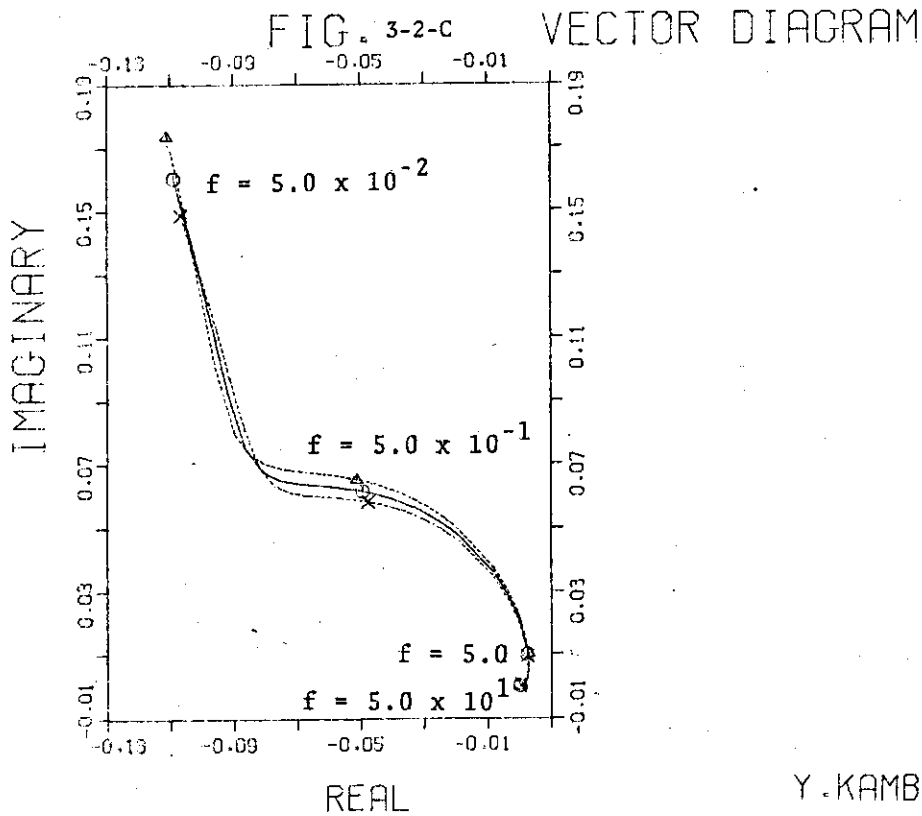
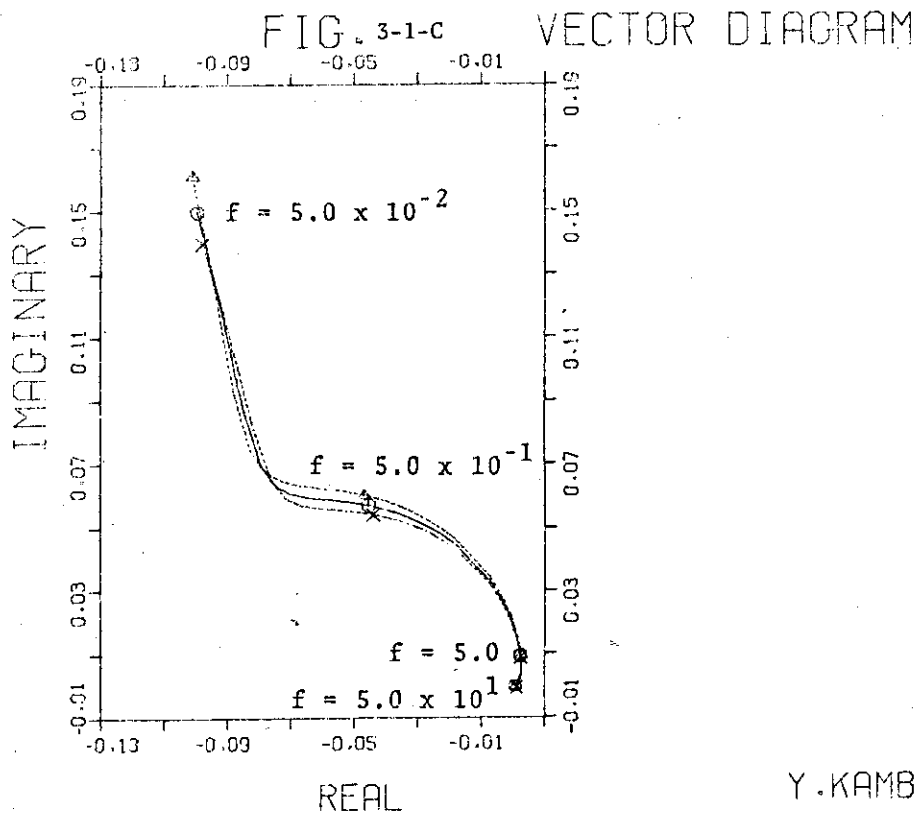


Fig.3-3 Frequency Characteristics  
 Terminal Voltage ( $\delta V/V_0$ )  $\rightarrow$  Plasma Position ( $\delta R/R_0$ )

$\Gamma_0 = 2.4$                        $\tau_c = 0.03$   
 $G = -0.6$  ---  $\Delta$  ---             $\tau_v = 0.5$   
           - 0.8 ---  $\circ$  ---             $\tau_t = 5.0$   
           - 1.0 ---  $\times$  ---

FIG. 3-3-A BODE DIAGRAM (GAIN)

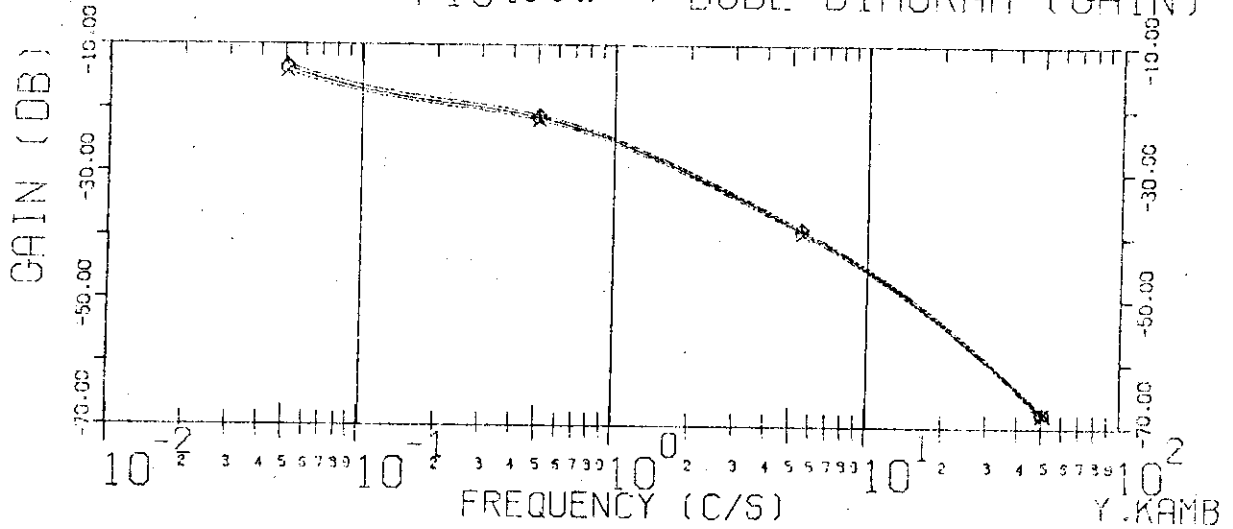


FIG. 3-3-B BODE DIAGRAM (PHASE)

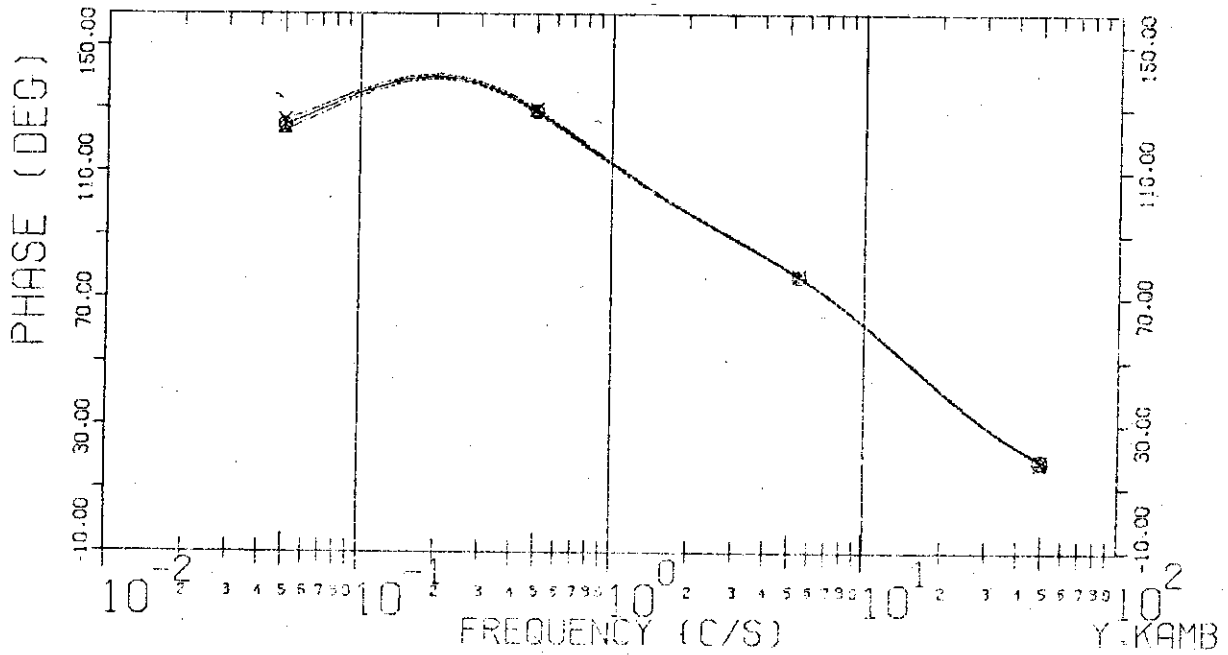


Fig. 3-4 Frequency Characteristics  
Terminal Voltage ( $\delta V/V_0$ )  $\rightarrow$  Plasma Position ( $\delta R/R_0$ )

$\Gamma_0 = 2.0$	---△---	$\tau_f = 0.03$
2.2	---○---	$\tau_V = 0.5$
2.4	---×---	$\tau_t = 5.0$
$G = -0.6$		

FIG. 3-4-A BODE DIAGRAM (GAIN)

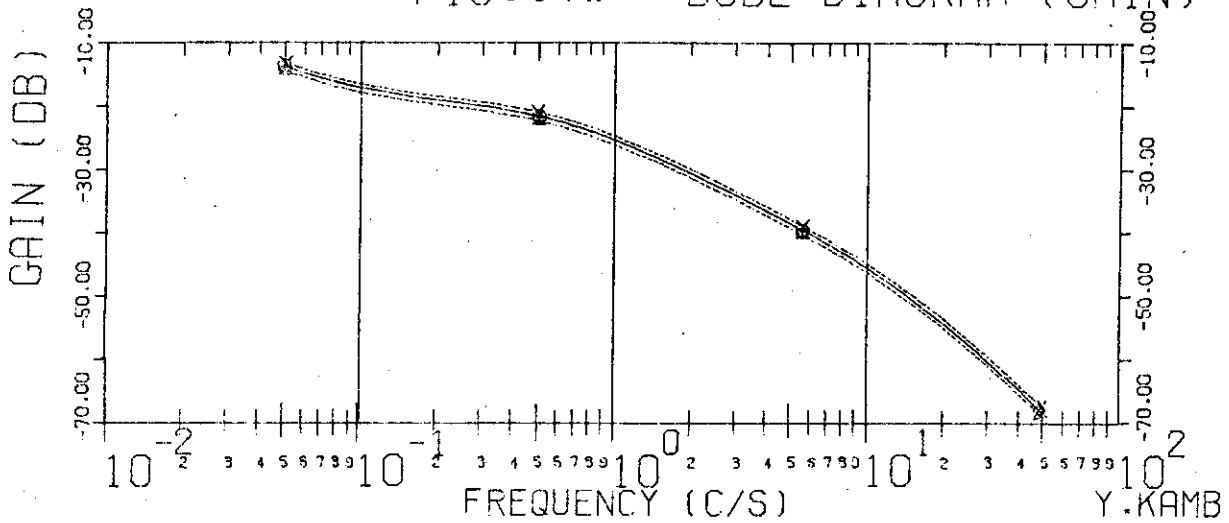
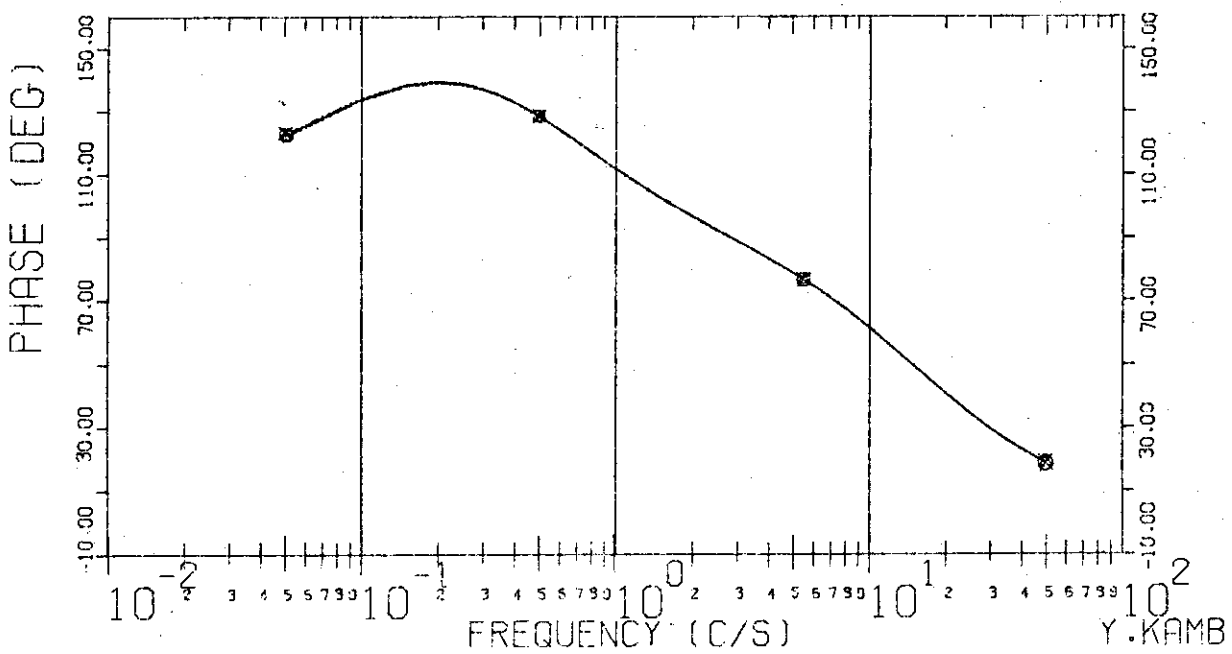


FIG. 3-4-B BODE DIAGRAM (PHASE)





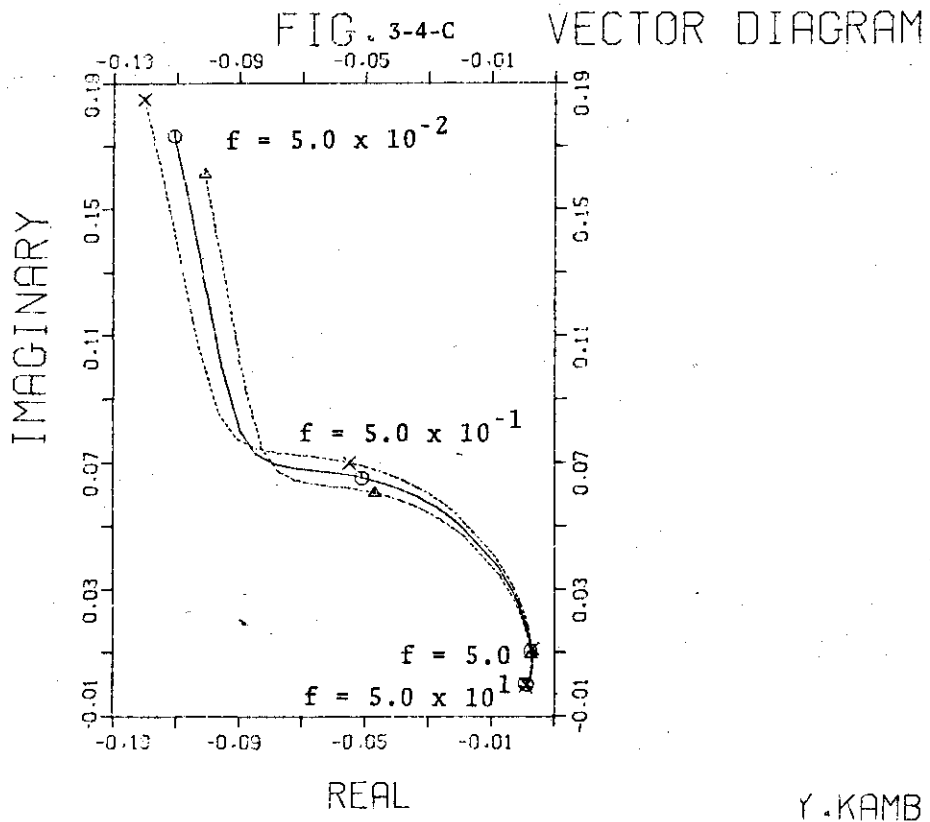
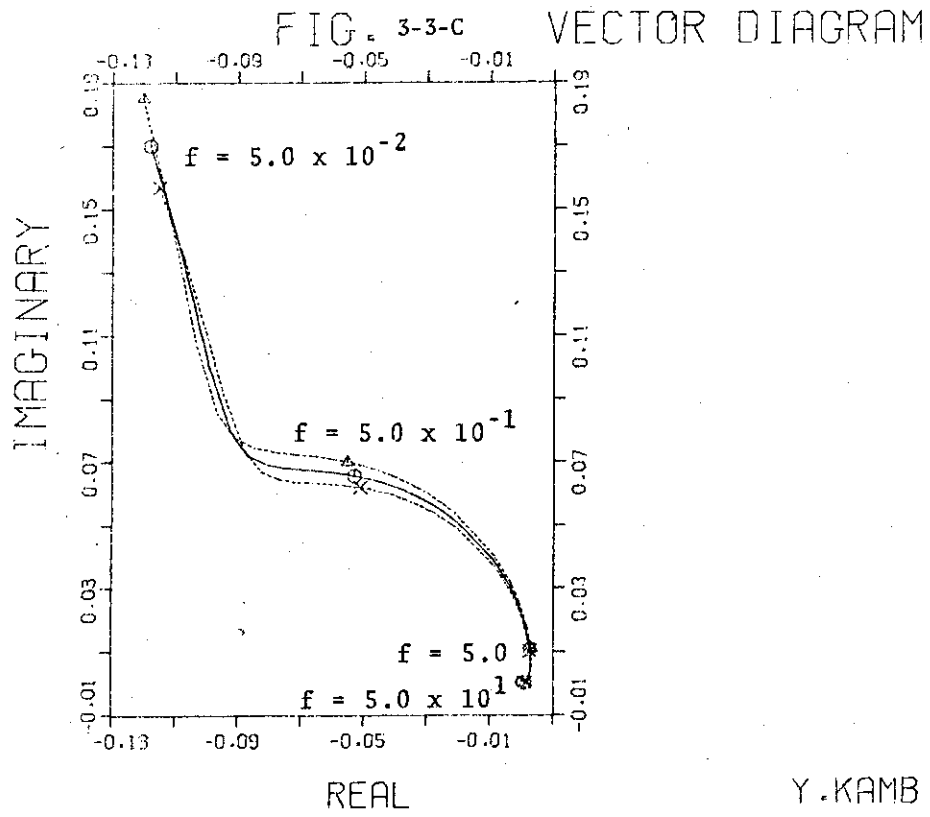


Fig. 3-5 Frequency Characteristics  
Terminal Voltage ( $\delta V/V_0$ )  $\rightarrow$  Plasma Position ( $\delta R/R_0$ )

$\Gamma_0 = 2.0$	---△---	$\tau_v = 0.03$
2.2	---○---	$\tau_v = 0.5$
2.4	---×---	$\tau_t = 5.0$
$G = -0.8$		

FIG. 3-5-A BODE DIAGRAM (GAIN)

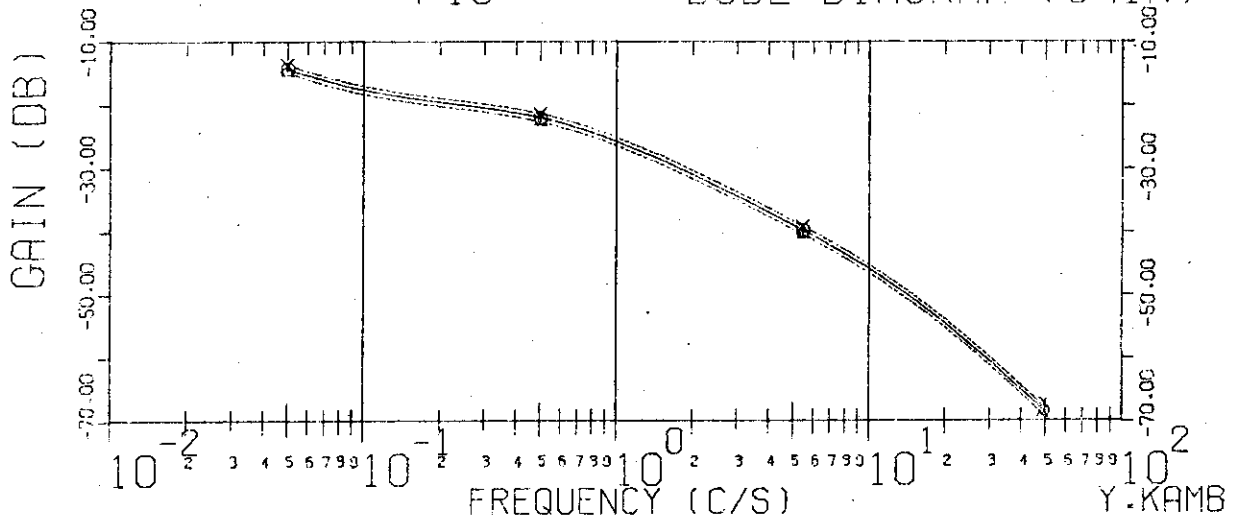


FIG. 3-5-B BODE DIAGRAM (PHASE)

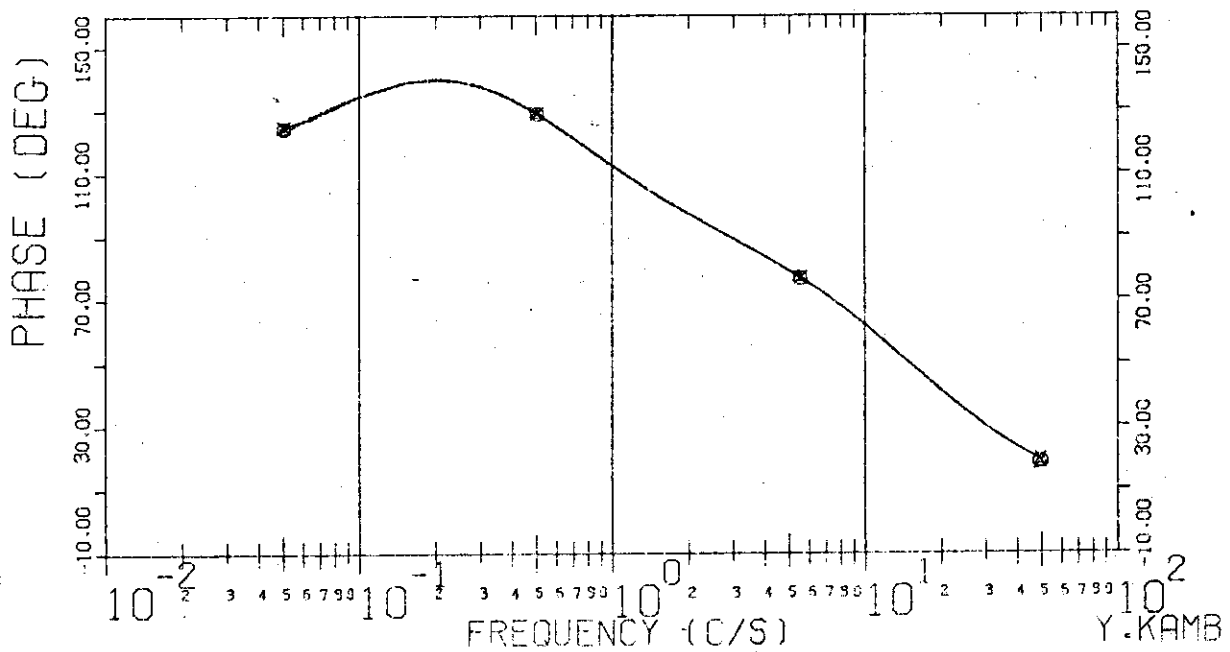


Fig. 3-6 Frequency Characteristics  
 Terminal Voltage ( $\delta V/V_0$ )  $\rightarrow$  Plasma Position ( $\delta R/R_0$ )

$\Gamma_0 = 2.0$	---△---	$\tau_x = 0.03$
2.2	---○---	$\tau_y = 0.5$
2.4	---×---	$\tau_t = 5.0$
$G = -1.0$		

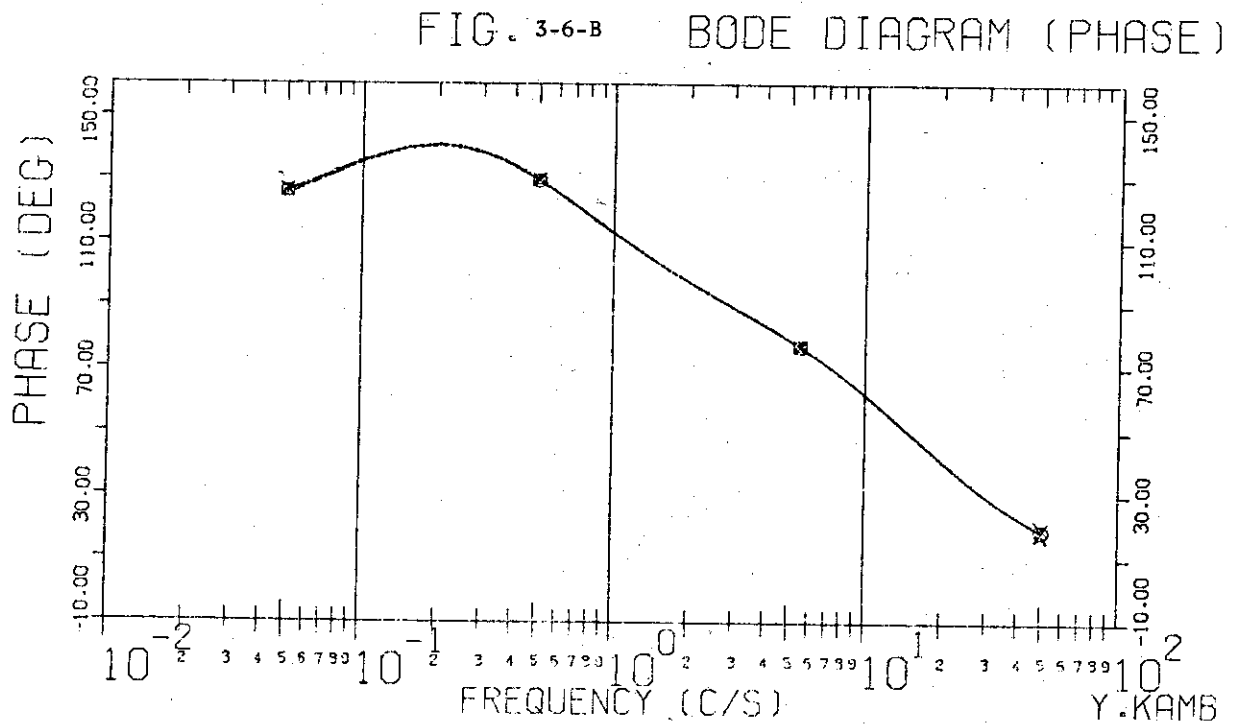
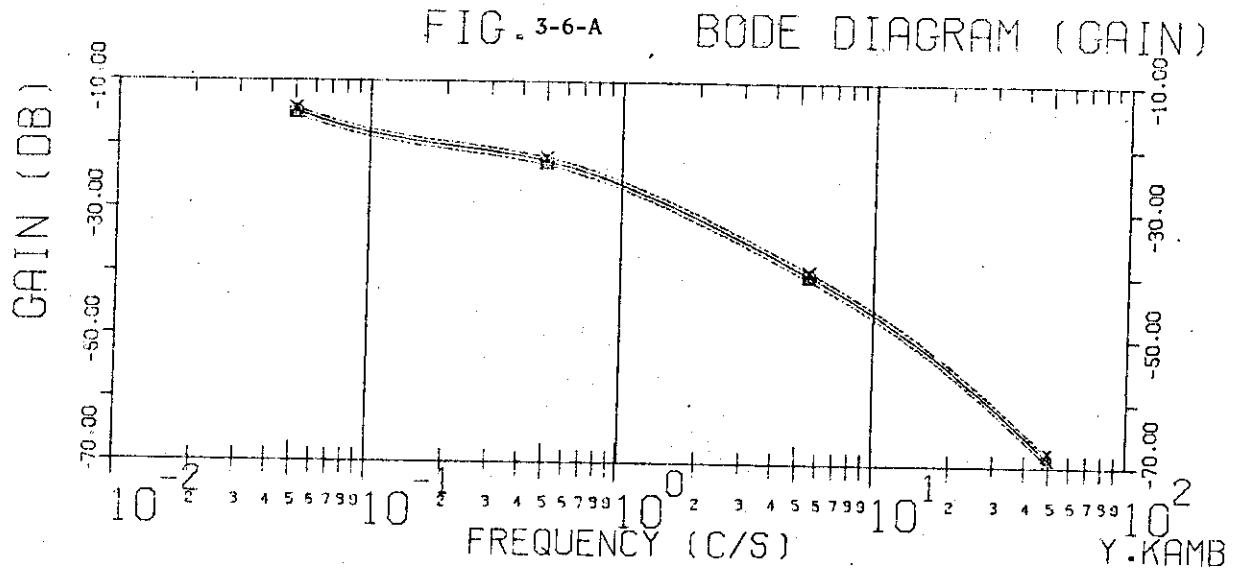
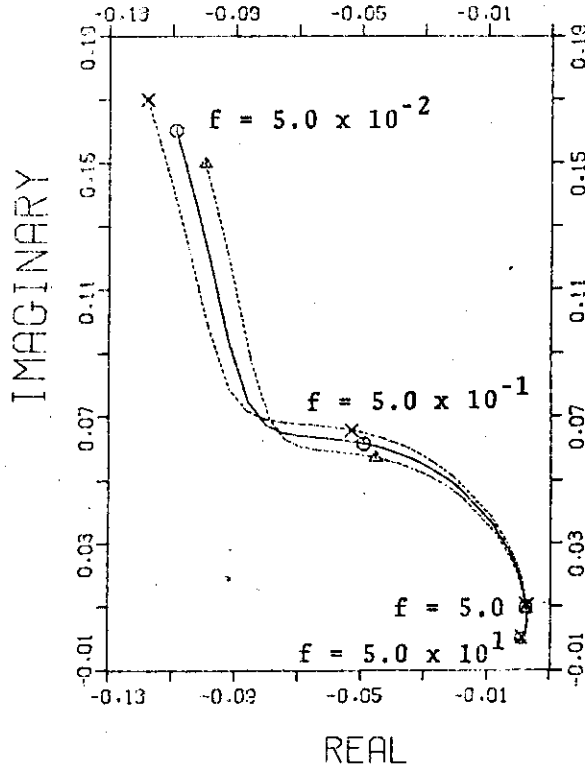
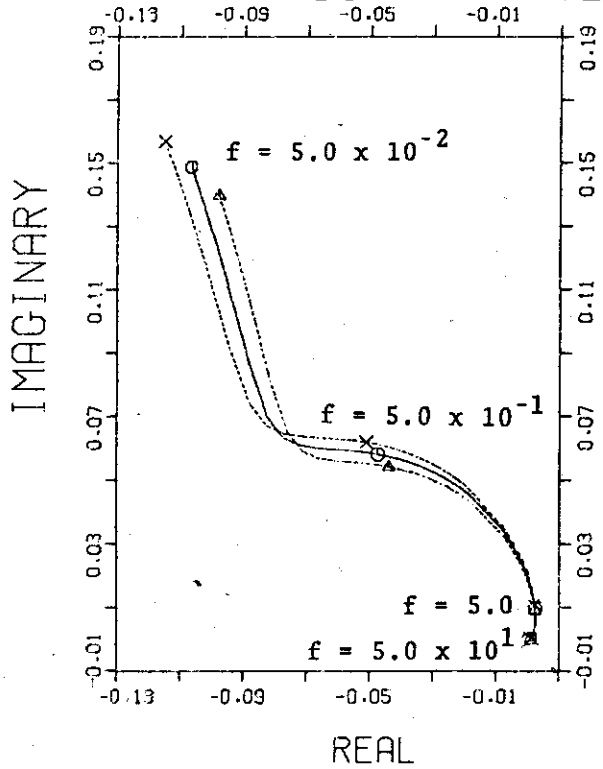


FIG. 3-5-C VECTOR DIAGRAM



Y. KAMB

FIG. 3-6-C VECTOR DIAGRAM



Y. KAMB

Fig. 4-1  
Frequency Characteristics  
Disturbance ( $\delta B_d/B_{vco}$ )  
—→ Plasma Position ( $\delta R/R_0$ )

$\Gamma_0 = 2.2$   
 $G = -0.8$   
 $\tau_L = 0.03$   
 $\tau_V = 1.0$   
 $\tau_t = 10.0$  ---  $\Delta$  ---  
 $5.0$  ---  $\circ$  ---  
 $2.0$  ---  $\times$  ---

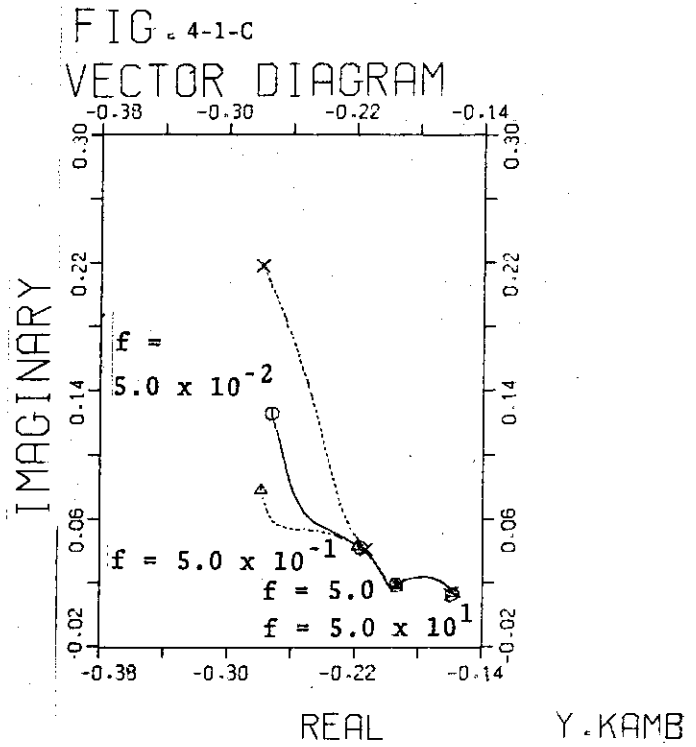


FIG. 4-1-A BODE DIAGRAM (GAIN)

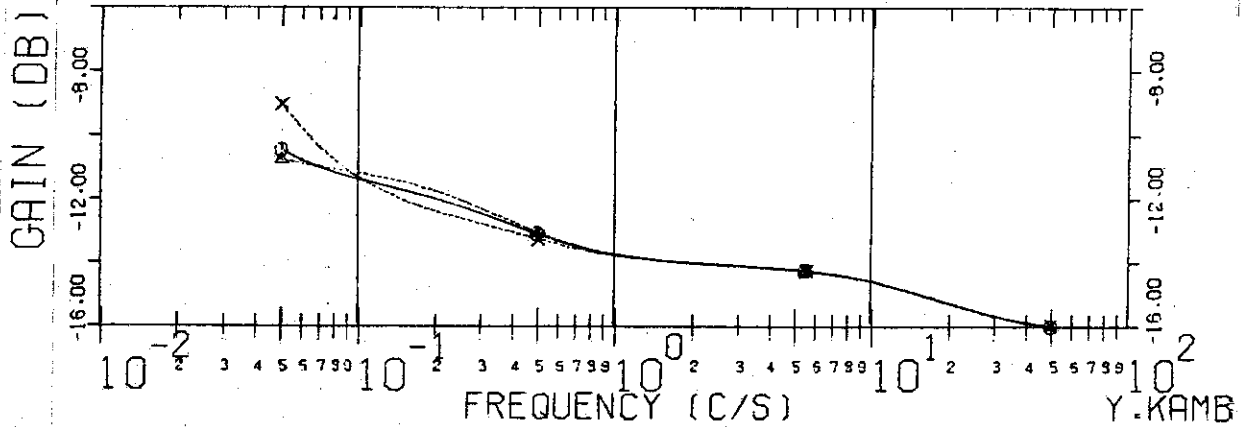


FIG. 4-1-B BODE DIAGRAM (PHASE)

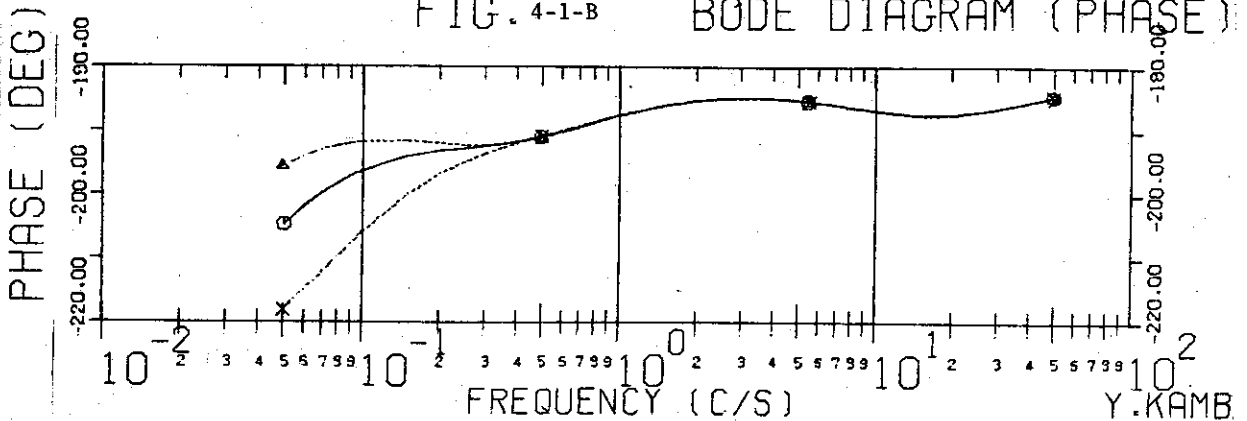


Fig. 4-2  
 Frequency Characteristics  
 Disturbance ( $\delta B_d/B_{vco}$ )  
 → Plasma Position ( $\delta R/R_0$ )

$\Gamma_0 = 2.2$   
 $G = -0.8$   
 $\tau_{xv} = 0.03$   
 $\tau_{v} = 0.5$   
 $\tau_t = 10.0$  —  $\Delta$  — —  
           5.0 —  $\circ$  — —  
           2.0 —  $\times$  — —

FIG. 4-2-C  
 VECTOR DIAGRAM

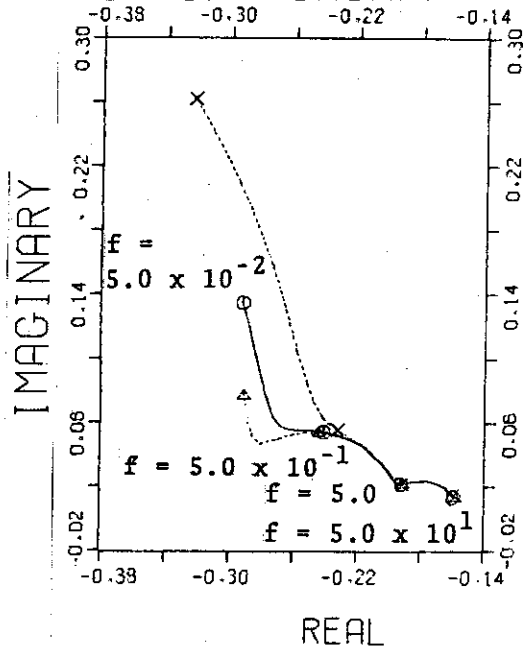


FIG. 4-2-A BODE DIAGRAM (GAIN)

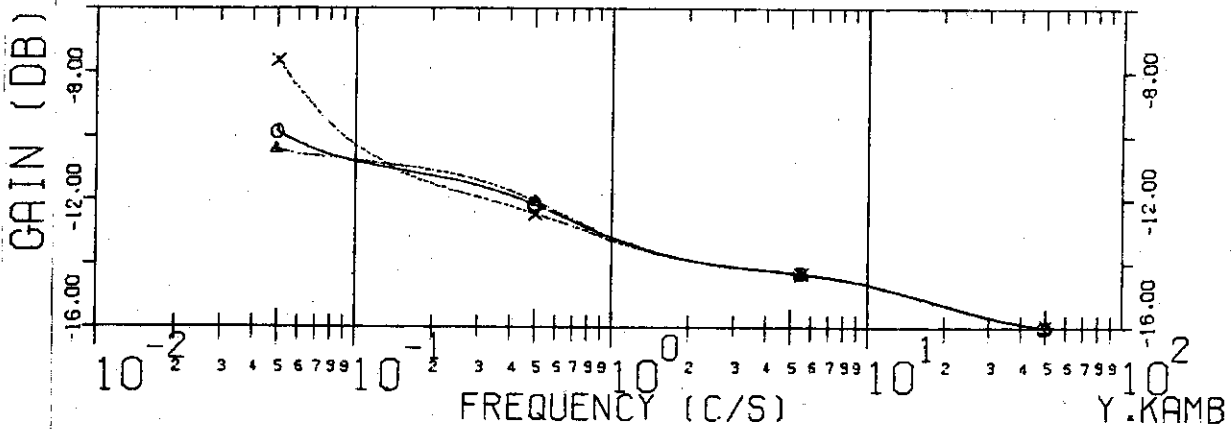


FIG. 4-2-B BODE DIAGRAM (PHASE)

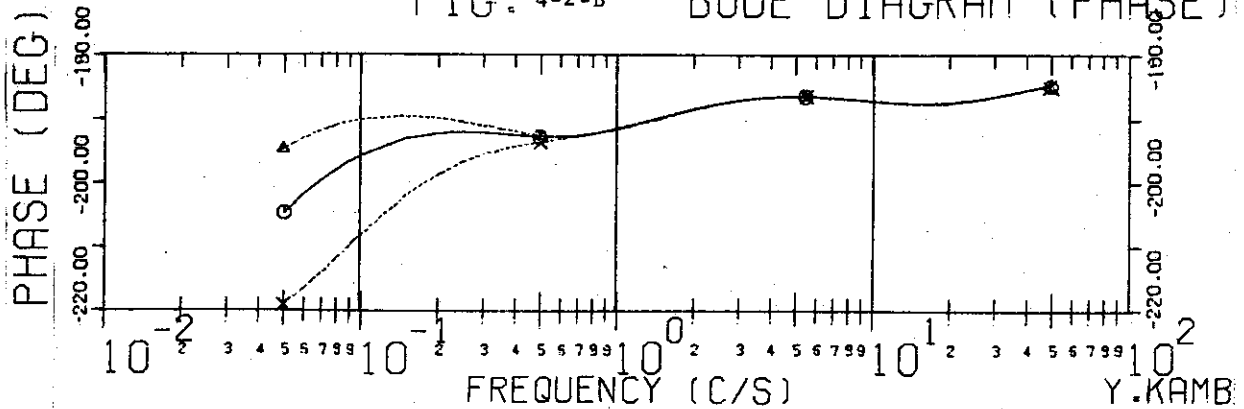


Fig. 4-3  
 Frequency Characteristics  
 Disturbance ( $\delta B_d/B_{vco}$ )  
 → Plasma Position ( $\delta R/R_0$ )

$\Gamma_0 = 2.2$   
 $G = -0.8$   
 $\tau_l = 0.03$   
 $\tau_v = 0.2$   
 $\tau_t = 10.0$  ---△---  
           5.0    —○—  
           2.0    ---×---

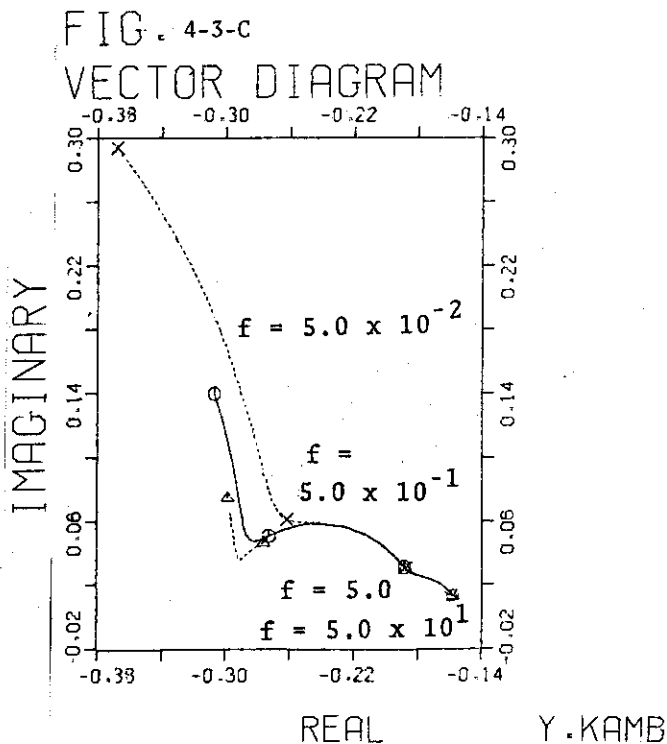


FIG. 4-3-A BODE DIAGRAM (GAIN)

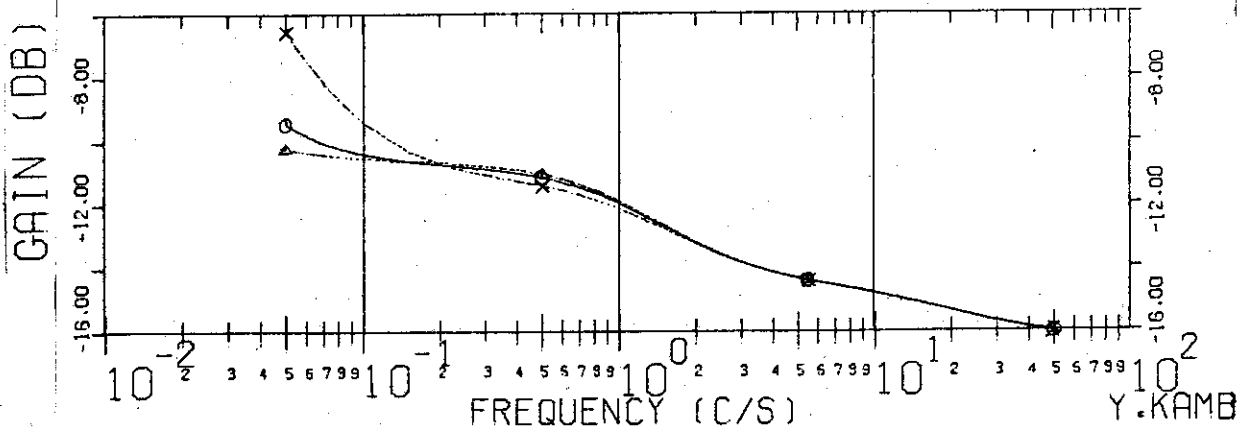


FIG. 4-3-B BODE DIAGRAM (PHASE)

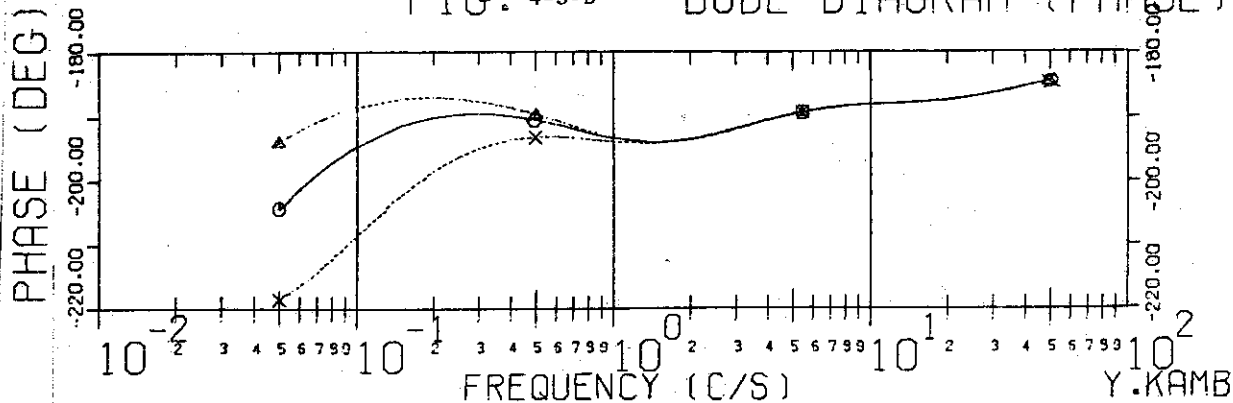


Fig. 4-4  
 Frequency Characteristics  
 Disturbance ( $\delta B_d/B_{vco}$ )  
 → Plasma Position ( $\delta R/R_0$ )

$\Gamma_0 = 2.2$   
 $G = -0.8$   
 $\tau_l = 0.02$   
 $\tau_v = 1.0$   
 $\tau_t = 10.0$  ---  $\Delta$  ---  
           5.0    ---  $\circ$  ---  
           2.0    ---  $\times$  ---

FIG. 4-4-C  
 VECTOR DIAGRAM

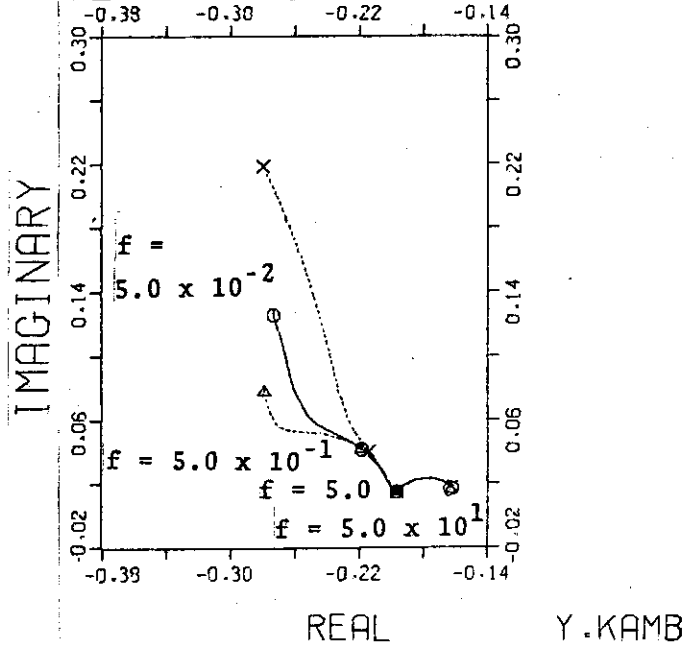


FIG. 4-4-A BODE DIAGRAM (GAIN)

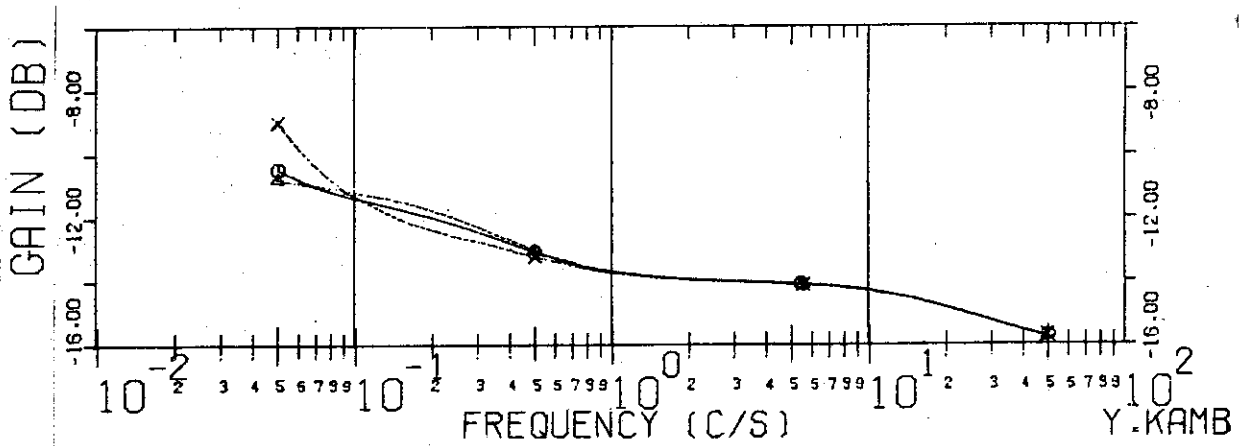


FIG. 4-4-B BODE DIAGRAM (PHASE)

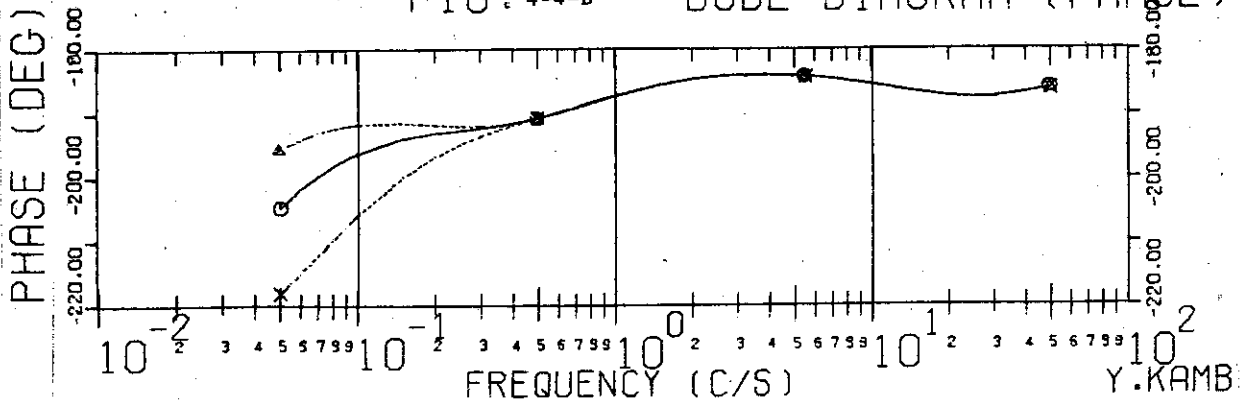




Fig. 4-5  
 Frequency Characteristics  
 Disturbance ( $\delta B_d/B_{vco}$ )  
 $\rightarrow$  Plasma Position ( $\delta R/R_0$ )

$\Gamma_0 = 2.2$   
 $G = -0.8$   
 $\tau_f = 0.02$   
 $\tau_v = 0.5$   
 $\tau_t = 10.0$  ---  $\Delta$  ---  
           5.0 ---  $\circ$  ---  
           2.0 ---  $\times$  ---

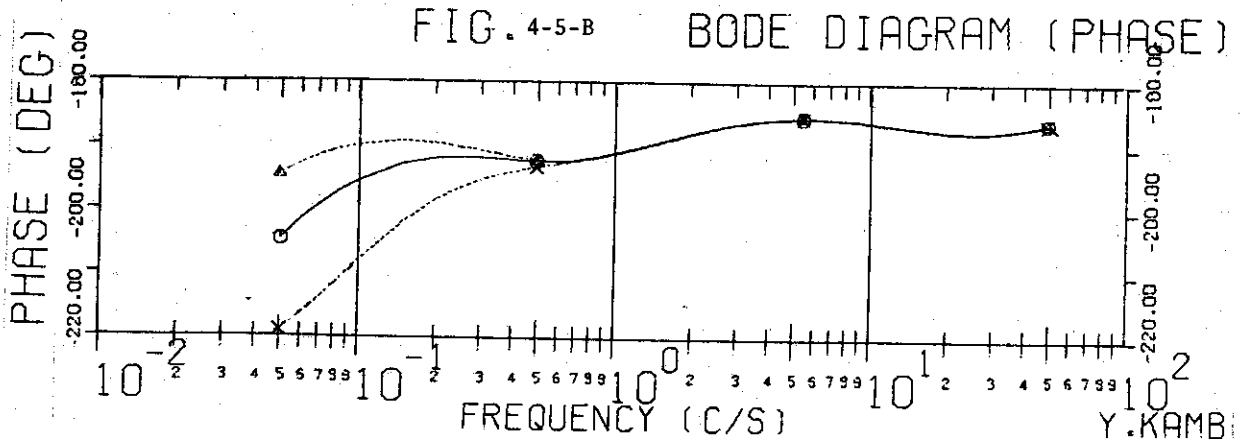
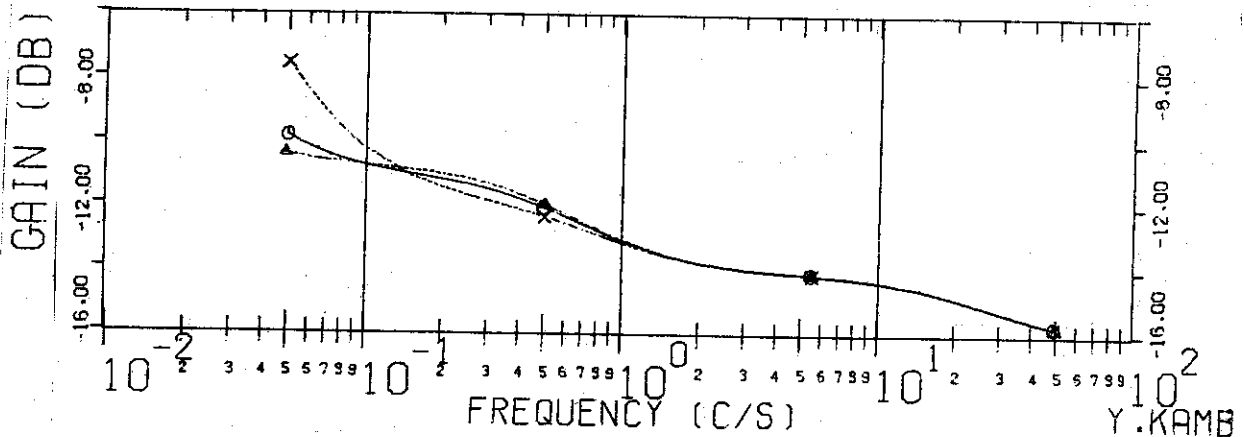
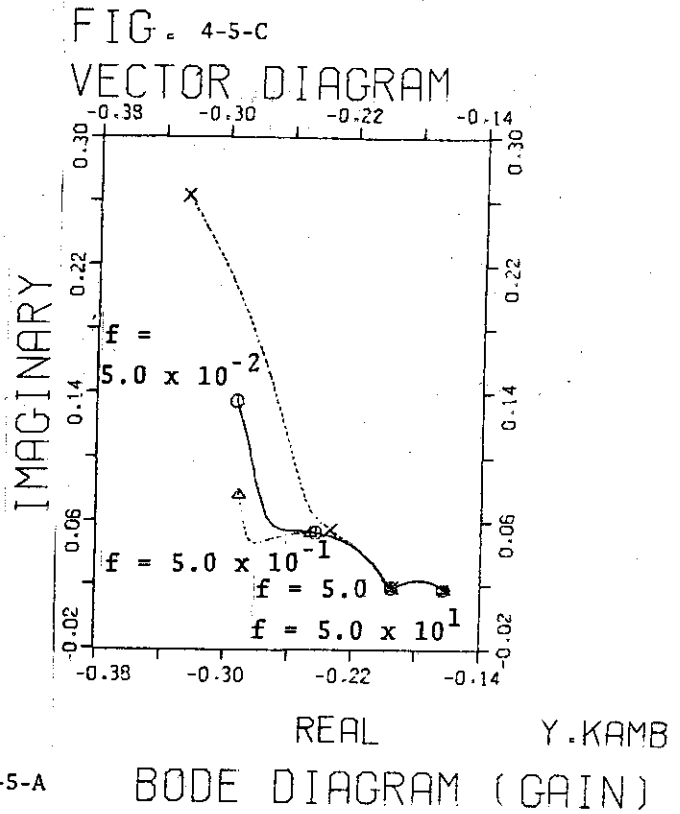


Fig. 4-6  
 Frequency Characteristics  
 Disturbance ( $\delta B_d/B_{vco}$ )  
 $\rightarrow$  Plasma Position ( $\delta R/R_0$ )

$\Gamma_0 = 2.2$   
 $G = -0.8$   
 $\tau_f = 0.02$   
 $\tau_v = 0.2$   
 $\tau_t = 10.0$  ---  $\Delta$  ---  
           5.0   ---  $\circ$  ---  
           2.0   ---  $\times$  ---

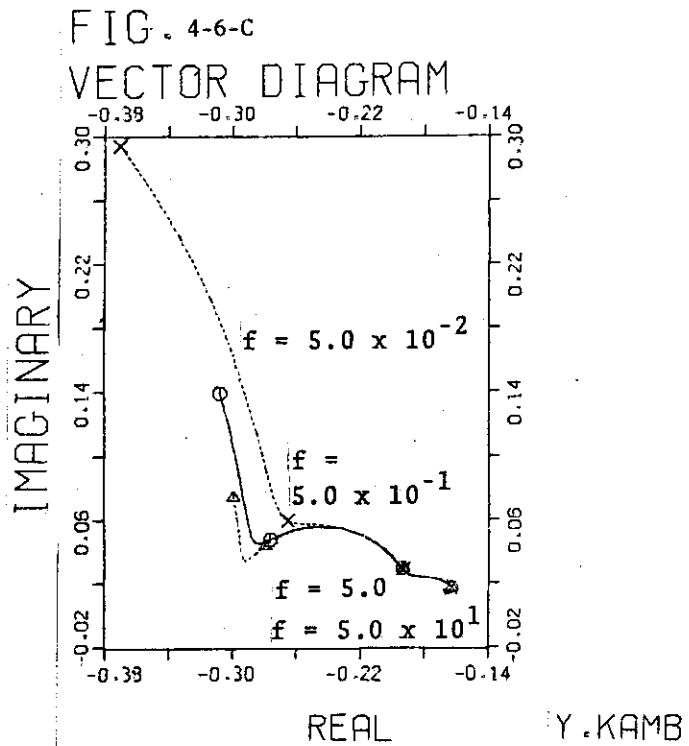


FIG. 4-6-A BODE DIAGRAM (GAIN)

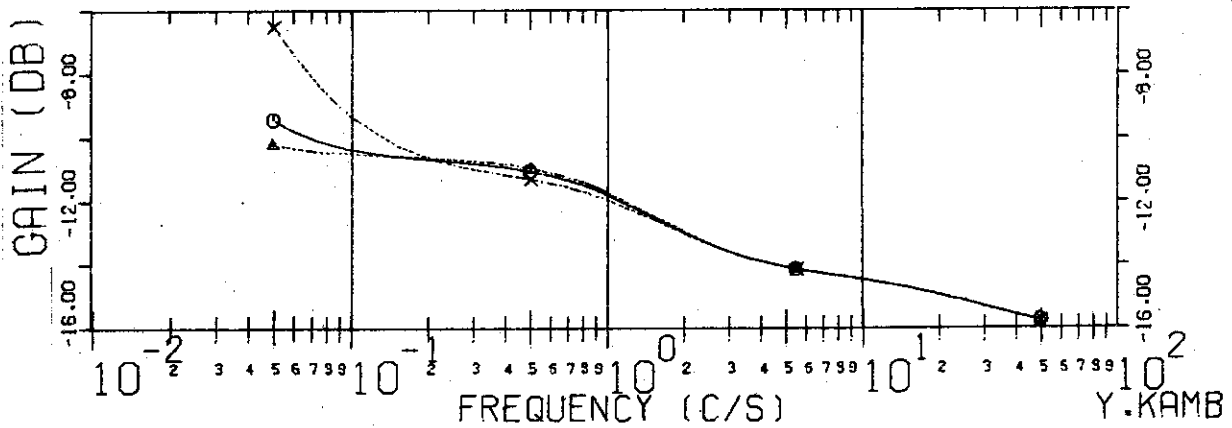


FIG. 4-6-B BODE DIAGRAM (PHASE)

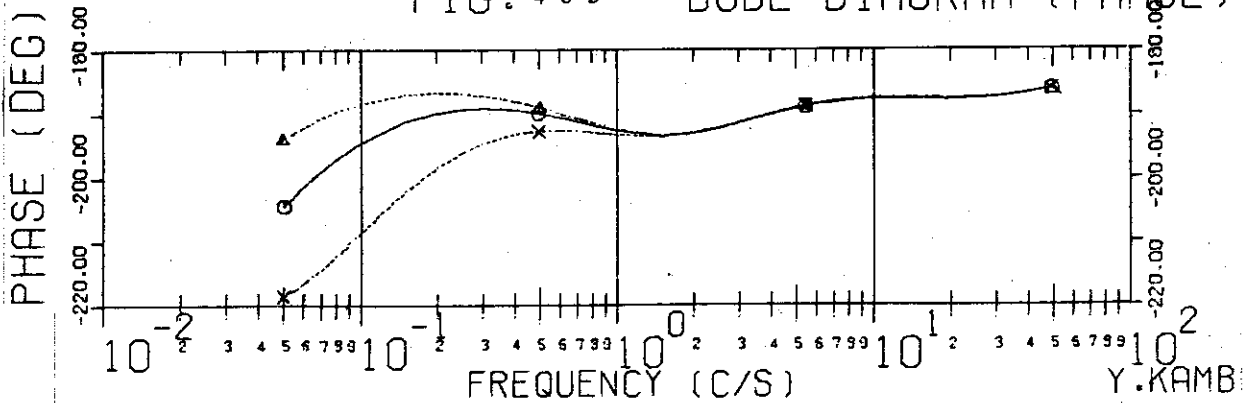


Fig. 4-7  
 Frequency Characteristics  
 Disturbance ( $\delta B_d/B_{vco}$ )  
 → Plasma Position ( $\delta R/R_0$ )

$\Gamma_0 = 2.2$   
 $G = -0.8$   
 $\tau_l = 0.01$   
 $\tau_v = 1.0$   
 $\tau_t = 10.0$  ---  $\Delta$  ---  
           5.0   ---  $\circ$  ---  
           2.0   ---  $\times$  ---

FIG. 4-7-C  
 VECTOR DIAGRAM

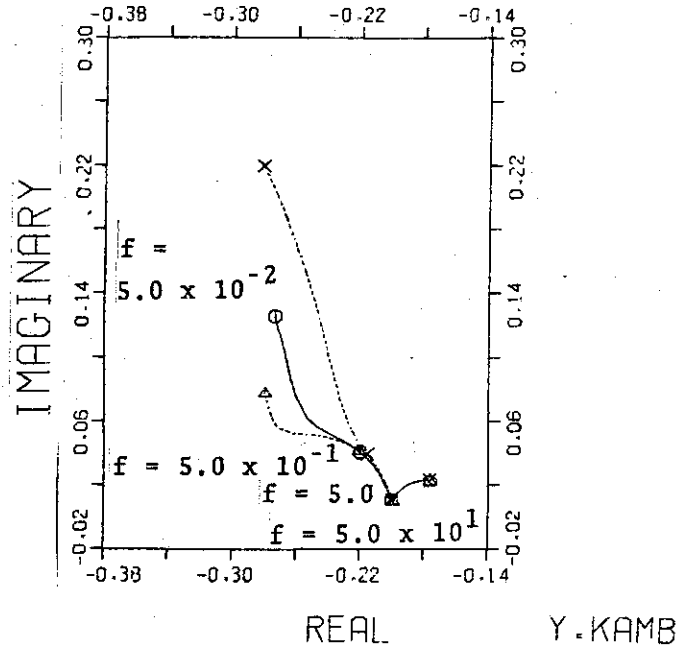


FIG. 4-7-A

BODE DIAGRAM (GAIN)

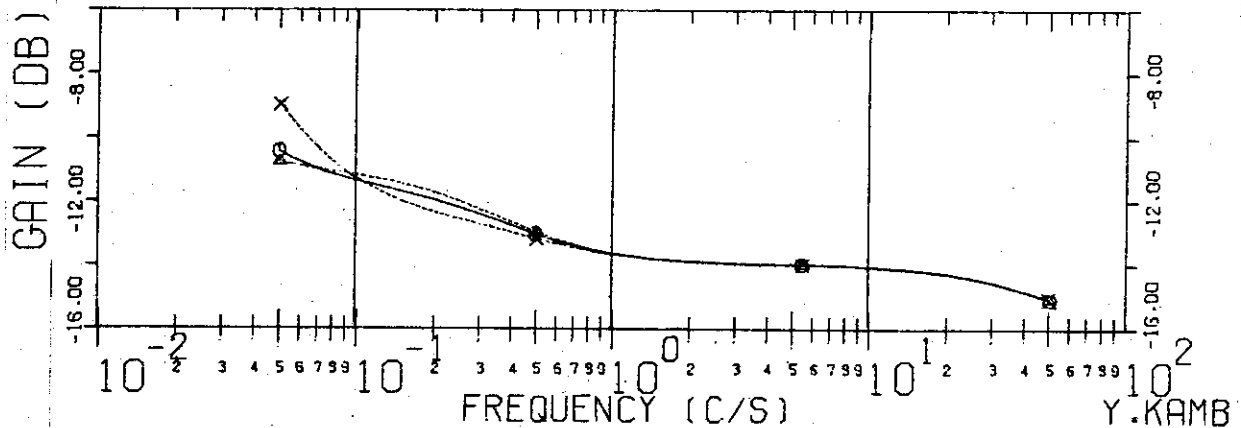


FIG. 4-7-B

BODE DIAGRAM (PHASE)

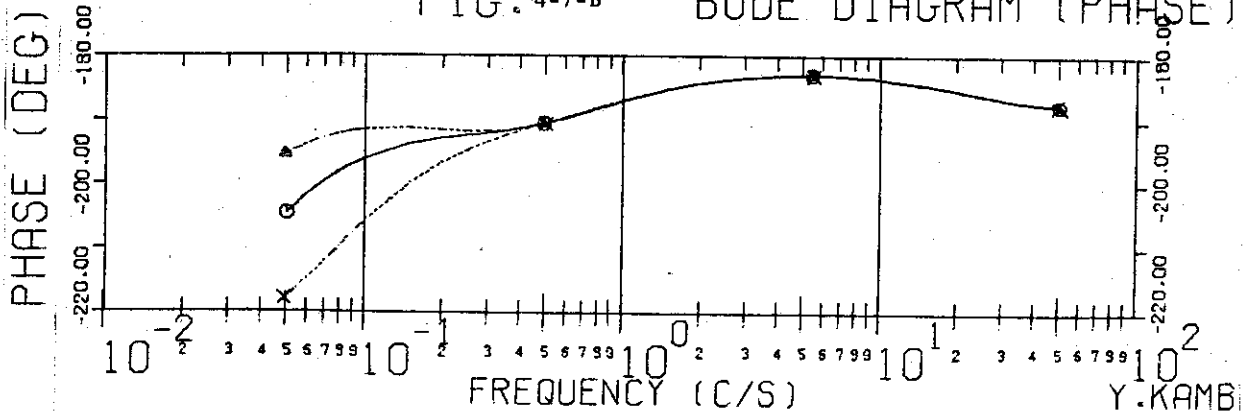


Fig. 4-8  
 Frequency Characteristics  
 Disturbance ( $\delta B_d/B_{vco}$ )  
 → Plasma Position ( $\delta R/R_0$ )

$\tau_0 = 2.2$   
 $G = -0.8$   
 $\tau_x = 0.01$   
 $\tau_y = 0.5$   
 $\tau_t = 10.0$  ---  $\Delta$  ---  
           5.0   —  $\circ$  —  
           2.0   —  $\times$  —

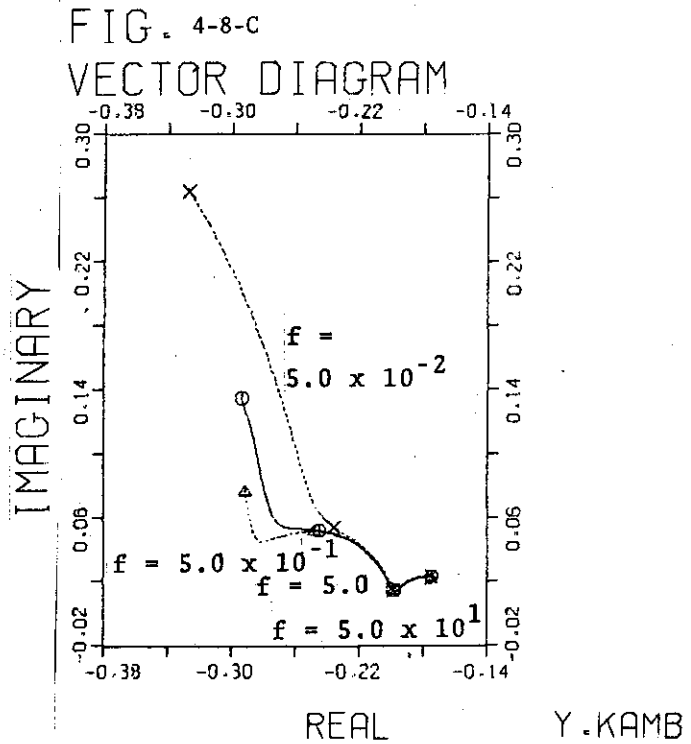


FIG. 4-8-A BODE DIAGRAM (GAIN)

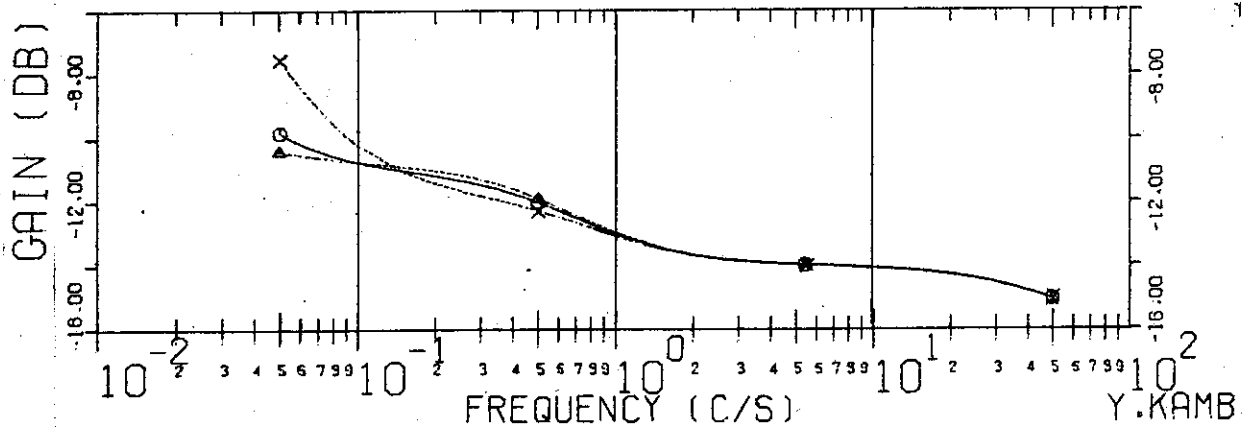


FIG. 4-8-B BODE DIAGRAM (PHASE)

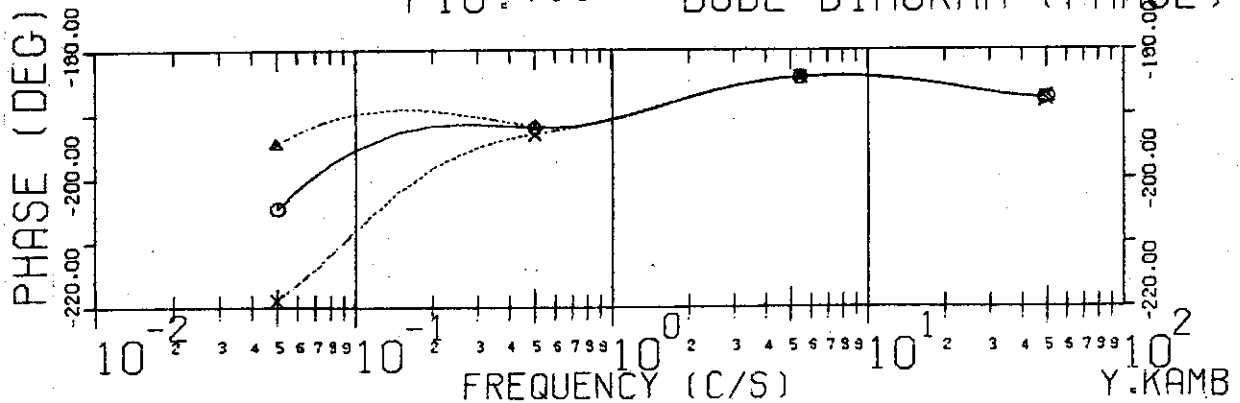


Fig. 4-9  
 Frequency Characteristics  
 Disturbance ( $\delta B_d/B_{vco}$ )  
 → Plasma Position ( $\delta R/R_0$ )

$\Gamma_0 = 2.2$   
 $G = -0.8$   
 $\tau_L = 0.01$   
 $\tau_V = 0.2$   
 $\tau_t = 10.0$  ---  $\Delta$  ---  
           5.0 ---  $\circ$  ---  
           2.0 ---  $\times$  ---

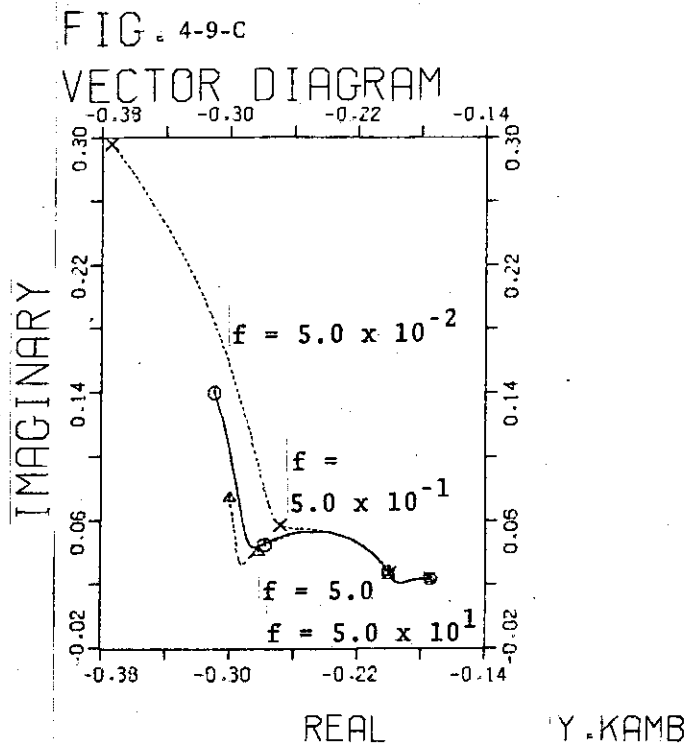


FIG. 4-9-A BODE DIAGRAM (GAIN)

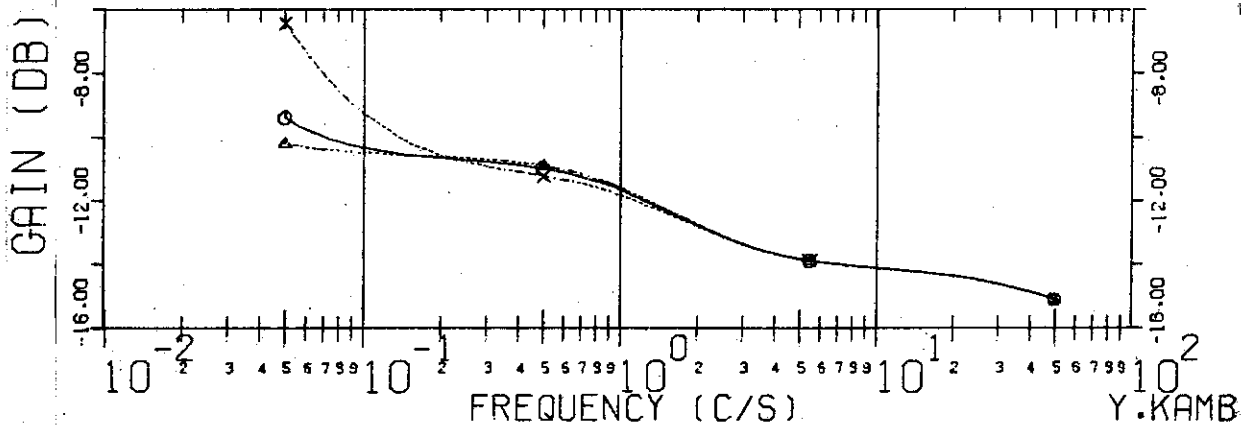


FIG. 4-9-B BODE DIAGRAM (PHASE)

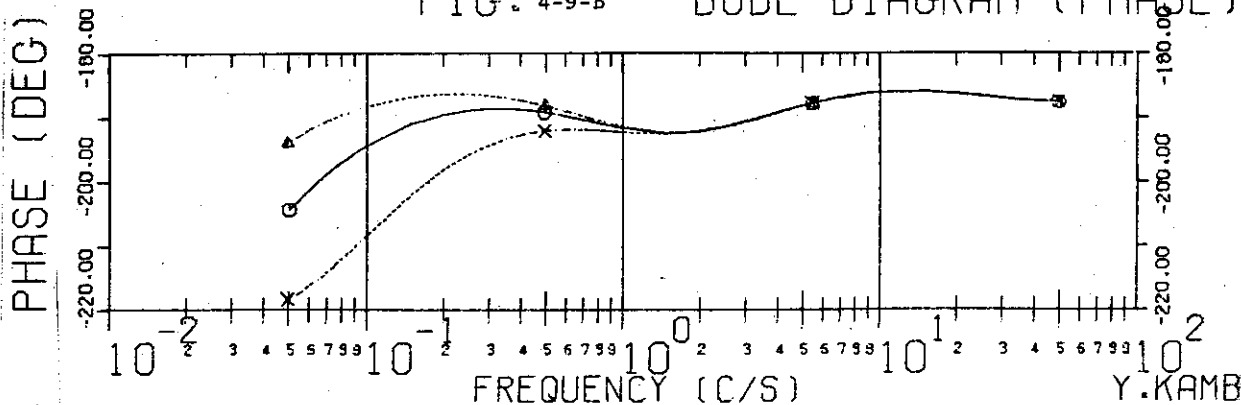


Fig. 4-10  
 Frequency Characteristics  
 Disturbance ( $\delta B_d/B_{vco}$ )  
 $\rightarrow$  Plasma Position ( $\delta R/R_0$ )

$\Gamma_0 = 2.2$   
 $G = -0.8$   
 $\tau_l = 0.03$   
 $\tau_v = 1.0$  ---  $\Delta$  ---  
           0.5 ---  $\circ$  ---  
           0.2 ---  $\times$  ---  
 $\tau_t = 10.0$

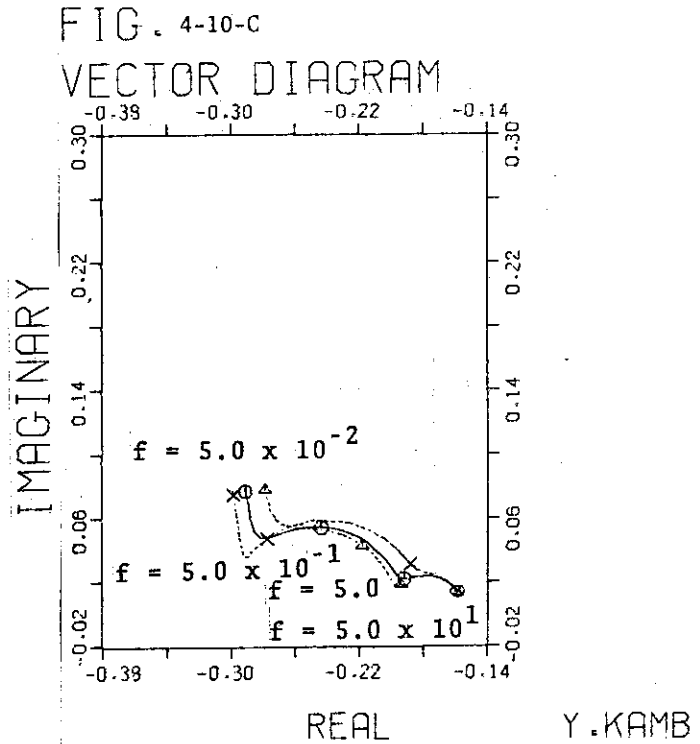


FIG. 4-10-A BODE DIAGRAM (GAIN)

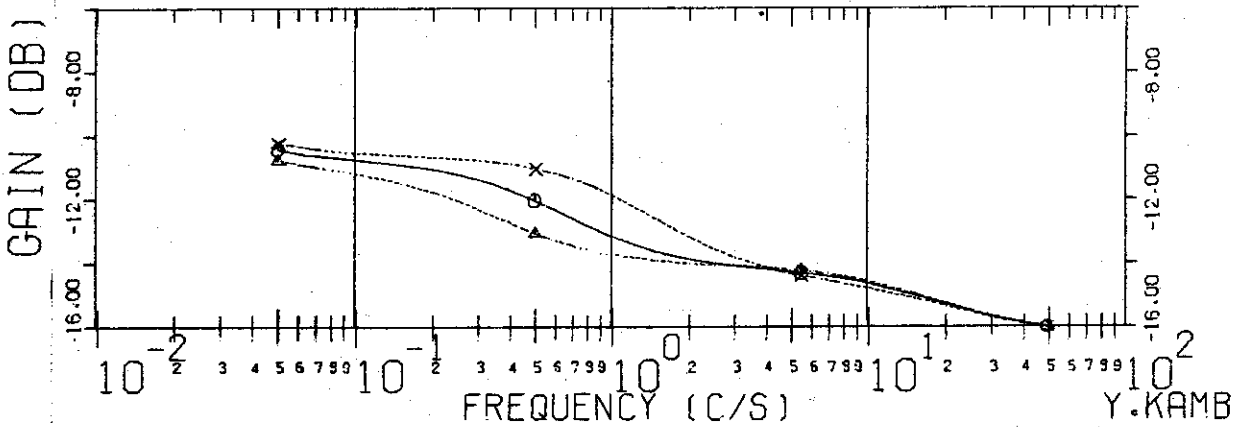


FIG. 4-10-B BODE DIAGRAM (PHASE)

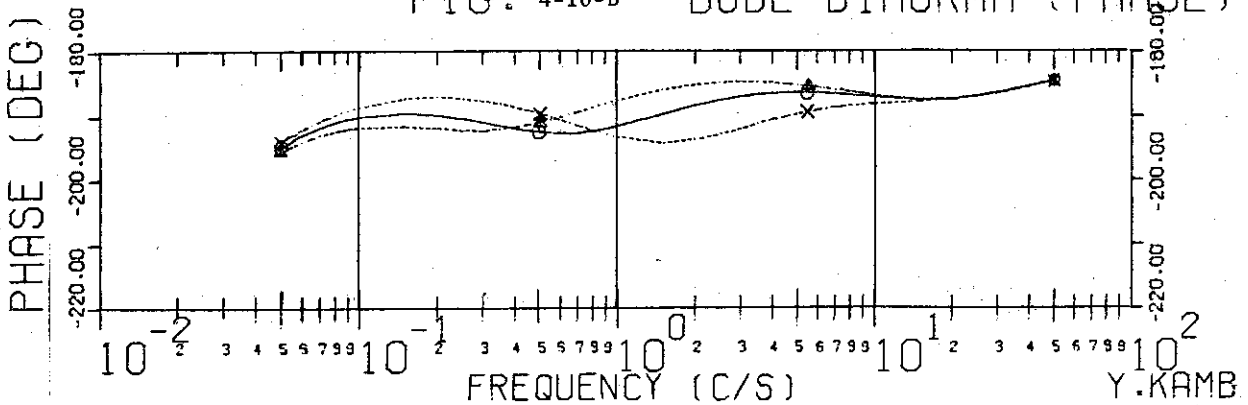


Fig. 4-11  
 Frequency Characteristics  
 Disturbance ( $\delta B_d/B_{vco}$ )  
 → Plasma Position ( $\delta R/R_0$ )

$\Gamma_0 = 2.2$   
 $G = -0.8$   
 $\tau_f = 0.02$   
 $\tau_v = 1.0$  ---  $\Delta$  ---  
           0.5 ---  $\circ$  ---  
           0.2 ---  $\times$  ---  
 $\tau_t = 10.0$

FIG. 4-11-C  
 VECTOR DIAGRAM

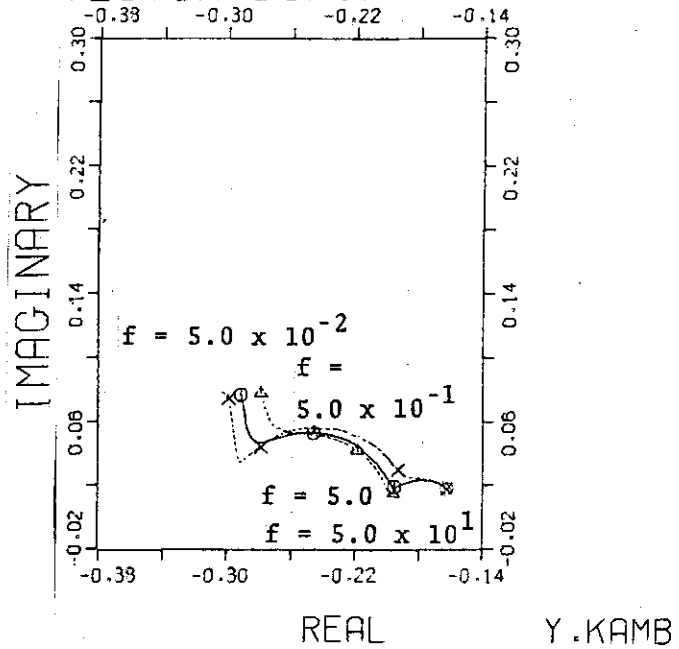


FIG. 4-11-A BODE DIAGRAM (GAIN)

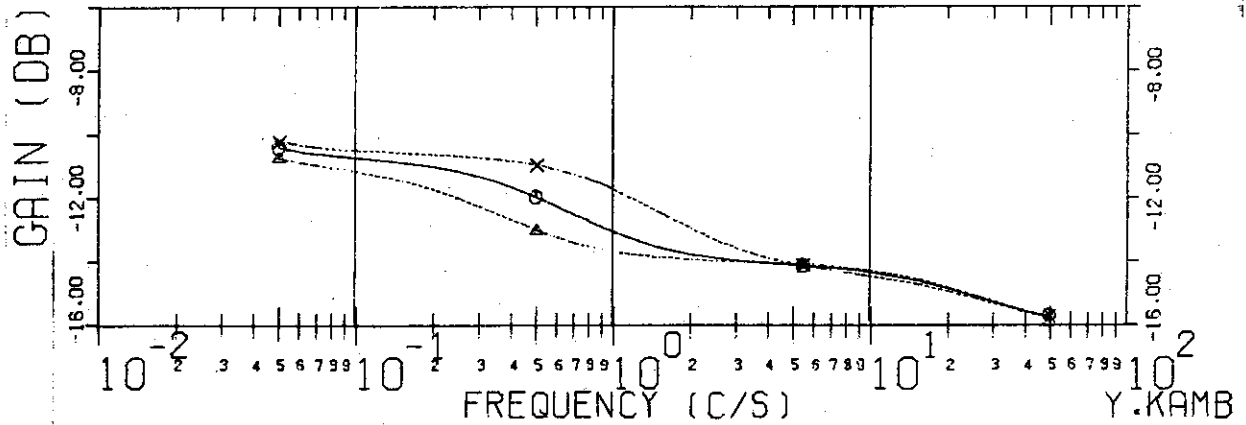


FIG. 4-11-B BODE DIAGRAM (PHASE)

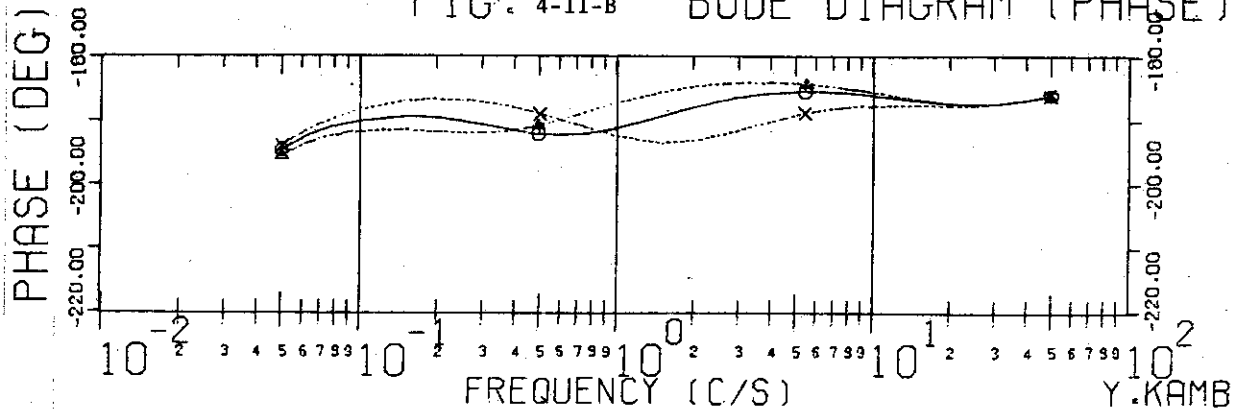


Fig. 4-12  
 Frequency Characteristics  
 Disturbance ( $\delta B_d/B_{vco}$ )  
 → Plasma Position ( $\delta R/R_0$ )

$\Gamma_0 = 2.2$   
 $G = -0.8$   
 $\tau_f = 0.01$   
 $\tau_v = 1.0$  ---  $\Delta$  ---  
           0.5    ---  $\circ$  ---  
           0.2    ---  $\times$  ---  
 $\tau_t = 10.0$

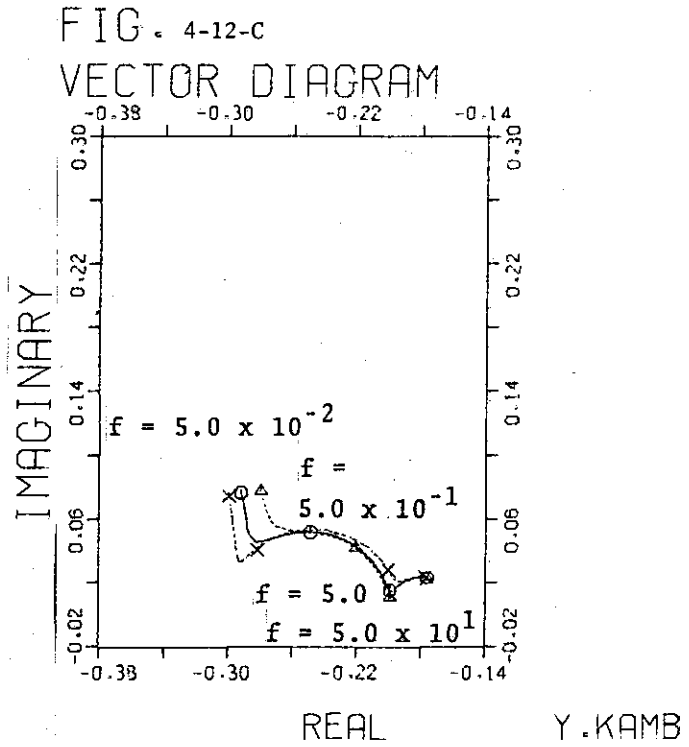


FIG. 4-12-A BODE DIAGRAM (GAIN)

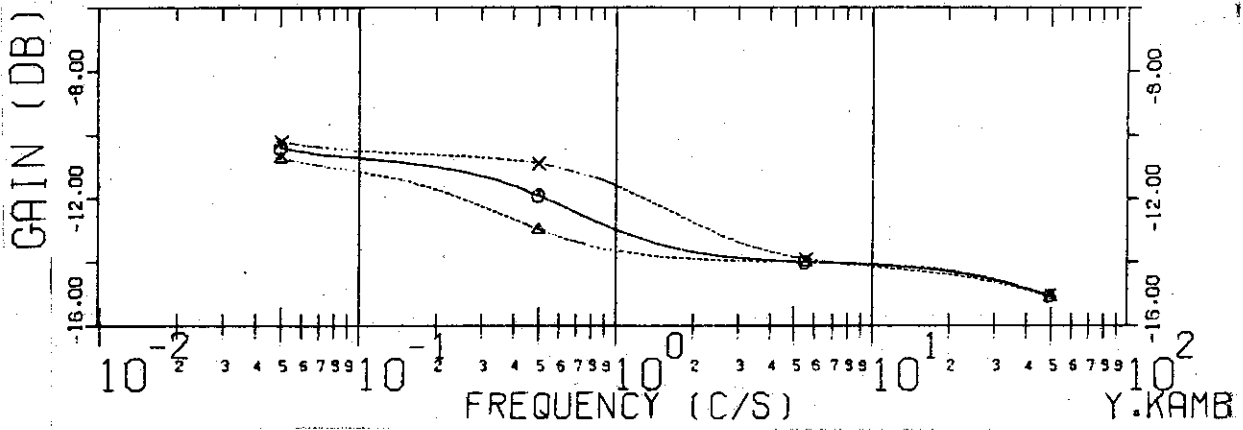


FIG. 4-12-B BODE DIAGRAM (PHASE)

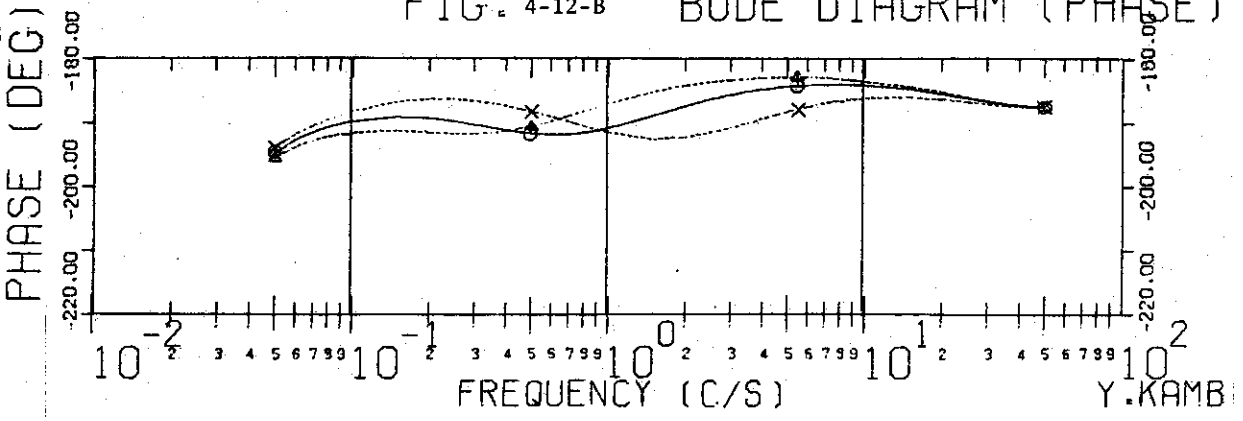




Fig. 4-13  
 Frequency Characteristics  
 Disturbance ( $\delta B_d/B_{vco}$ )  
 → Plasma Position ( $\delta R/R_0$ )

$\Gamma_0 = 2.2$   
 $G = -0.8$   
 $\tau_f = 0.03$   
 $\tau_v = 1.0$  ---  $\Delta$  ---  
           0.5 ---  $\circ$  ---  
           0.2 ---  $\times$  ---  
 $\tau_t = 5.0$

FIG. 4-13-C  
 VECTOR DIAGRAM

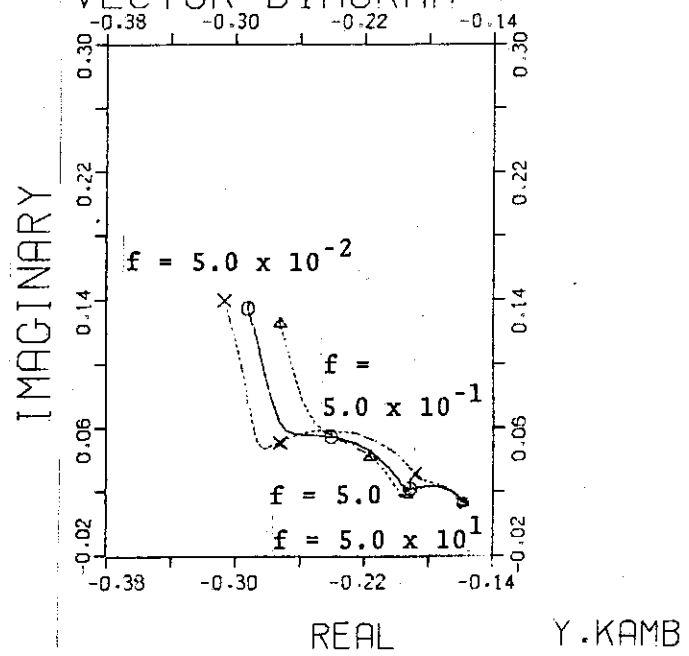


FIG. 4-13-A BODE DIAGRAM (GAIN)

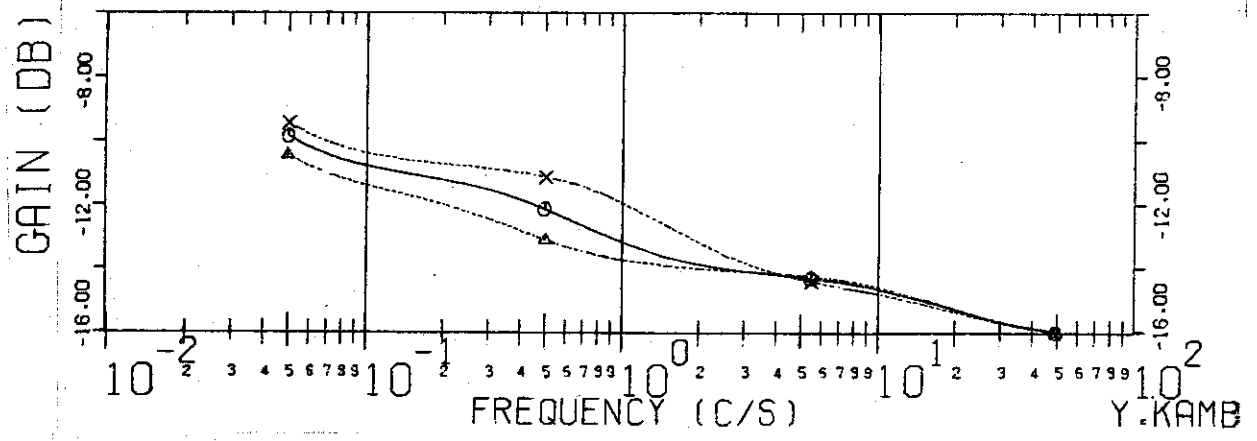


FIG. 4-13-B BODE DIAGRAM (PHASE)

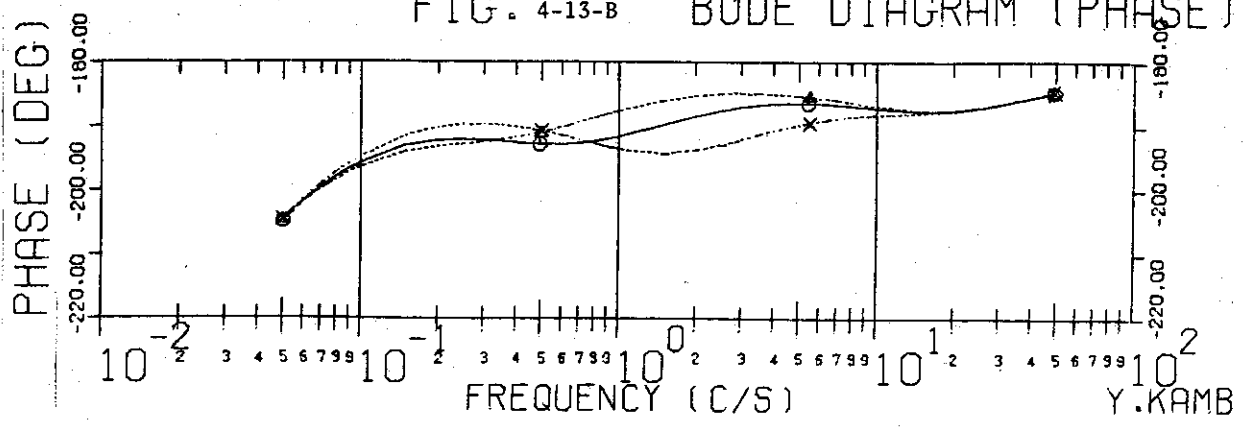


Fig. 4-14  
 Frequency Characteristics  
 Disturbance ( $\delta B_d/B_{vco}$ )  
 → Plasma Position ( $\delta R/R_0$ )

$\Gamma_0 = 2.2$   
 $G = -0.8$   
 $\tau_l = 0.02$   
 $\tau_v = 1.0$  ---  $\Delta$  ---  
           0.5 ---  $\circ$  ---  
           0.2 ---  $\times$  ---  
 $\tau_t = 5.0$

FIG. 4-14-C  
 VECTOR DIAGRAM

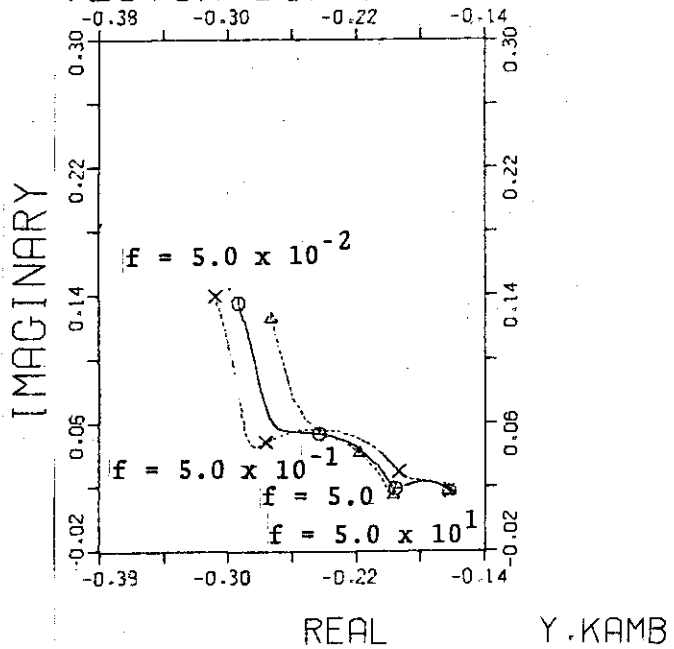


FIG. 4-14-A BODE DIAGRAM (GAIN)

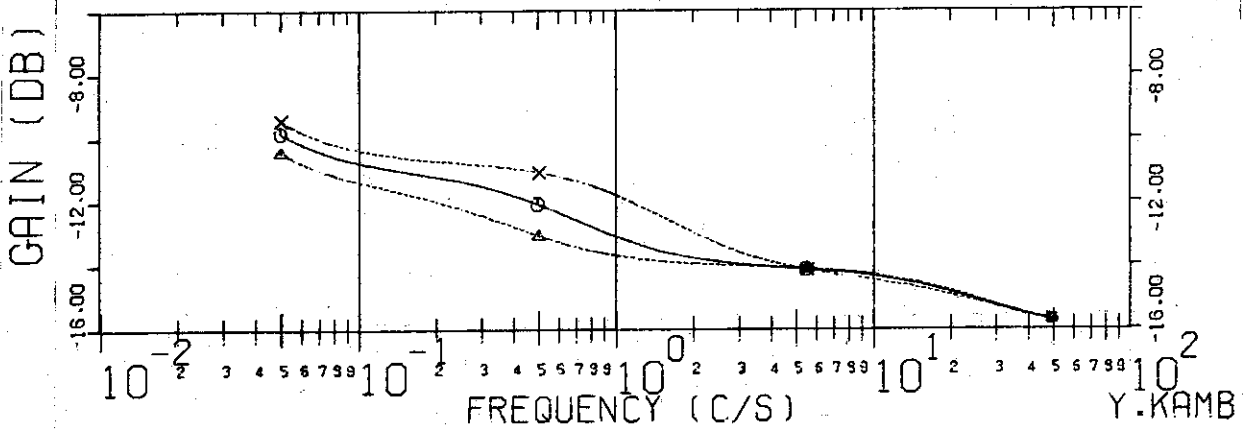


FIG. 4-14-B BODE DIAGRAM (PHASE)

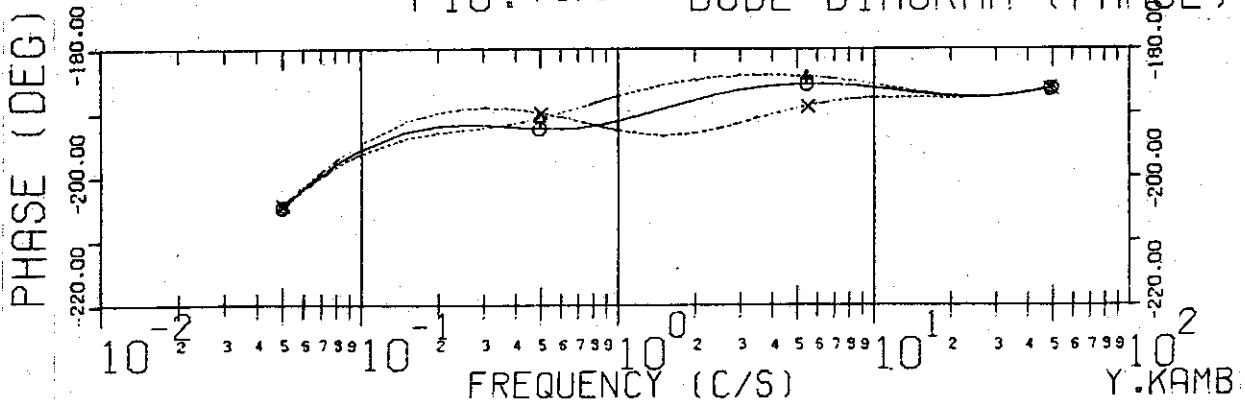


Fig. 4-15  
 Frequency Characteristics  
 Disturbance ( $\delta B_d/B_{vco}$ )  
 → Plasma Position ( $\delta R/R_0$ )

$\Gamma_0 = 2.2$   
 $G = -0.8$   
 $\tau_d = 0.01$   
 $\tau_v = 1.0$  —  $\Delta$  —  
           0.5 —  $\circ$  —  
           0.2 —  $\times$  —  
 $\tau_t = 5.0$

FIG. 4-15-C  
 VECTOR DIAGRAM

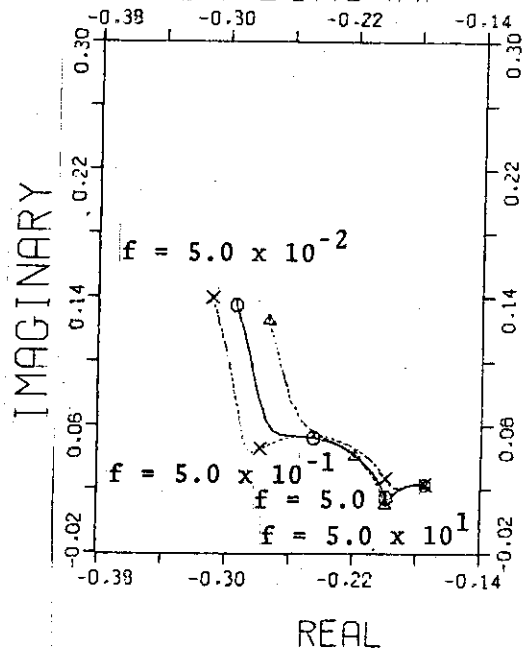


FIG. 4-15-A

BODE DIAGRAM (GAIN)

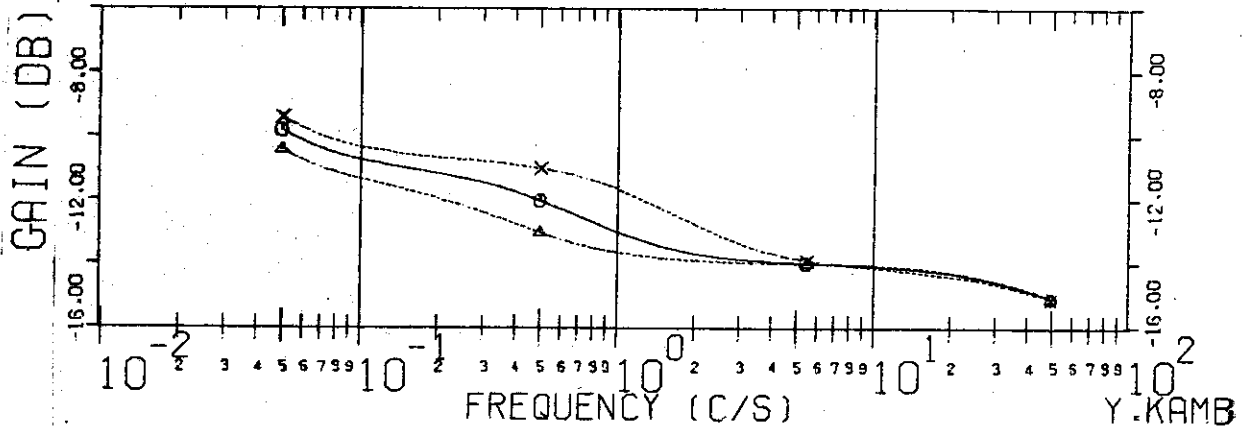


FIG. 4-15-B

BODE DIAGRAM (PHASE)

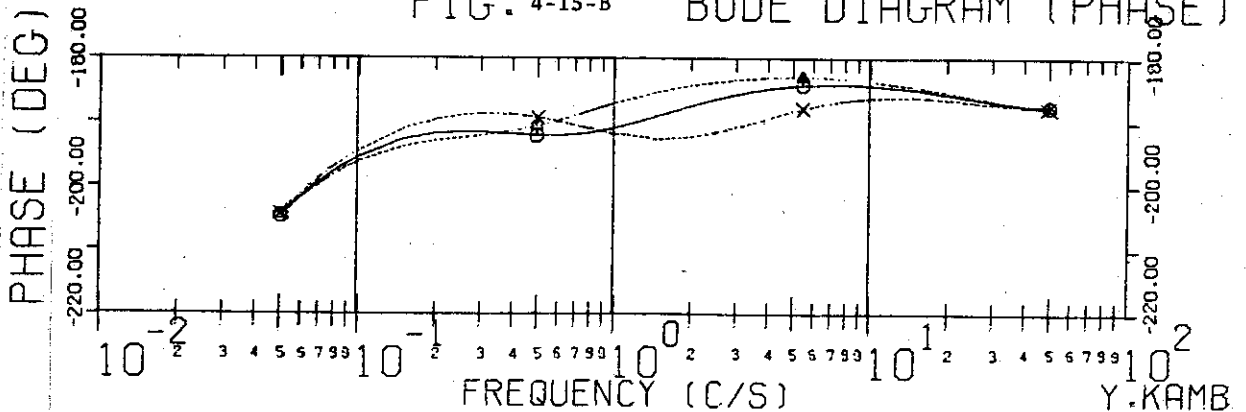


Fig. 4-16  
Frequency Characteristics  
Disturbance ( $\delta B_d/B_{vco}$ )  
→ Plasma Position ( $\delta R/R_0$ )

$T_0 = 2.2$   
 $G = -0.8$   
 $\tau_L = 0.03$   
 $\tau_V = 1.0$  —  $\Delta$  —  
 $0.5$  —  $\circ$  —  
 $0.2$  —  $\times$  —  
 $\tau_t = 2.0$

FIG. 4-16-C  
VECTOR DIAGRAM

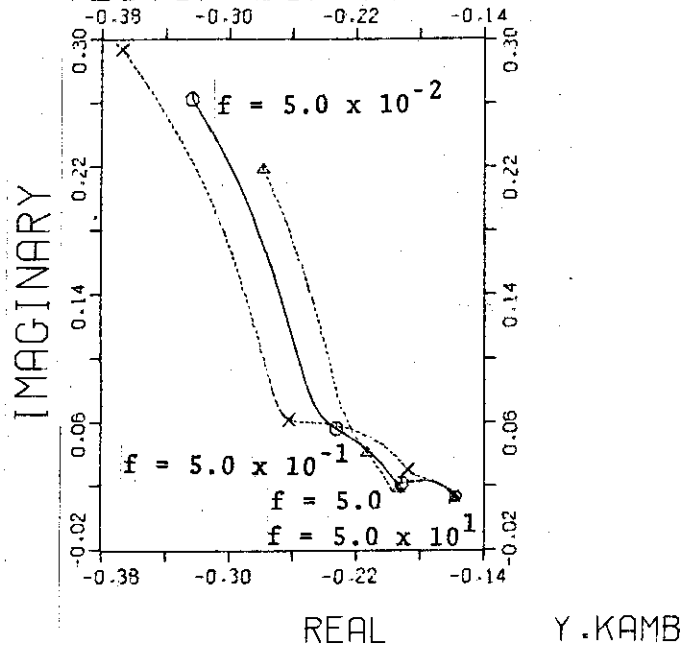


FIG. 4-16-A BODE DIAGRAM (GAIN)

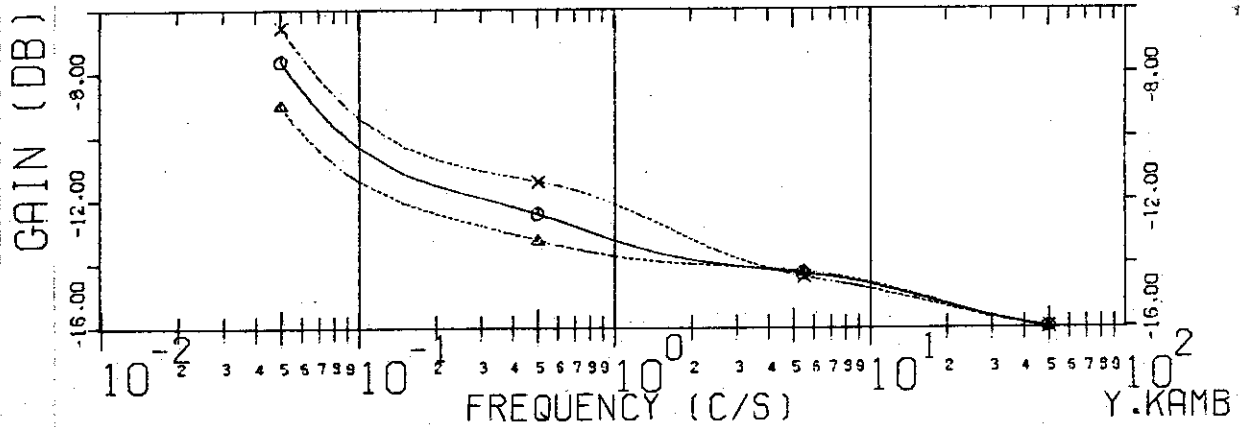


FIG. 4-16-B BODE DIAGRAM (PHASE)

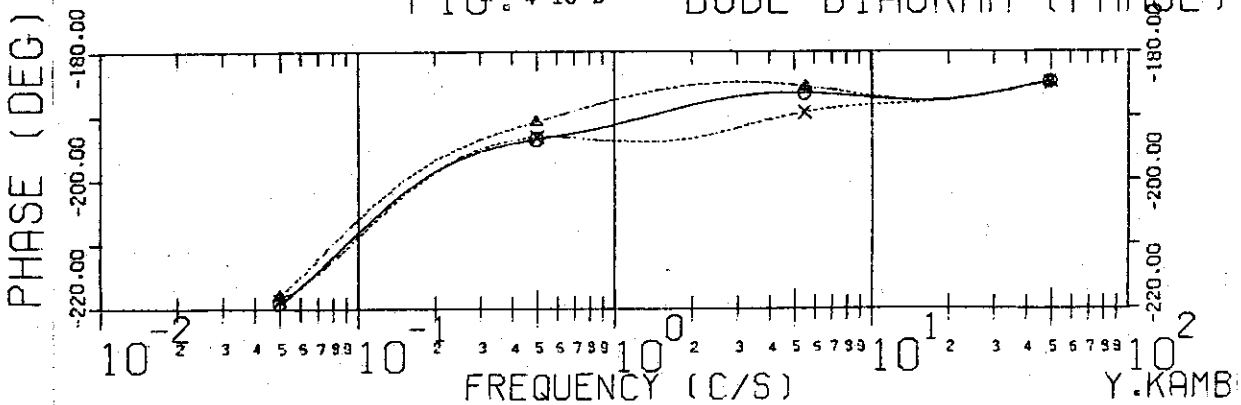


Fig. 4-17  
 Frequency Characteristics  
 Disturbance ( $\delta B_d/B_{vco}$ )  
 —→ Plasma Position ( $\delta R/R_0$ )

$\Gamma_0 = 2.2$   
 $G = -0.8$   
 $\tau_p = 0.02$   
 $\tau_v = 1.0$  —  $\Delta$  —  
           0.5 —  $\circ$  —  
           0.2 —  $\times$  —  
 $\tau_t = 2.0$

FIG. 4-17-C  
 VECTOR DIAGRAM

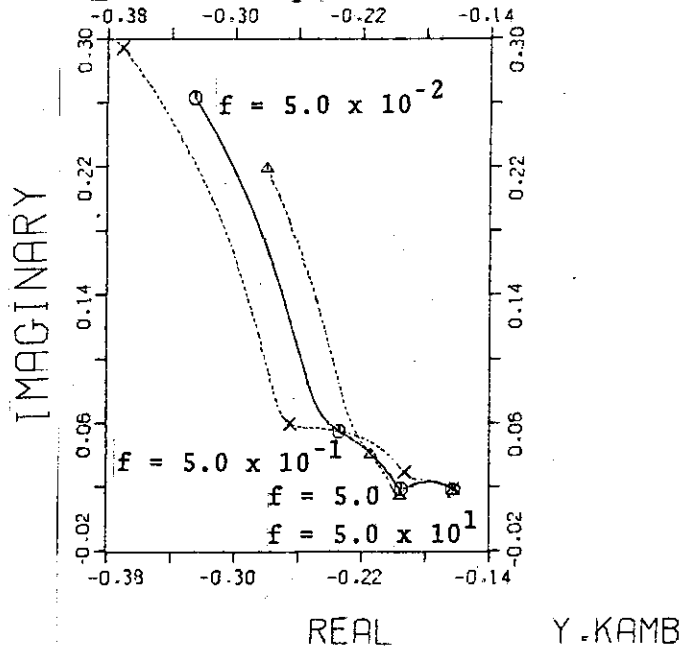


FIG. 4-17-A BODE DIAGRAM (GAIN)

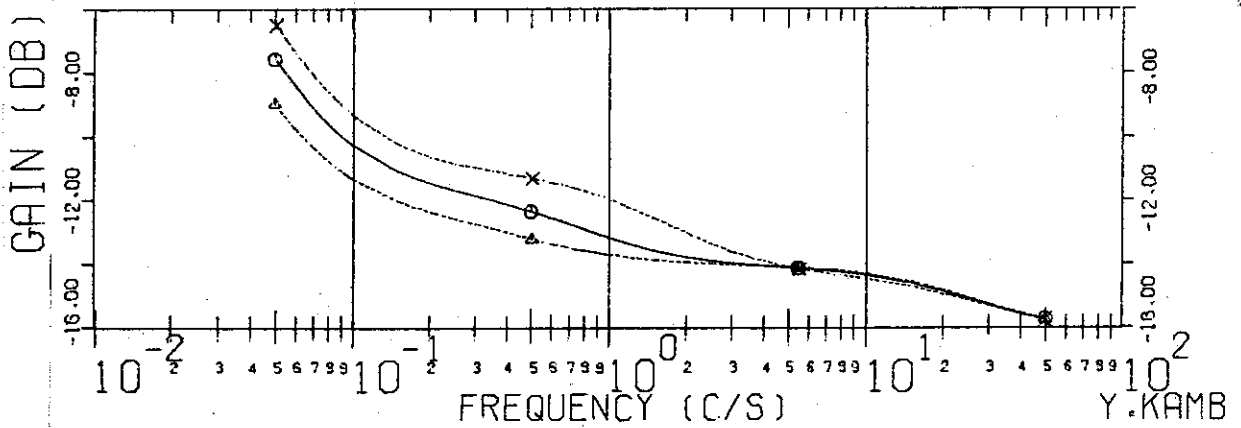


FIG. 4-17-B BODE DIAGRAM (PHASE)

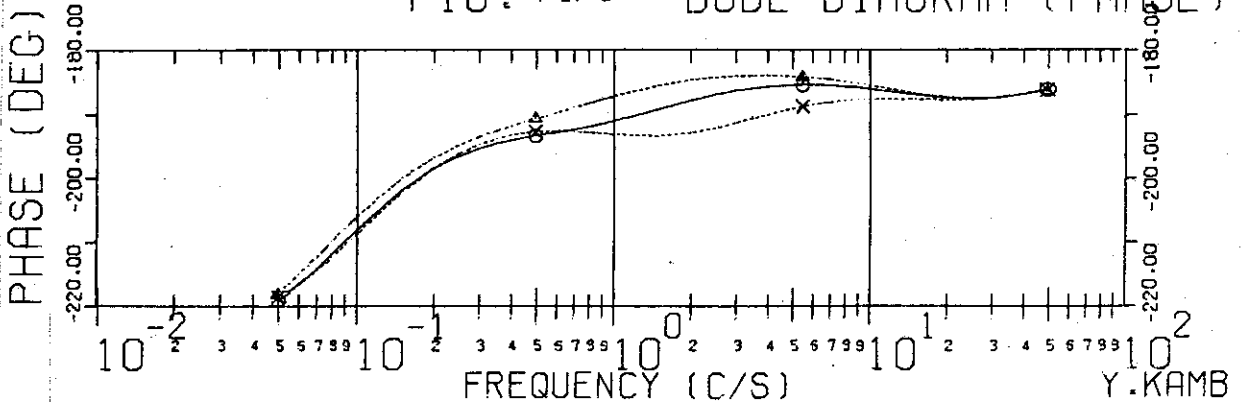


Fig. 4-18  
 Frequency Characteristics  
 Disturbance ( $\delta B_d/B_{vco}$ )  
 —→ Plasma Position ( $\delta R/R_0$ )

$\Gamma_0 = 2.2$   
 $G = -0.8$   
 $\tau_f = 0.01$   
 $\tau_v = 1.0$  ---  $\Delta$  ---  
 $0.5$  ---  $\circ$  ---  
 $0.2$  ---  $\times$  ---  
 $\tau_t = 2.0$

FIG. 4-18-C  
 VECTOR DIAGRAM

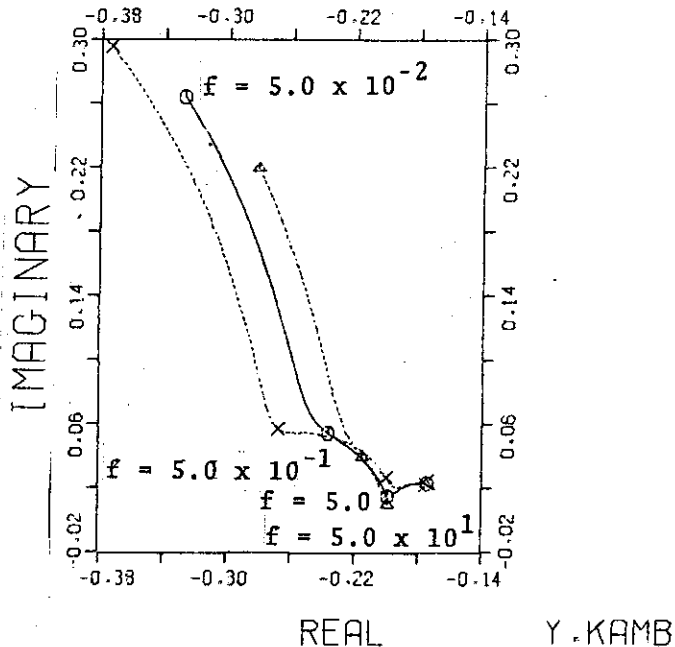


FIG. 4-18-A BODE DIAGRAM (GAIN)

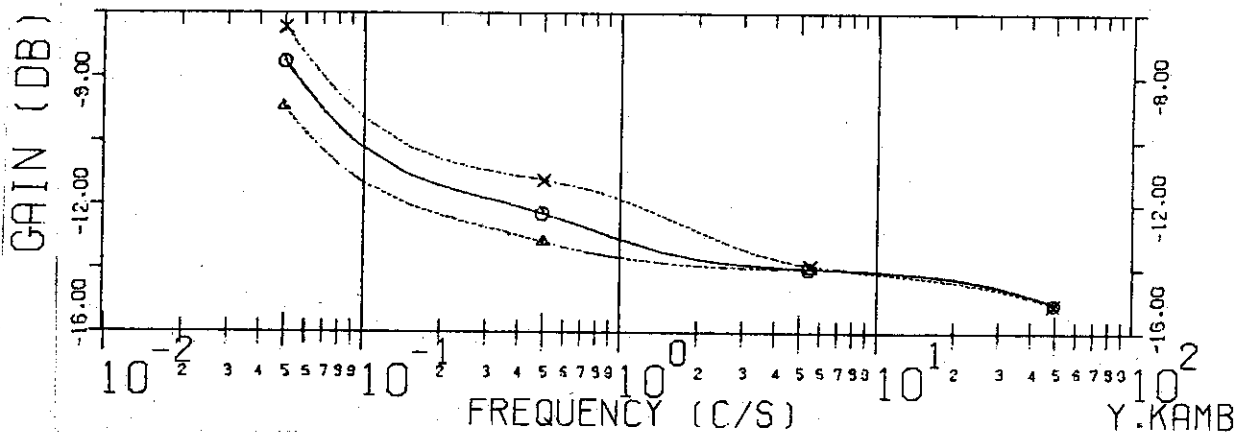


FIG. 4-18-B BODE DIAGRAM (PHASE)

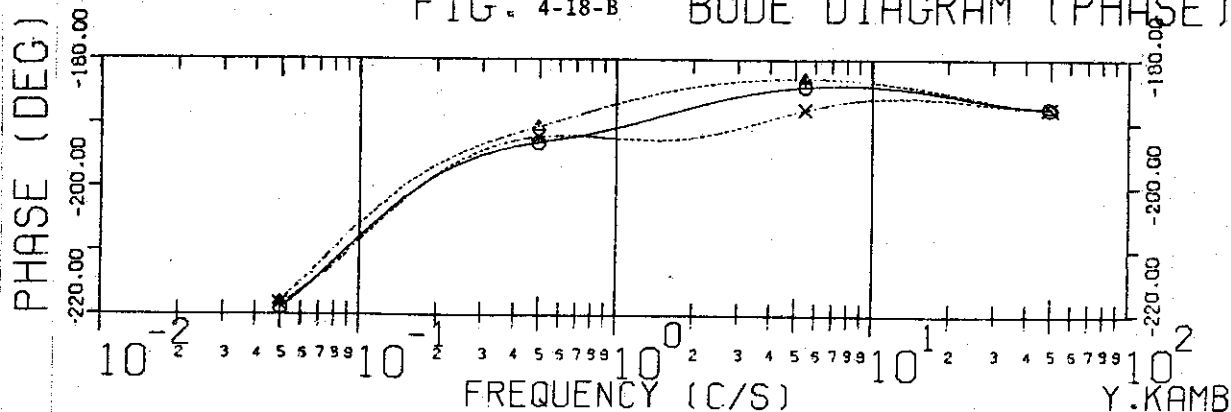


Fig. 4-19  
 Frequency Characteristics  
 Disturbance ( $\delta B_d/B_{vco}$ )  
 —→ Plasma Position ( $\delta R/R_0$ )

$\Gamma_0 = 2.2$   
 $G = -0.8$   
 $\tau_d = 0.03$  ---  $\Delta$  ---  
           0.02 ---  $\circ$  ---  
           0.01 ---  $\times$  ---  
 $\tau_v = 1.0$   
 $\tau_t = 10.0$

FIG. 4-19-C  
 VECTOR DIAGRAM

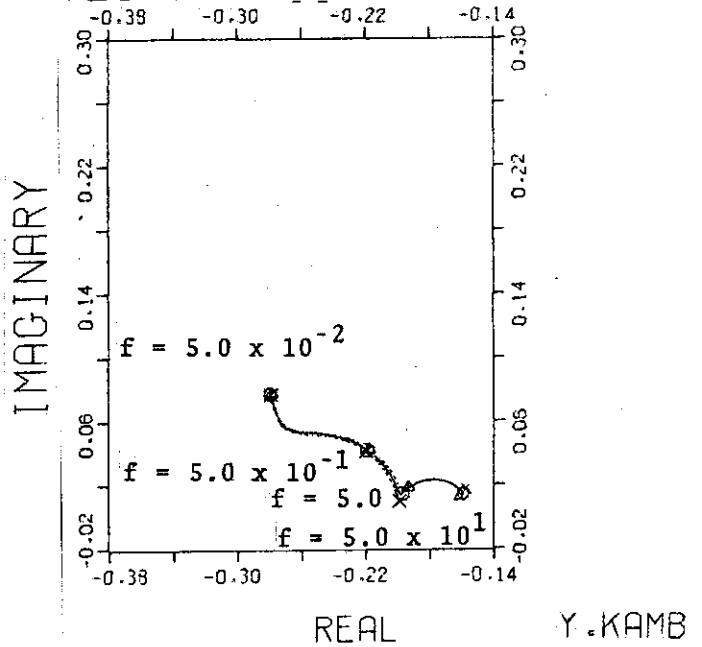


FIG. 4-19-A BODE DIAGRAM (GAIN)

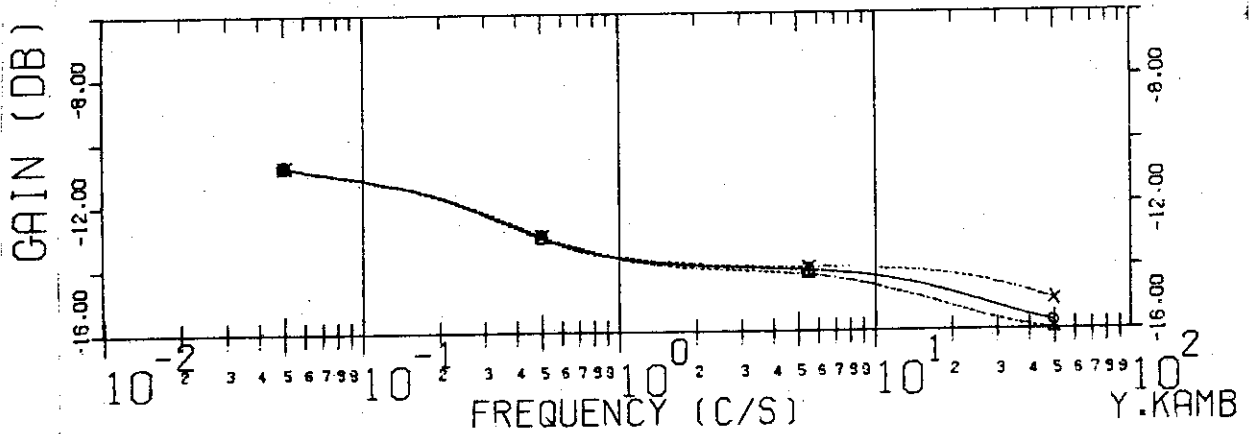


FIG. 4-19-B BODE DIAGRAM (PHASE)

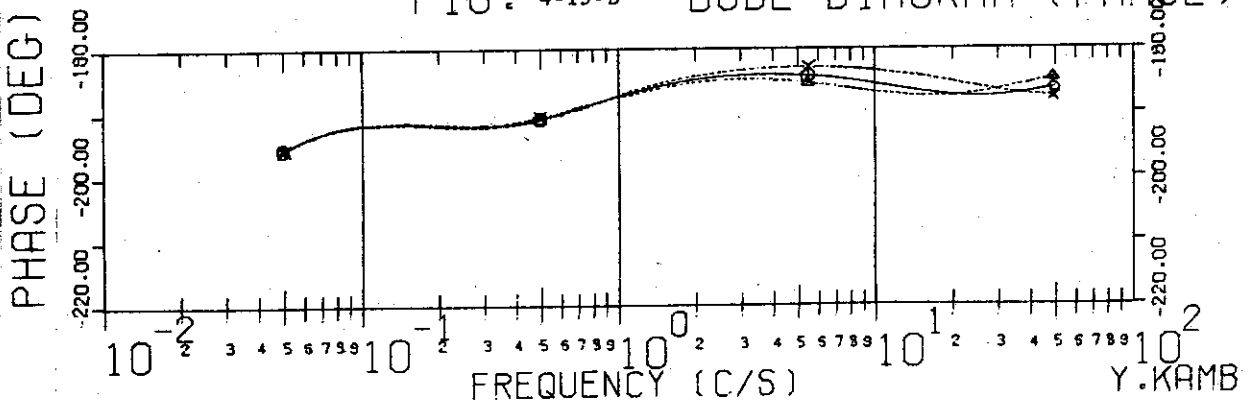


Fig. 4-20  
 Frequency Characteristics  
 Disturbance ( $\delta B_d/B_{VCO}$ )  
 $\rightarrow$  Plasma Position ( $\delta R/R_0$ )

$\Gamma_0 = 2.2$   
 $G = -0.8$   
 $\tau_\chi = 0.03$  ---  $\Delta$  ---  
           0.02 ---  $\circ$  ---  
           0.01 ---  $\times$  ---  
 $\tau_V = 1.0$   
 $\tau_t = 5.0$

FIG. 4-20-C  
 VECTOR DIAGRAM

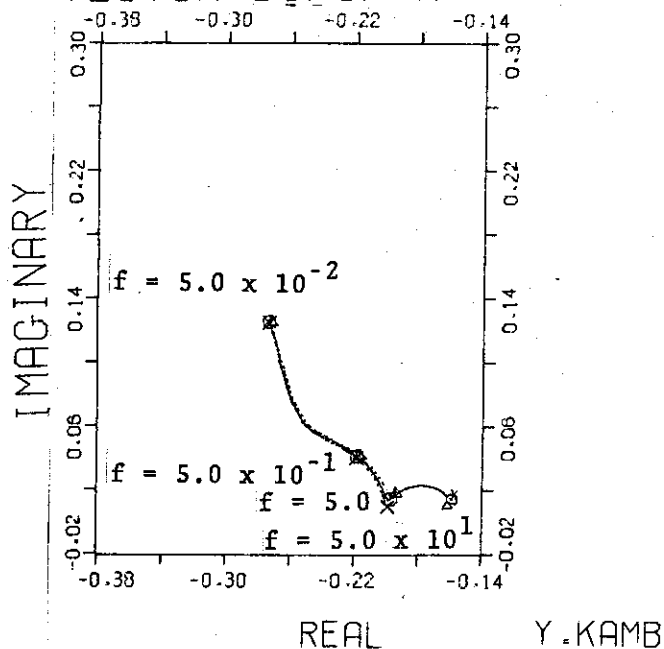


FIG. 4-20-A BODE DIAGRAM (GAIN)

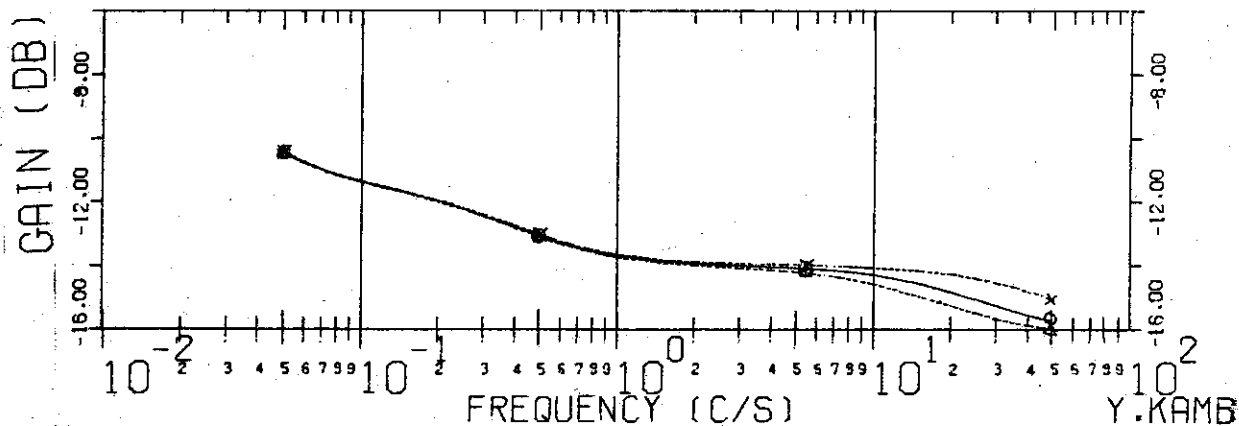


FIG. 4-20-B BODE DIAGRAM (PHASE)

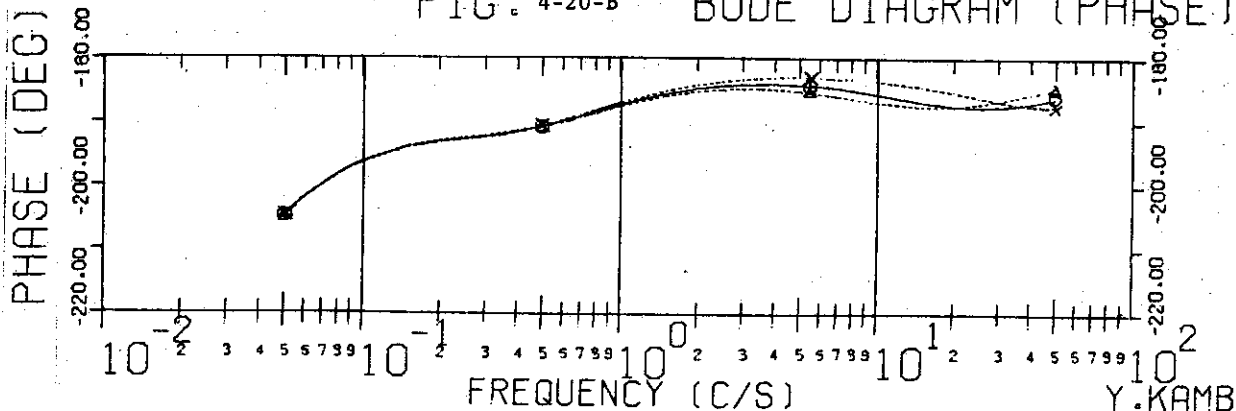




Fig. 4-21  
 Frequency Characteristics  
 Disturbance ( $\delta B_d/B_{vco}$ )  
 → Plasma Position ( $\delta R/R_0$ )

$\Gamma_0 = 2.2$   
 $G = -0.8$   
 $\tau_L = 0.03$  ---  $\Delta$  ---  
           0.02 ---  $\circ$  ---  
           0.01 ---  $\times$  ---  
 $\tau_V = 1.0$   
 $\tau_t = 2.0$

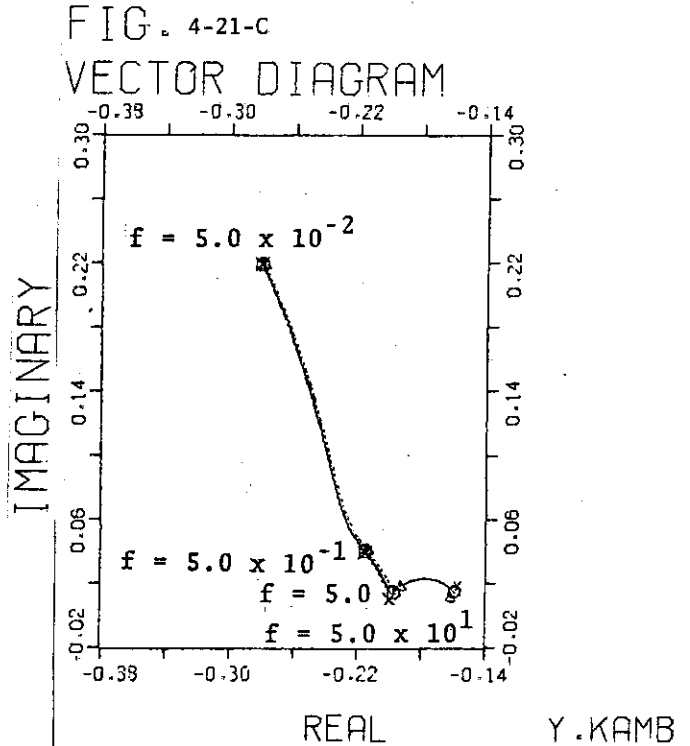


FIG. 4-21-A BODE DIAGRAM (GAIN)

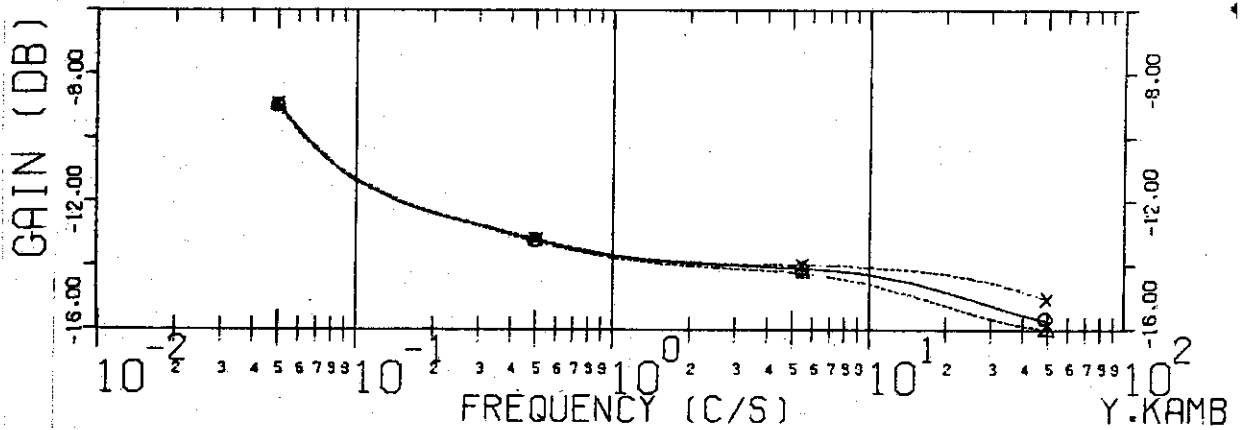


FIG. 4-21-B BODE DIAGRAM (PHASE)

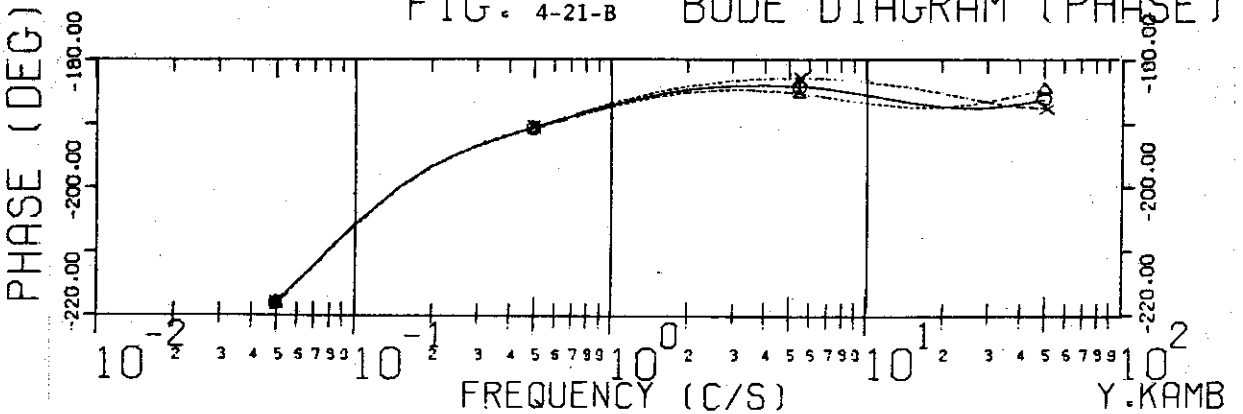


Fig. 4-22  
 Frequency Characteristics  
 Disturbance ( $\delta B_d/B_{vco}$ )  
 → Plasma Position ( $\delta R/R_0$ )

$\Gamma_0 = 2.2$   
 $G = -0.8$   
 $\tau_l = 0.03$  —  $\Delta$  — —  
           0.02 —  $\circ$  — —  
           0.01 —  $\times$  — —  
 $\tau_v = 0.5$   
 $\tau_t = 10.0$

FIG. 4-22-C  
 VECTOR DIAGRAM

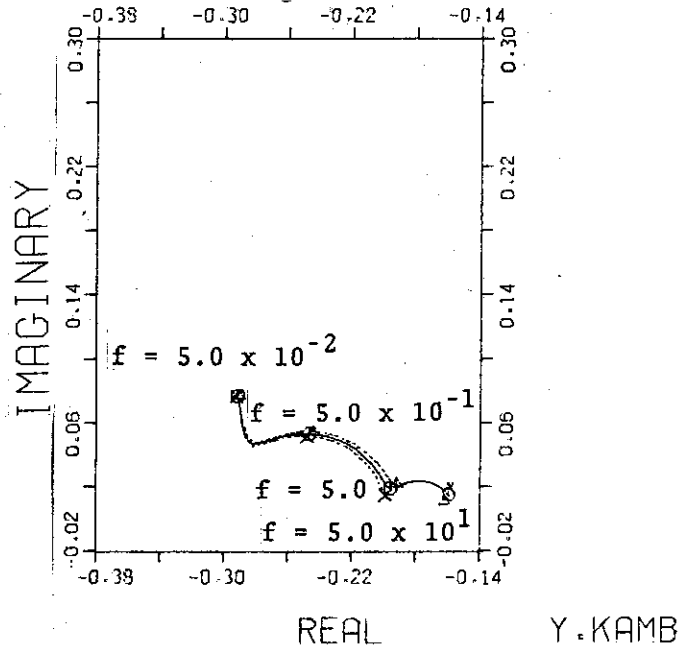


FIG. 4-22-A BODE DIAGRAM (GAIN)

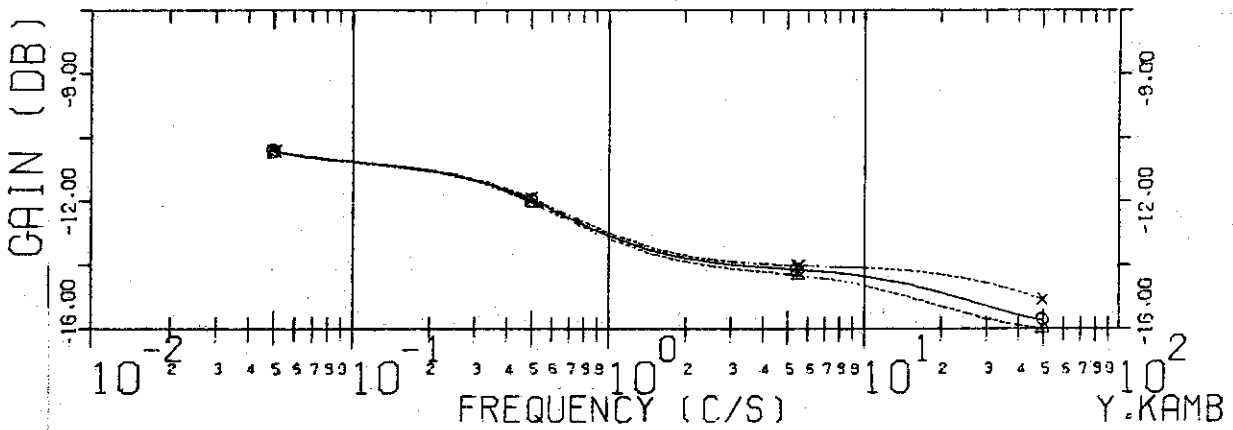


FIG. 4-22-B BODE DIAGRAM (PHASE)

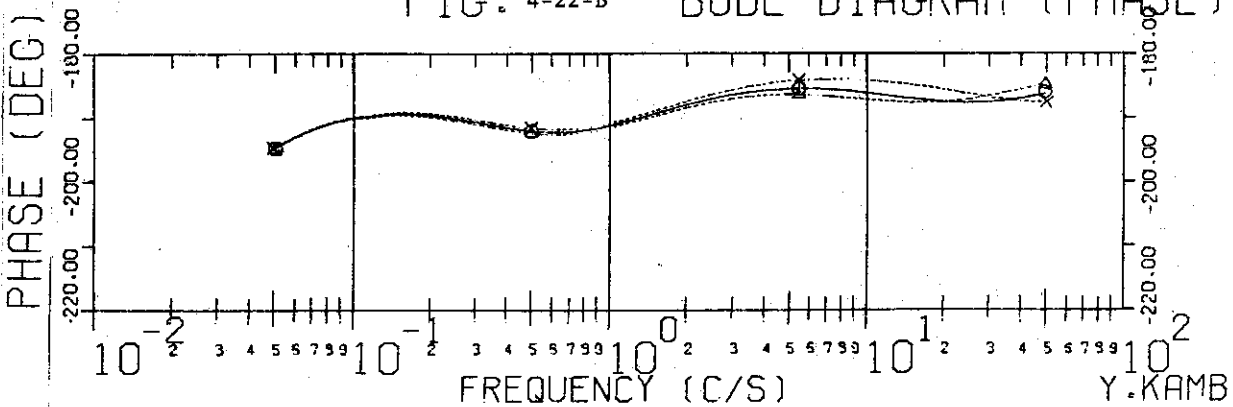


Fig. 4-23  
 Frequency Characteristics  
 Disturbance ( $\delta B_d/B_{vco}$ )  
 —→ Plasma Position ( $\delta R/R_0$ )

$\Gamma_0 = 2.2$   
 $G = -0.8$   
 $\tau_l = 0.03$  ---  $\Delta$  ---  
 $0.02$  ---  $\circ$  ---  
 $0.01$  ---  $\times$  ---  
 $\tau_v = 0.5$   
 $\tau_t = 5.0$

FIG. 4-23-C  
 VECTOR DIAGRAM

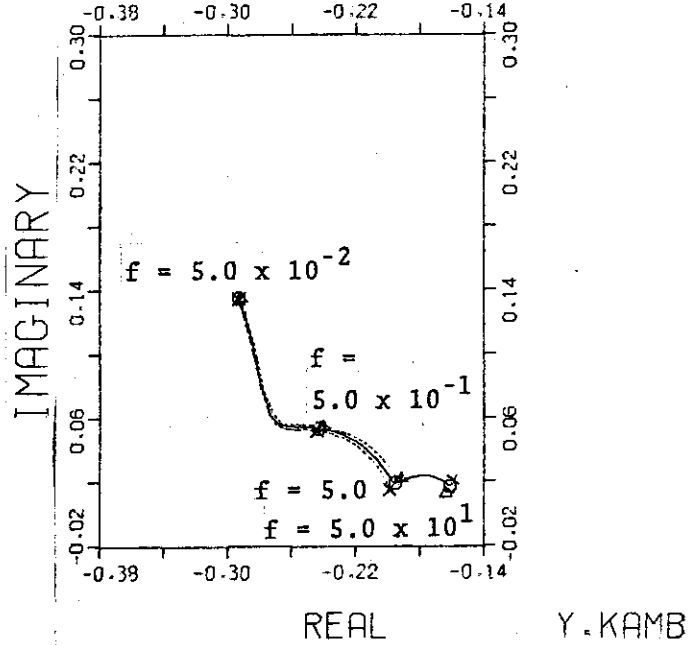


FIG. 4-23-A BODE DIAGRAM (GAIN)

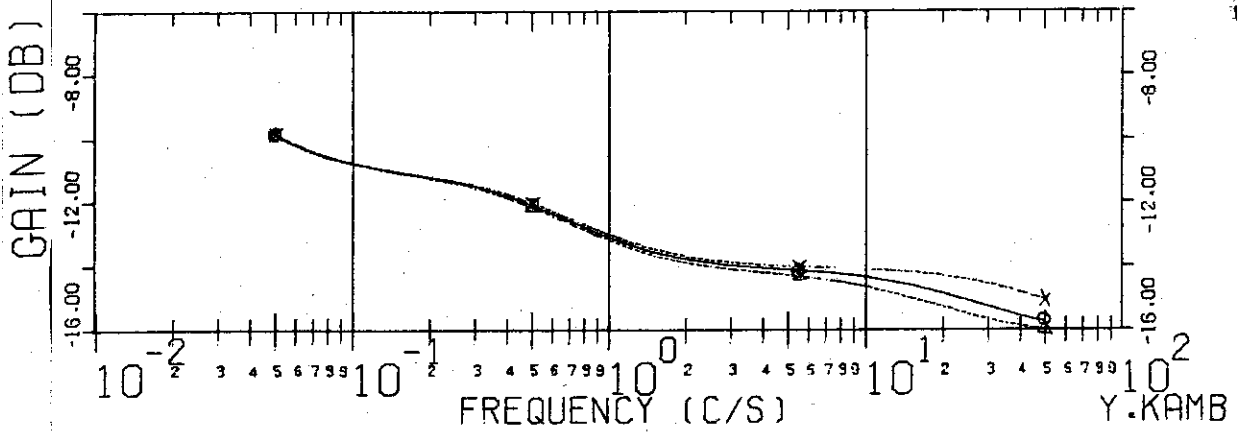


FIG. 4-23-B BODE DIAGRAM (PHASE)

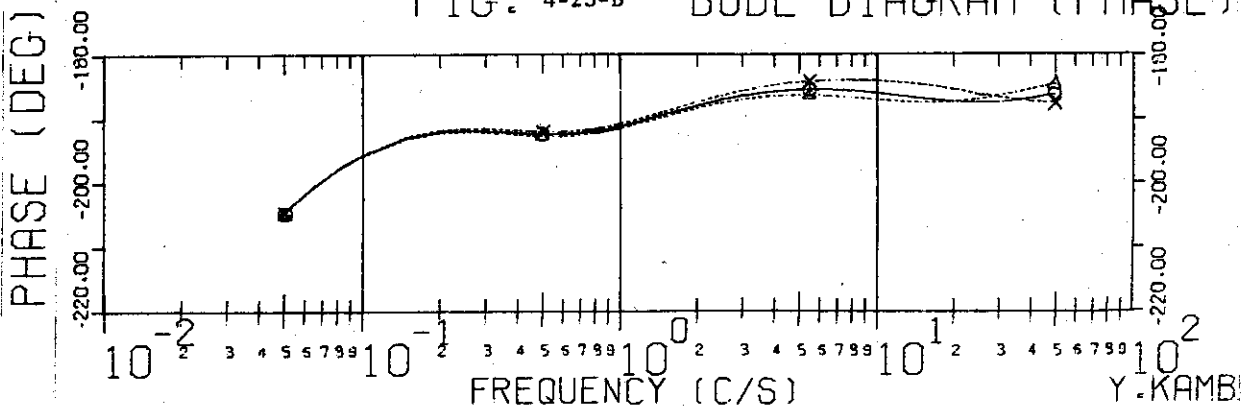


Fig. 4-24  
 Frequency Characteristics  
 Disturbance ( $\delta B_d/B_{vco}$ )  
 → Plasma Position ( $\delta R/R_0$ )

$\Gamma_0 = 2.2$   
 $\xi = -0.8$   
 $\tau_L = 0.03$  ---  $\Delta$  ---  
           0.02 ---  $\circ$  ---  
           0.01 ---  $\times$  ---  
 $\tau_V = 0.5$   
 $\tau_t = 2.0$

FIG. 4-24-C  
 VECTOR DIAGRAM

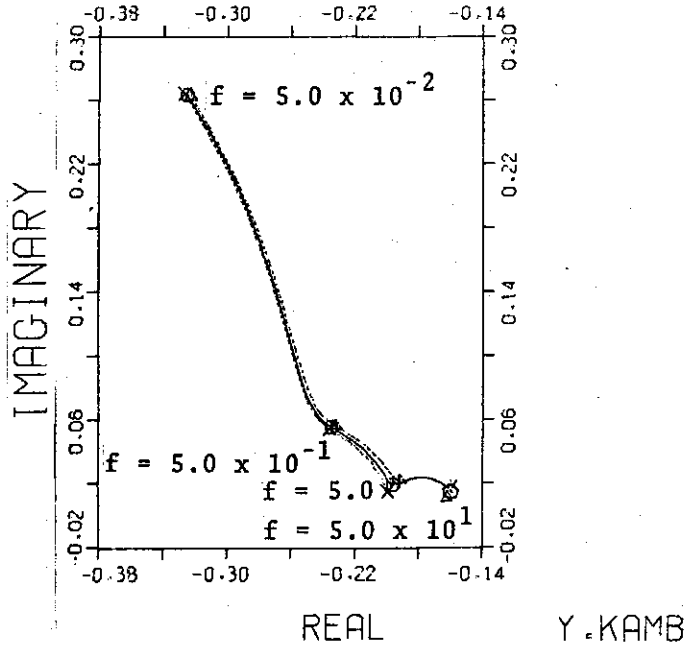


FIG. 4-24-A BODE DIAGRAM (GAIN)

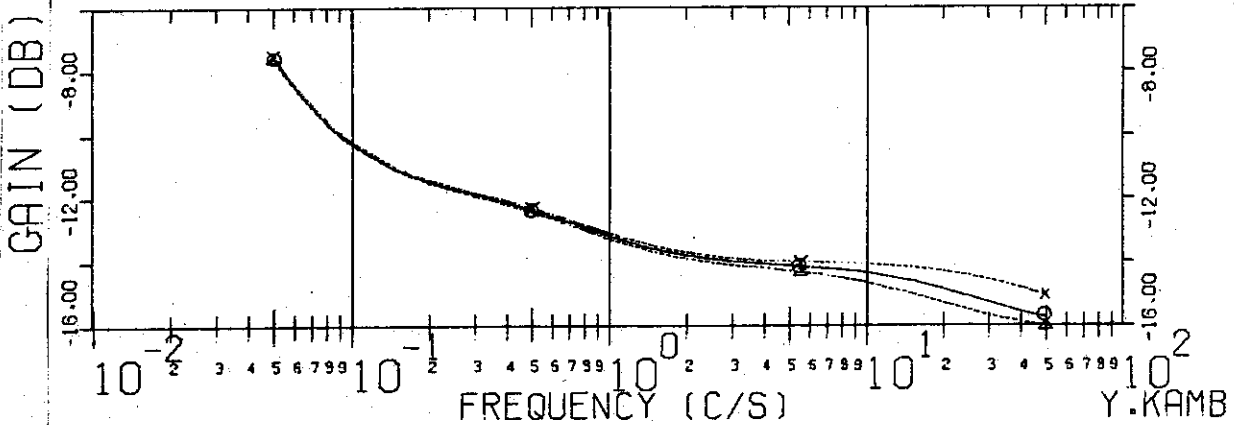


FIG. 4-24-B BODE DIAGRAM (PHASE)

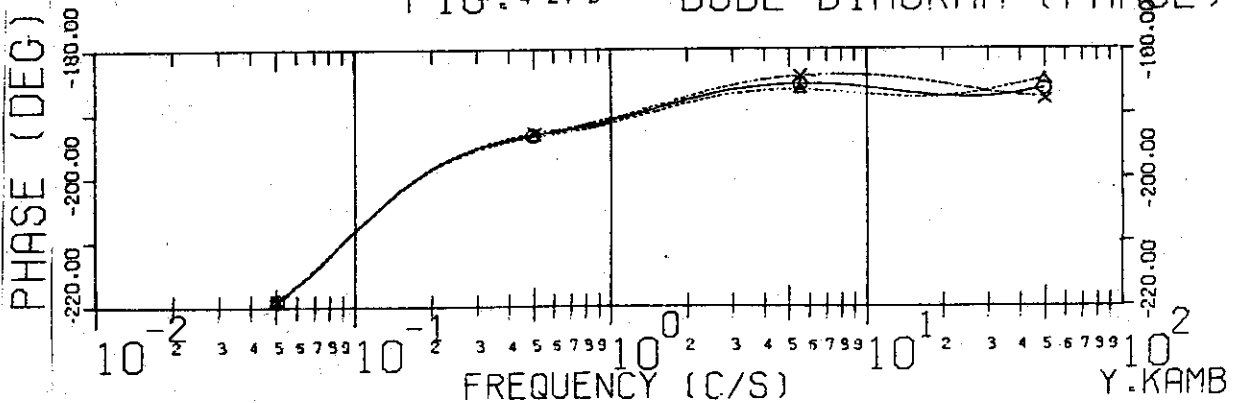


Fig. 4-25  
 Frequency Characteristics  
 Disturbance ( $\delta B_d/B_{vco}$ )  
 → Plasma Position ( $\delta R/R_0$ )

$\Gamma_0 = 2.2$   
 $G = -0.8$   
 $\tau_f = 0.03$  ---  $\Delta$  ---  
           0.02 ---  $\circ$  ---  
           0.01 ---  $\times$  ---  
 $\tau_v = 0.2$   
 $\tau_t = 10.0$

FIG. 4-25-C

VECTOR DIAGRAM

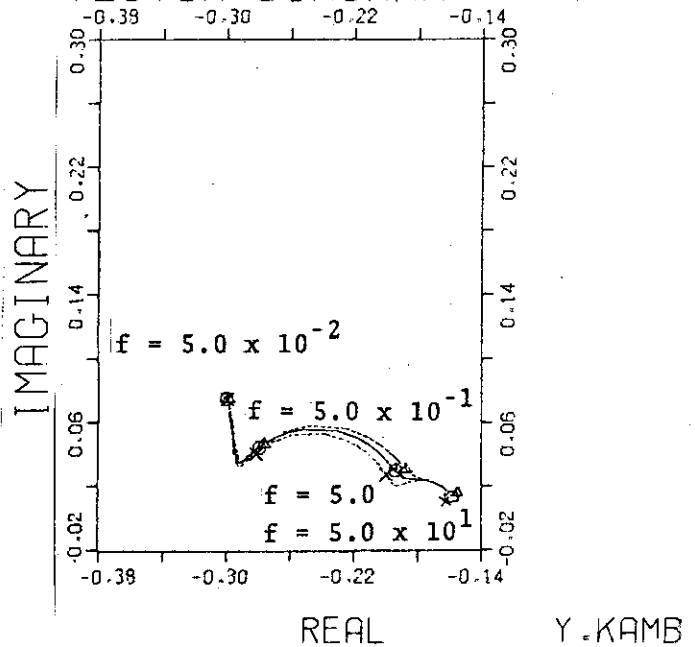


FIG. 4-25-A

BODE DIAGRAM (GAIN)

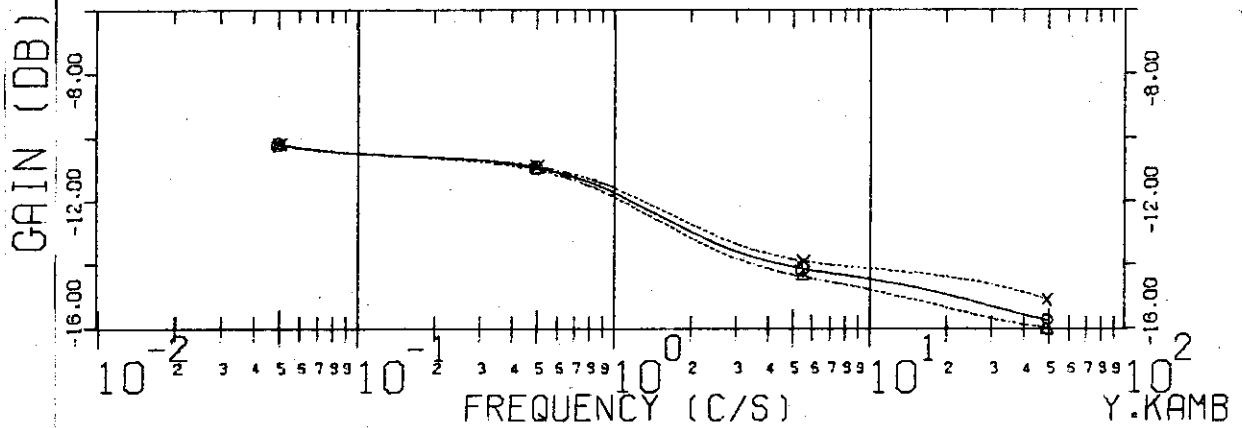


FIG. 4-25-B

BODE DIAGRAM (PHASE)

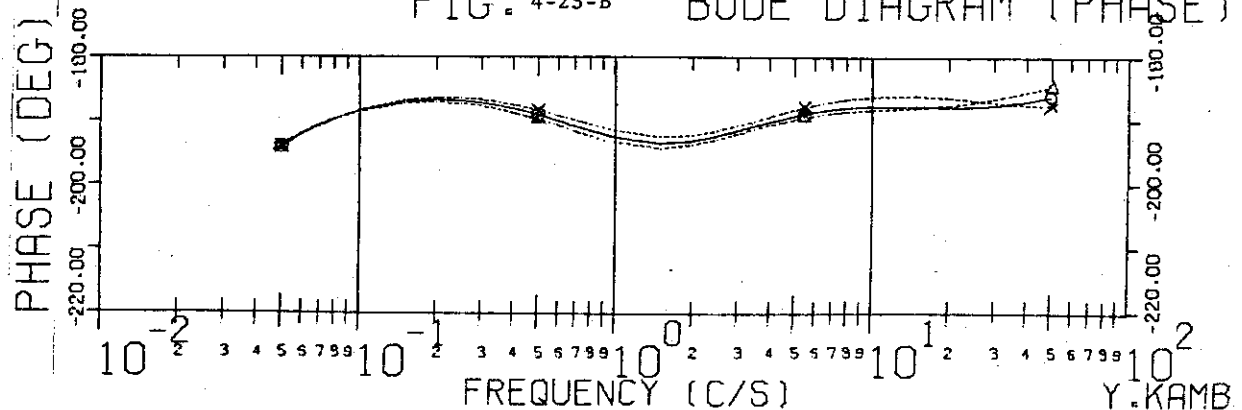


Fig. 4-26  
 Frequency Characteristics  
 Disturbance ( $\delta B_d/B_{vco}$ )  
 — Plasma Position ( $\delta R/R_0$ )

$\Gamma_0 = 2.2$   
 $G = -0.8$   
 $\tau_f = 0.03$  —  $\Delta$  ---  
           0.02 —  $\circ$  ---  
           0.01 —  $\times$  ---  
 $\tau_v = 0.2$   
 $\tau_t = 5.0$

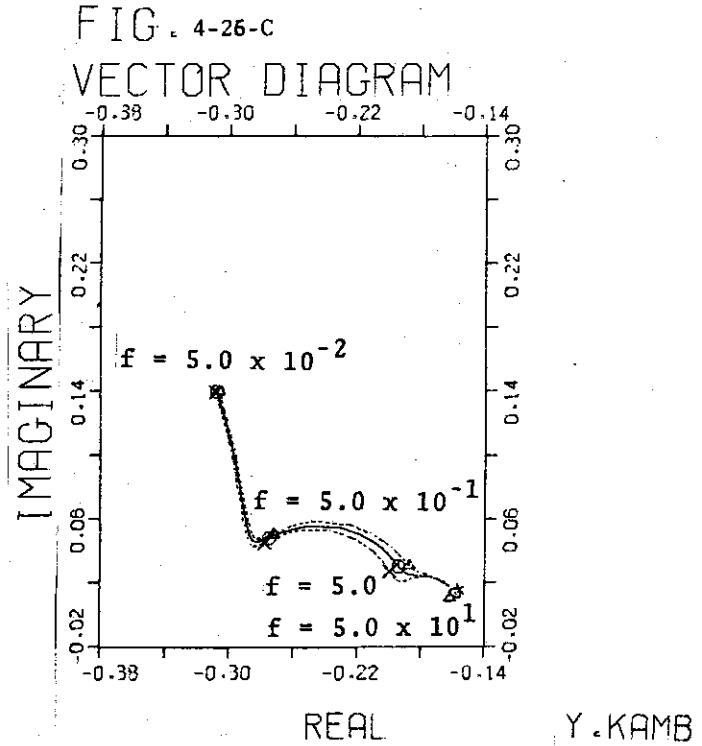


FIG. 4-26-A BODE DIAGRAM (GAIN)

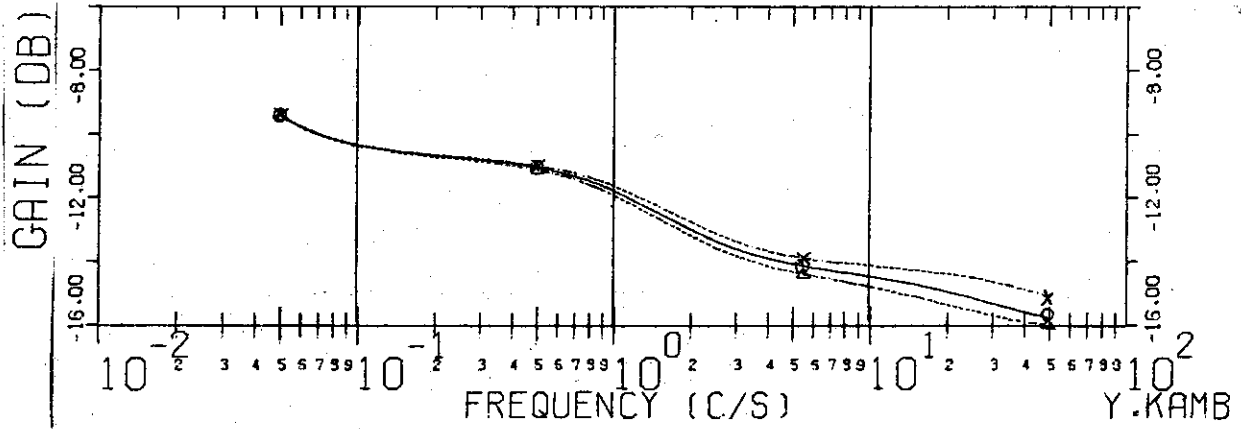


FIG. 4-26-B BODE DIAGRAM (PHASE)

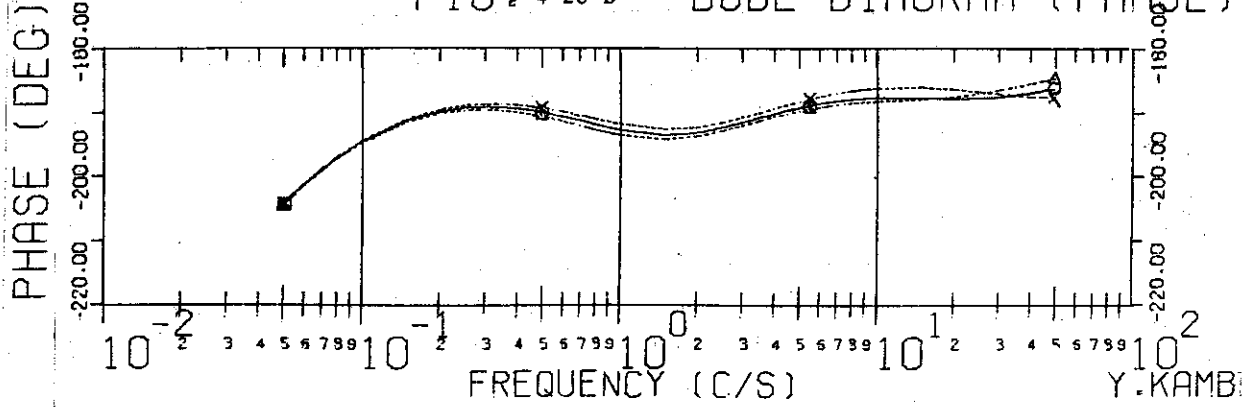


Fig. 4-27  
 Frequency Characteristics  
 Disturbance ( $\delta B_d/B_{vco}$ )  
 → Plasma Position ( $\delta R/R_0$ )

$\Gamma_0 = 2.2$   
 $G = -0.8$   
 $\tau_l = 0.03$  ---  $\Delta$  ---  
           0.02 ---  $\circ$  ---  
           0.01 ---  $\times$  ---  
 $\tau_v = 0.2$   
 $\tau_t = 2.0$

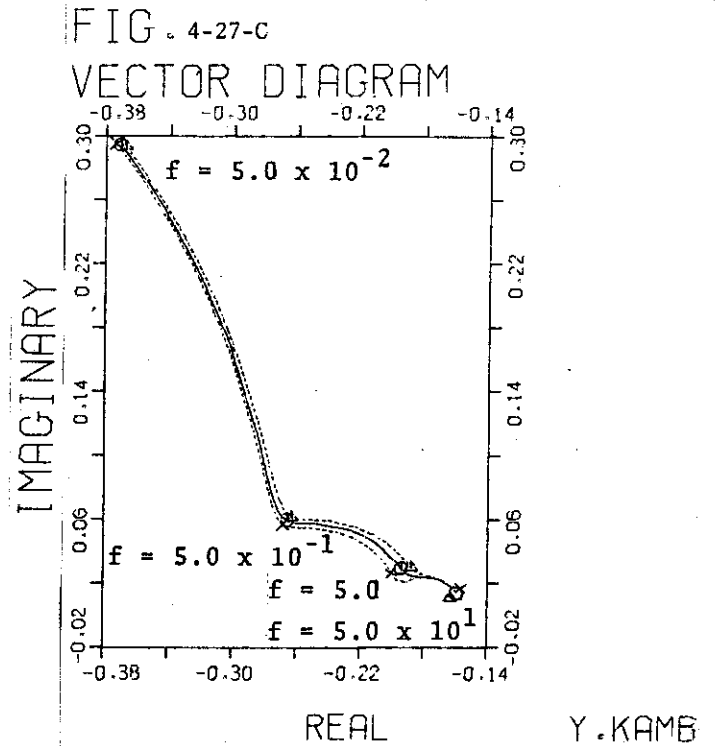


FIG. 4-27-A BODE DIAGRAM (GAIN)

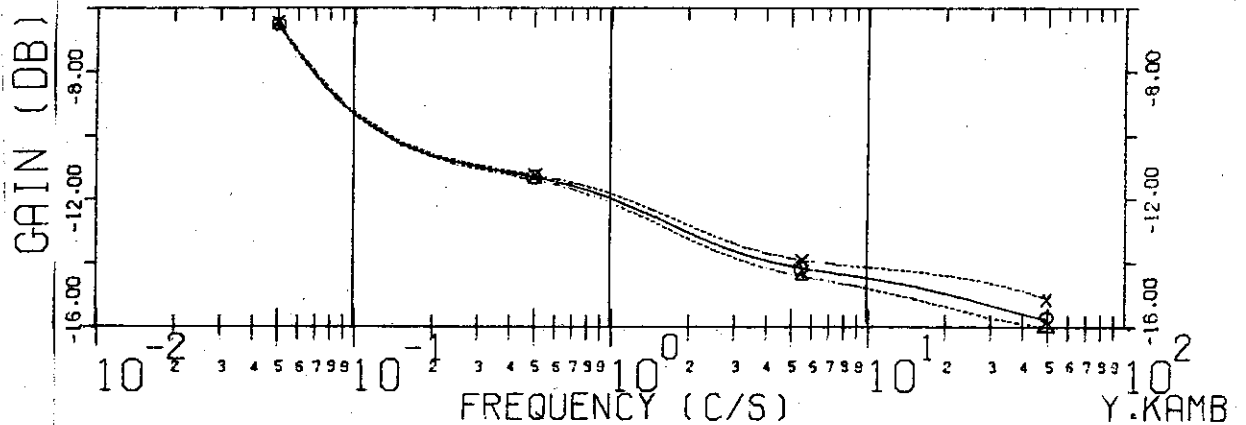
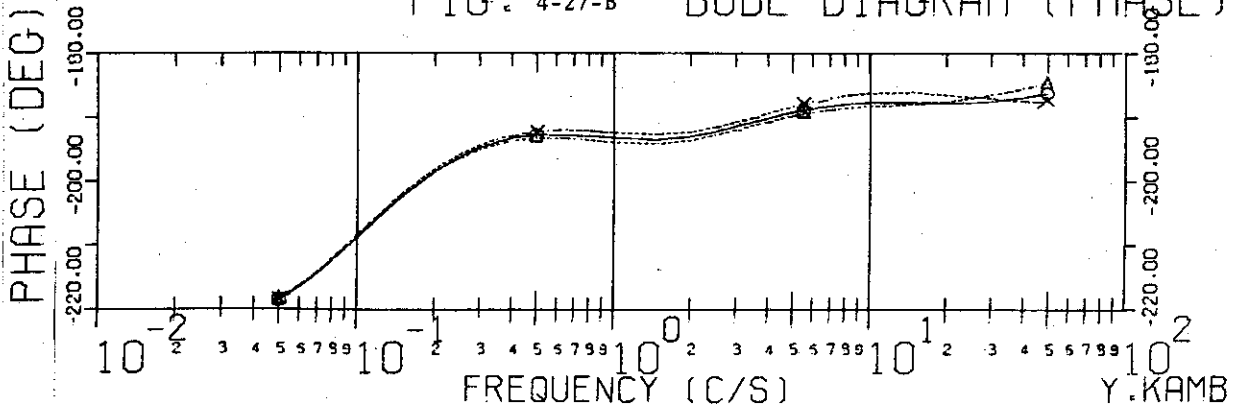


FIG. 4-27-B BODE DIAGRAM (PHASE)









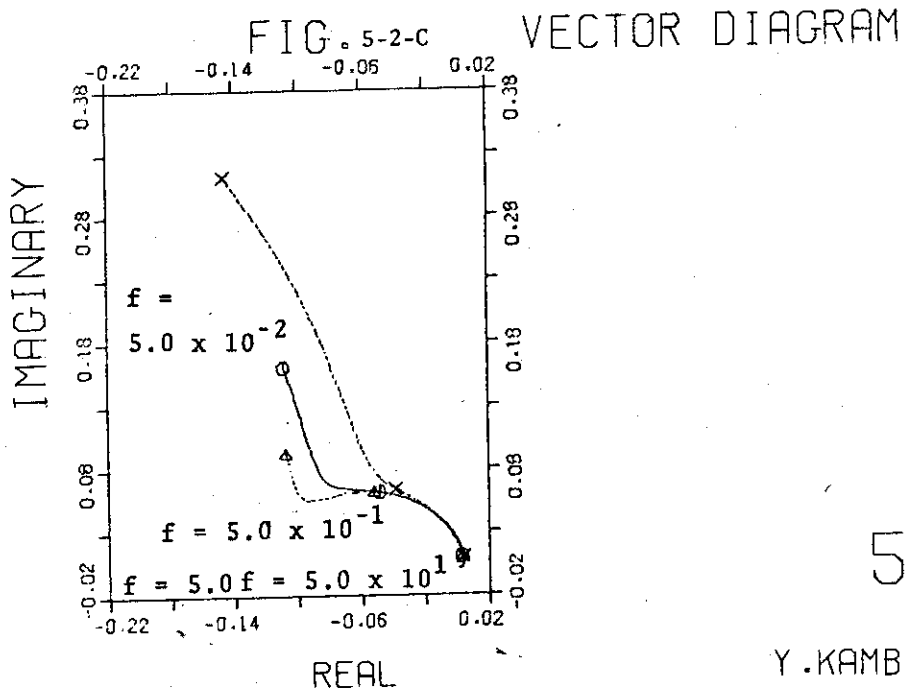
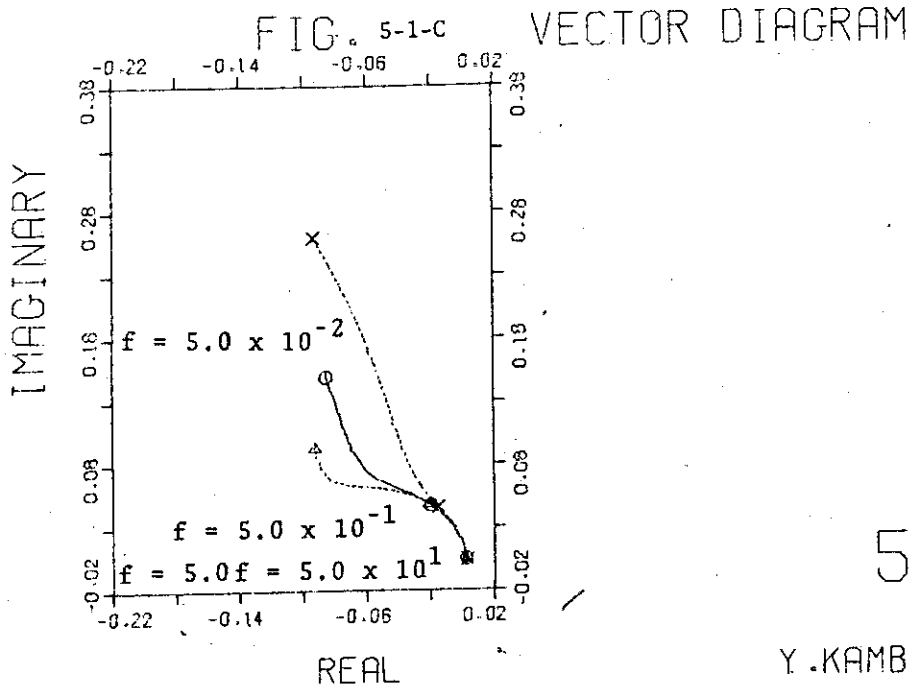
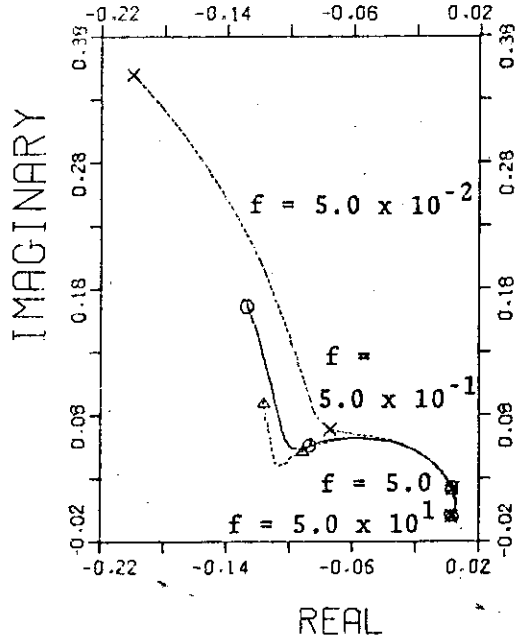






FIG. 5-3-C

VECTOR DIAGRAM

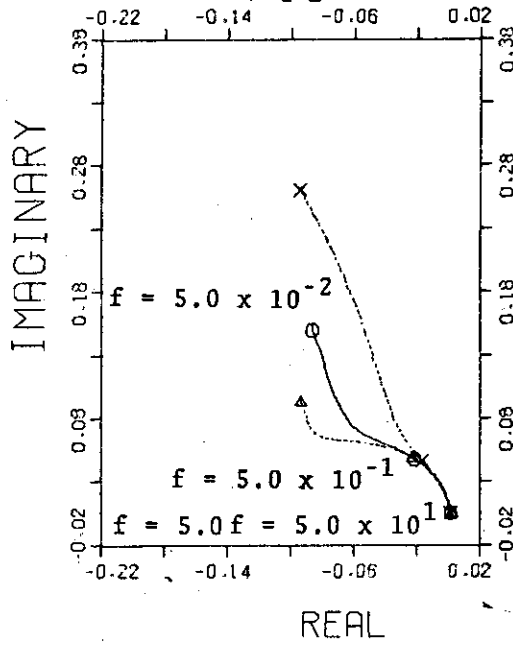


5

Y.KAMB

FIG. 5-4-C

VECTOR DIAGRAM



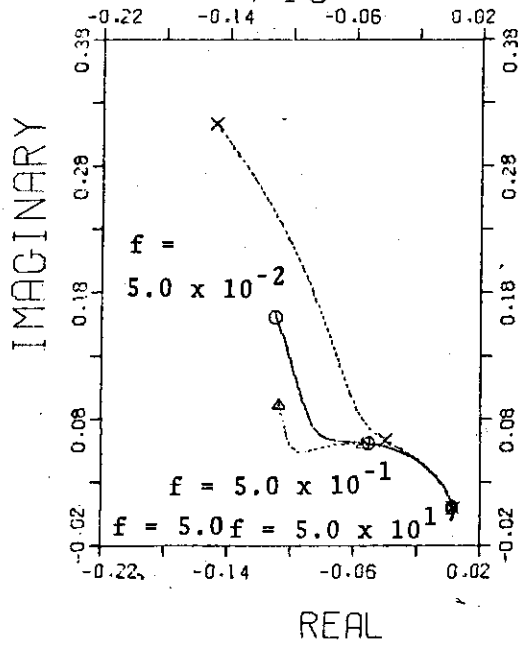
5

Y.KAMB





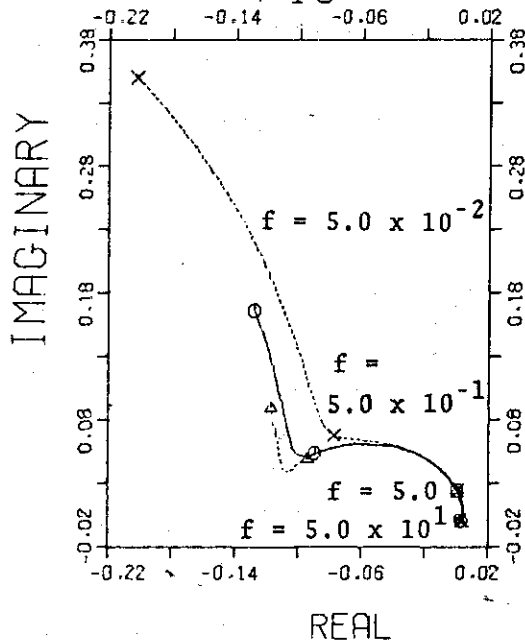
FIG. 5-5-C VECTOR DIAGRAM



6

Y.KAMB

FIG. 5-6-C VECTOR DIAGRAM



6

Y.KAMB







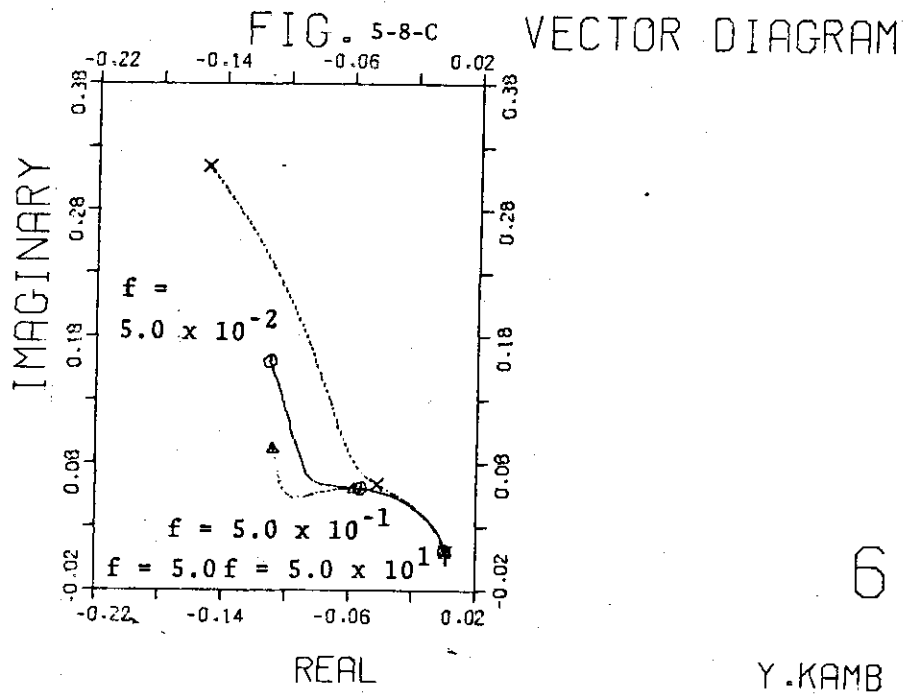
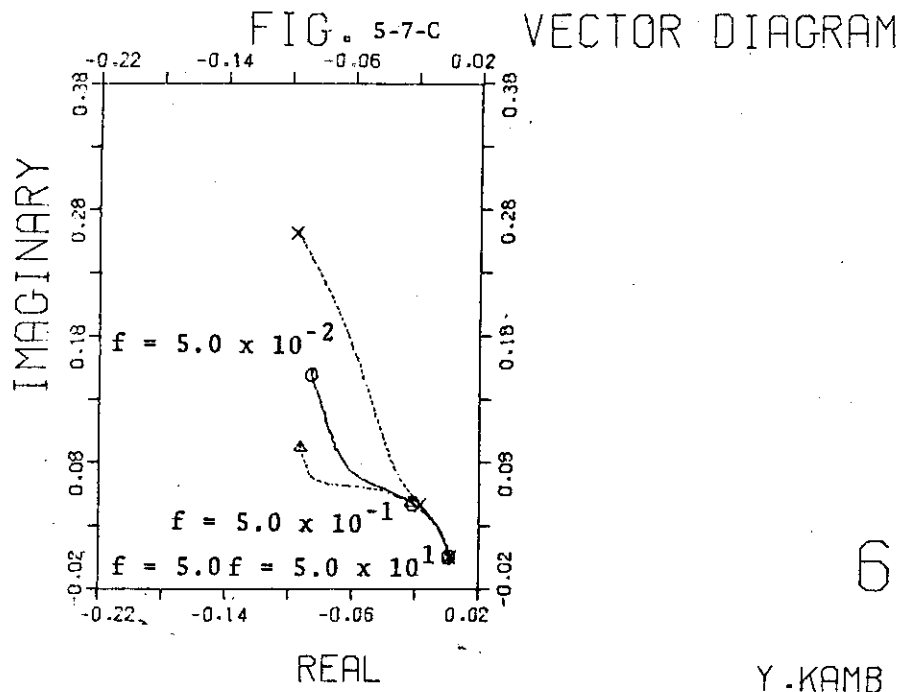
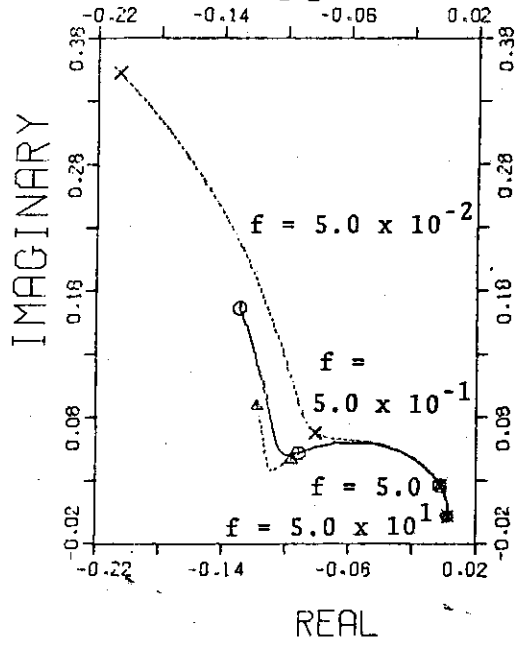






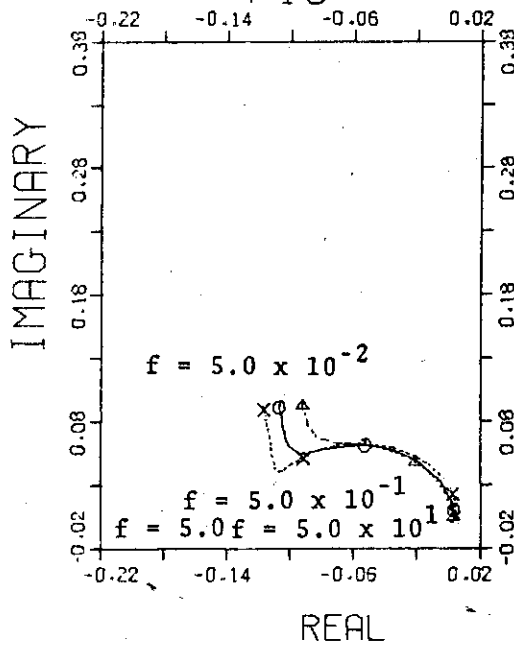
FIG. 5-9-C VECTOR DIAGRAM



6

Y.KAMB

FIG. 5-10-C VECTOR DIAGRAM



6

Y.KAMB



Fig. 5-12 Frequency Characteristics

Terminal Voltage ( $\delta V/V_0$ )  $\rightarrow$  Plasma Position ( $\delta R/R_0$ )

$\Gamma_0 = 2.2$	$\tau_x = 0.01$	$\tau_v = 1.0$	--- $\Delta$ ---	$\tau_t = 10.0$
		0.5	--- $\circ$ ---	
$G = -0.8$		0.2	--- $\times$ ---	

FIG. 5-12-A BODE DIAGRAM (GAIN)

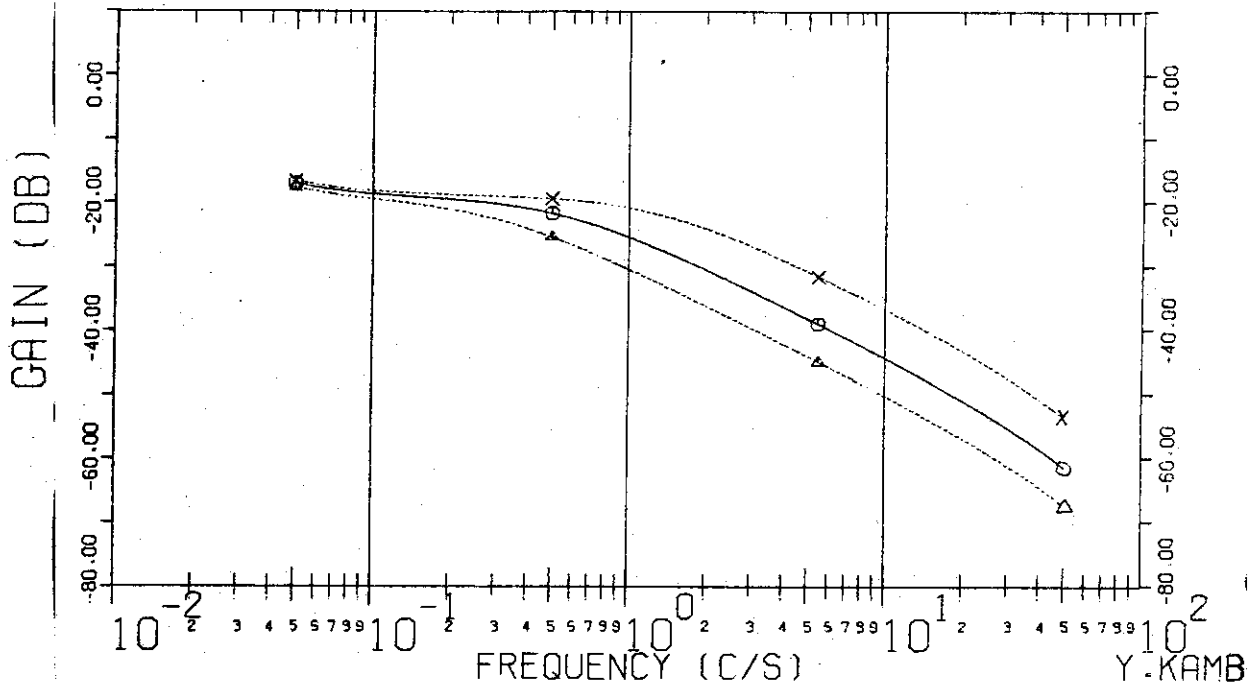


FIG. 5-12-B BODE DIAGRAM (PHASE)

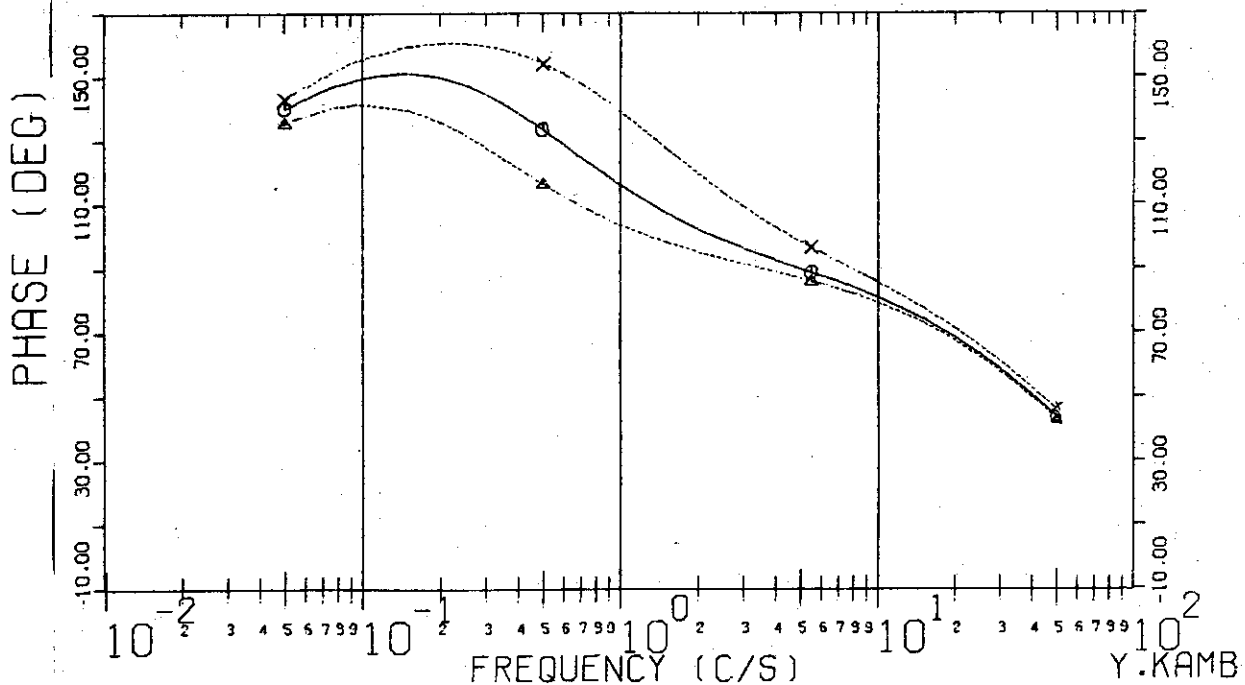
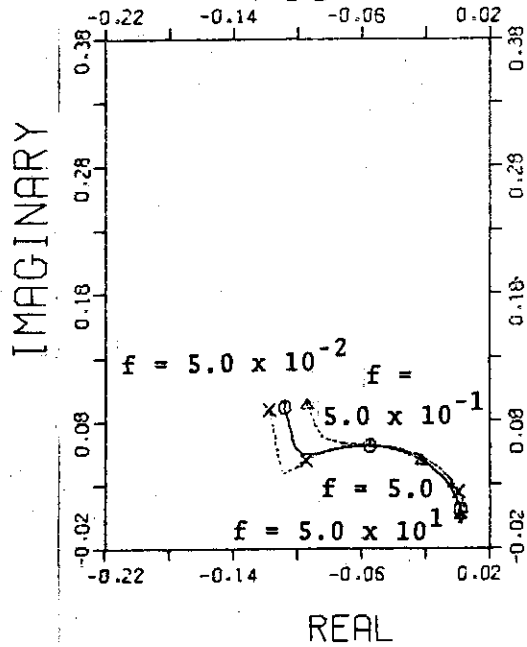




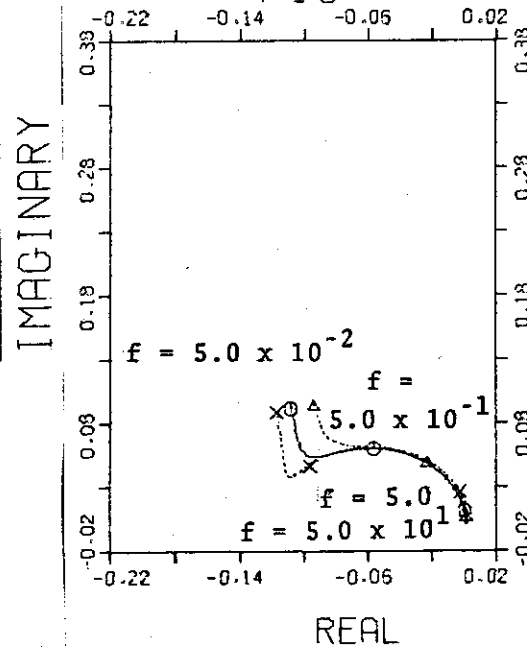
FIG. 5-11-C VECTOR DIAGRAM



6

Y.KAMB

FIG. 5-12-C VECTOR DIAGRAM



6

Y.KAMB



Fig. 5-14 Frequency Characteristics

Terminal Voltage ( $\delta V/V_0$ )  $\rightarrow$  Plasma Position ( $\delta R/R_0$ )

$\Gamma_0 = 2.2$	$\tau_l = 0.02$	$\tau_v = 1.0$	--- $\Delta$ ---	$\tau_t = 5.0$
$G = -0.8$		0.5	--- $\circ$ ---	
		0.2	--- $\times$ ---	

FIG. 5-14-A BODE DIAGRAM (GAIN)

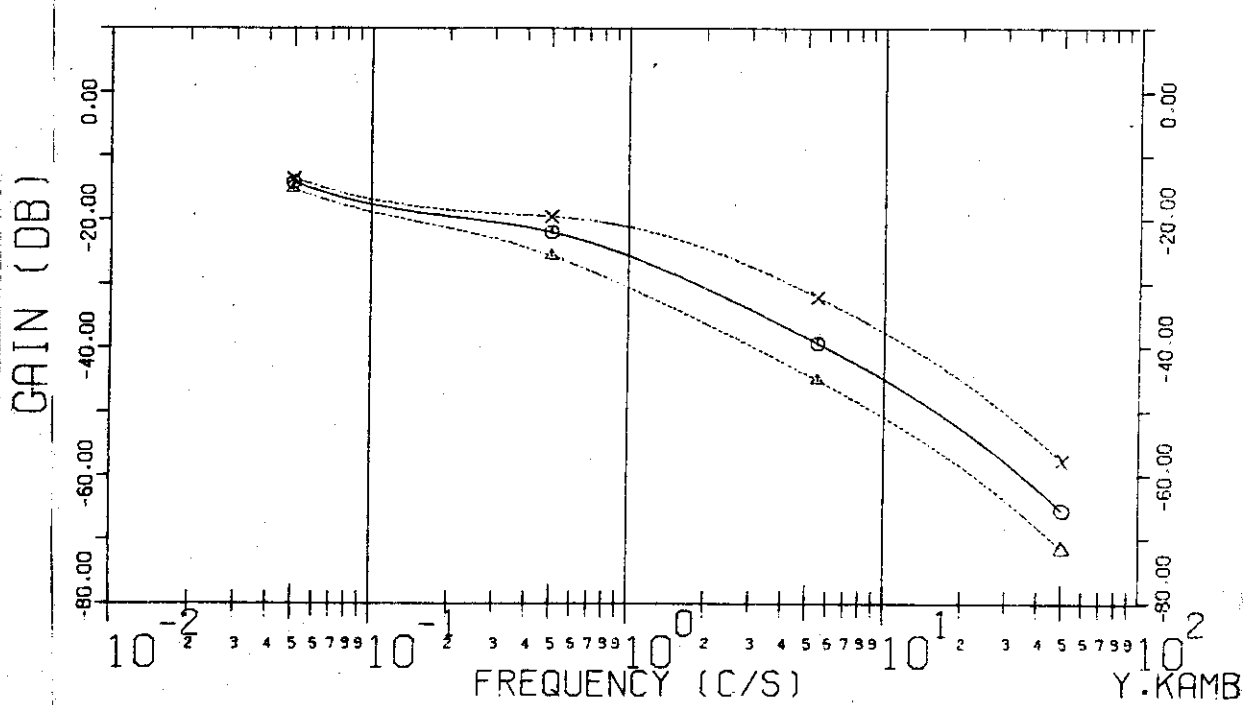
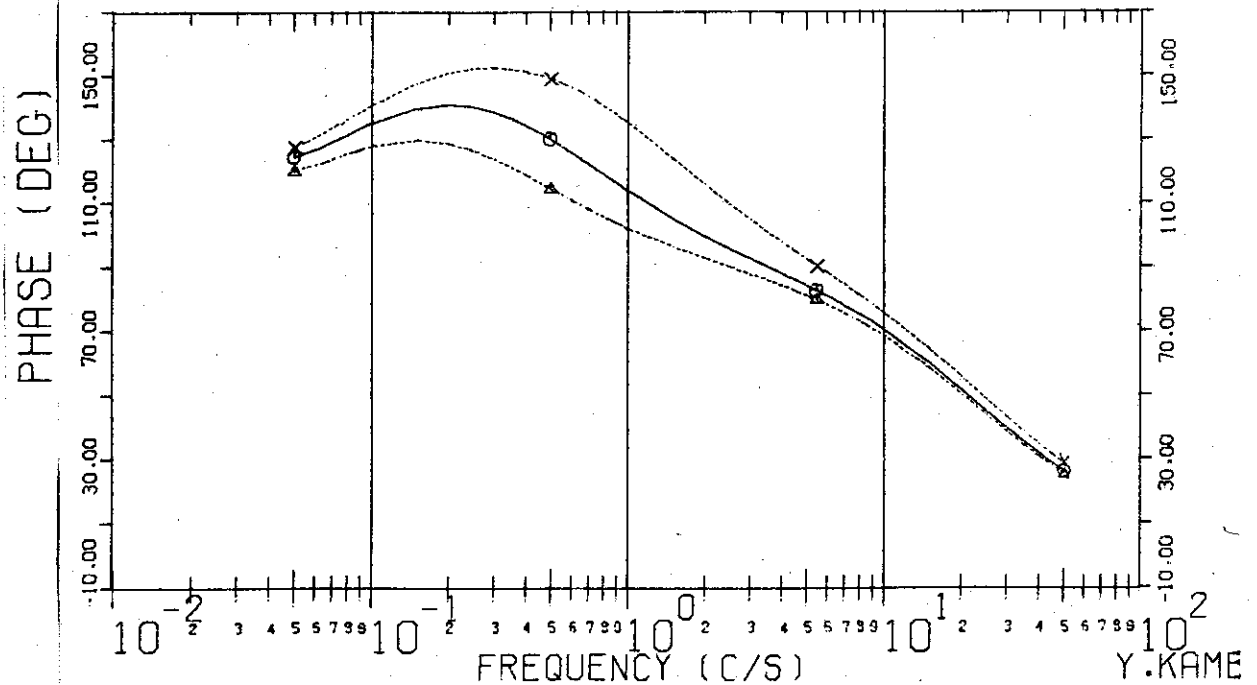


FIG. 5-14-B BODE DIAGRAM (PHASE)



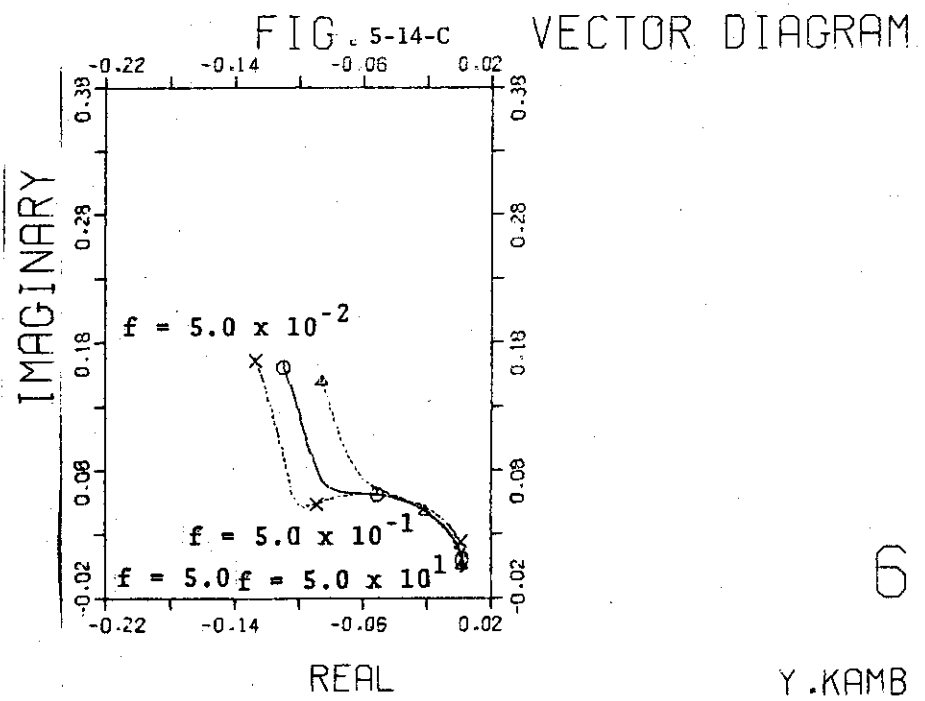
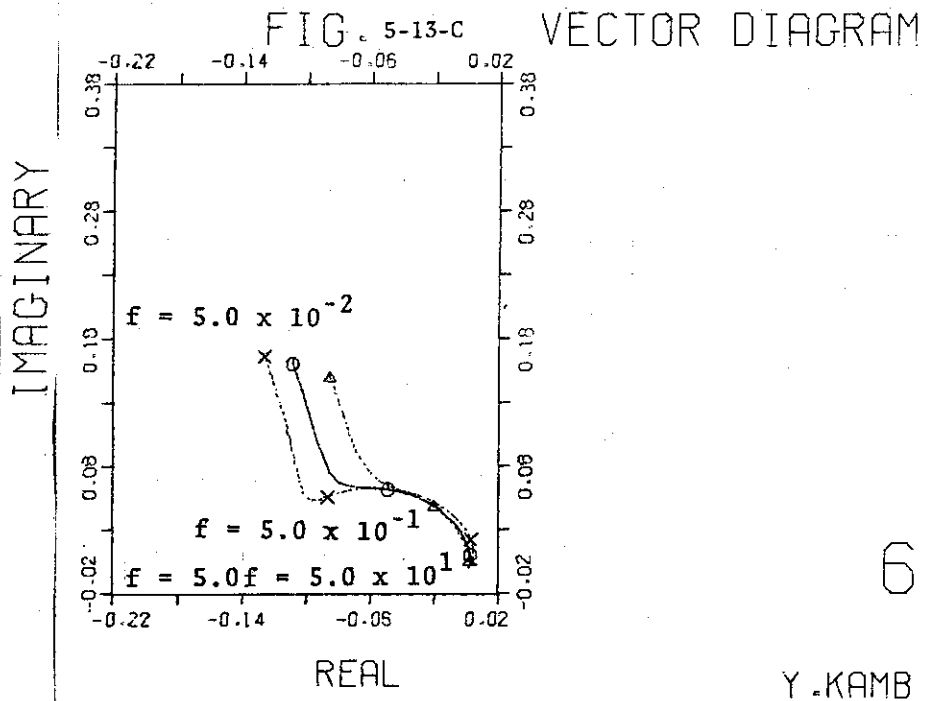
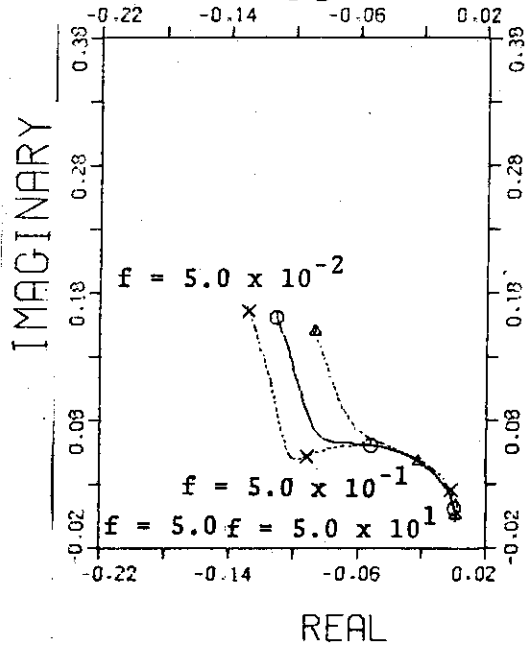






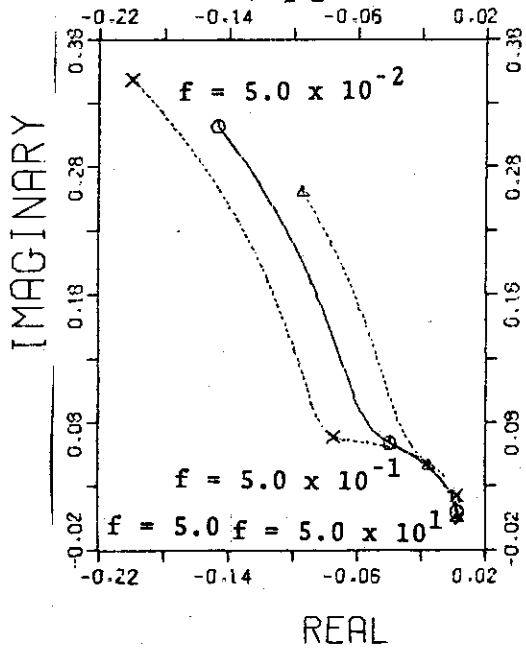
FIG. 5-15-C VECTOR DIAGRAM



7

Y.KAMB

FIG. 5-16-C VECTOR DIAGRAM



7

Y.KAMB

Fig. 5-17 Frequency Characteristics

Terminal Voltage ( $\delta V/V_0$ )  $\rightarrow$  Plasma Position ( $\delta R/R_0$ )

$\Gamma_0 = 2.2$	$\tau_k = 0.02$	$\tau_v = 1.0$	--- $\Delta$ ---	$\tau_t = 2.0$
$G = -0.8$		0.5	--- $\circ$ ---	
		0.2	--- $\times$ ---	

FIG. 5-17-A BODE DIAGRAM (GAIN)

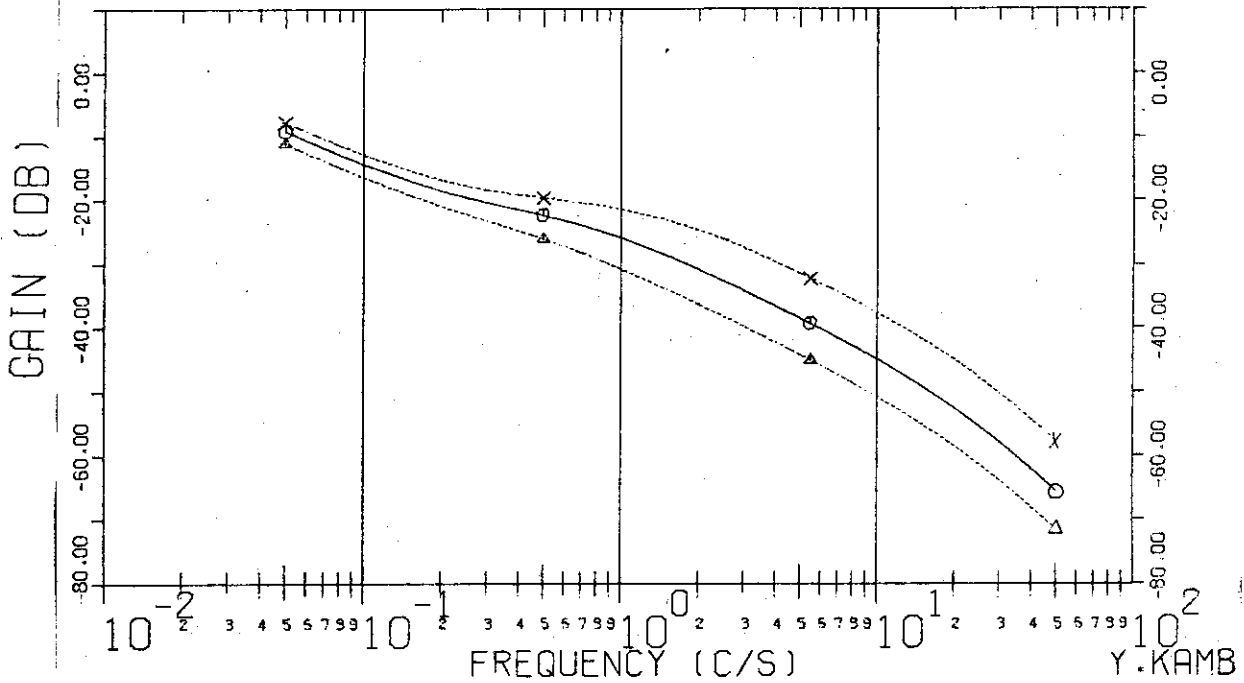


FIG. 5-17-B BODE DIAGRAM (PHASE)

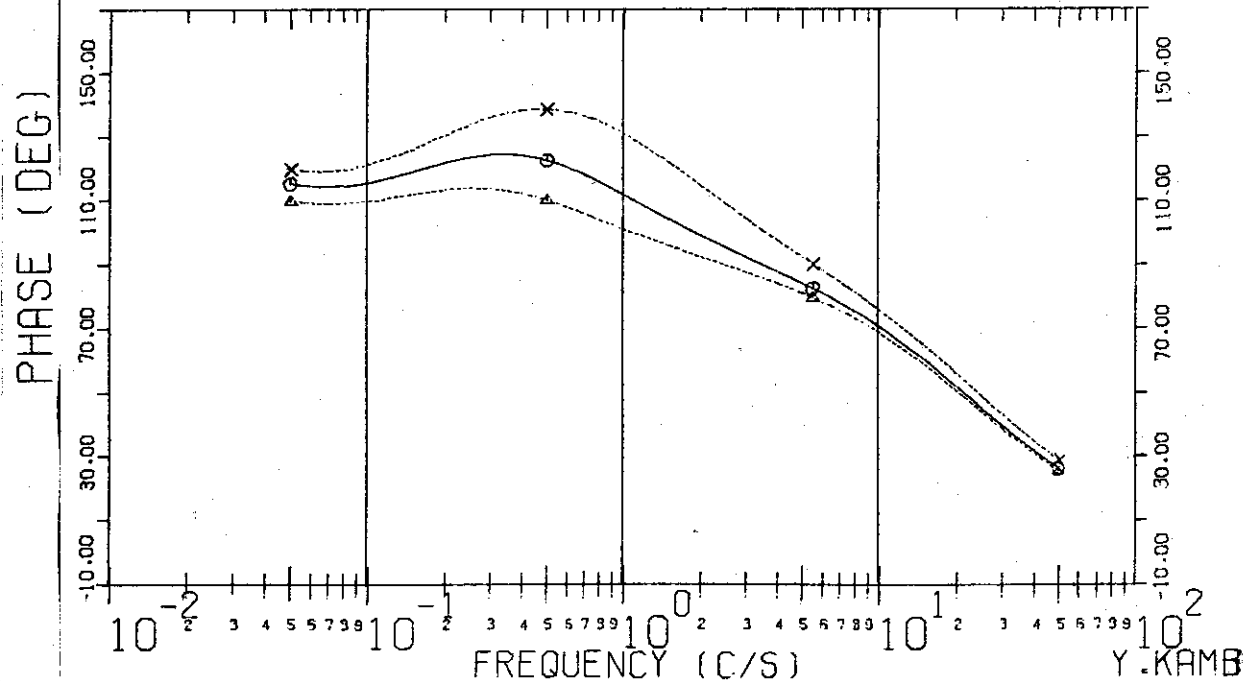




Fig.5-18 Frequency Characteristics  
 Terminal Voltage ( $\delta V/V_0$ )  $\rightarrow$  Plasma Position ( $\delta R/R_0$ )  
 $r_0 = 2.2$      $\tau_z = 0.01$      $\tau_y = 1.0$      $\tau_t = 2.0$   
 $G = -0.8$                          0.5     $\circ$                          0.2     $\times$

FIG. 5-18-A BODE DIAGRAM (GAIN)

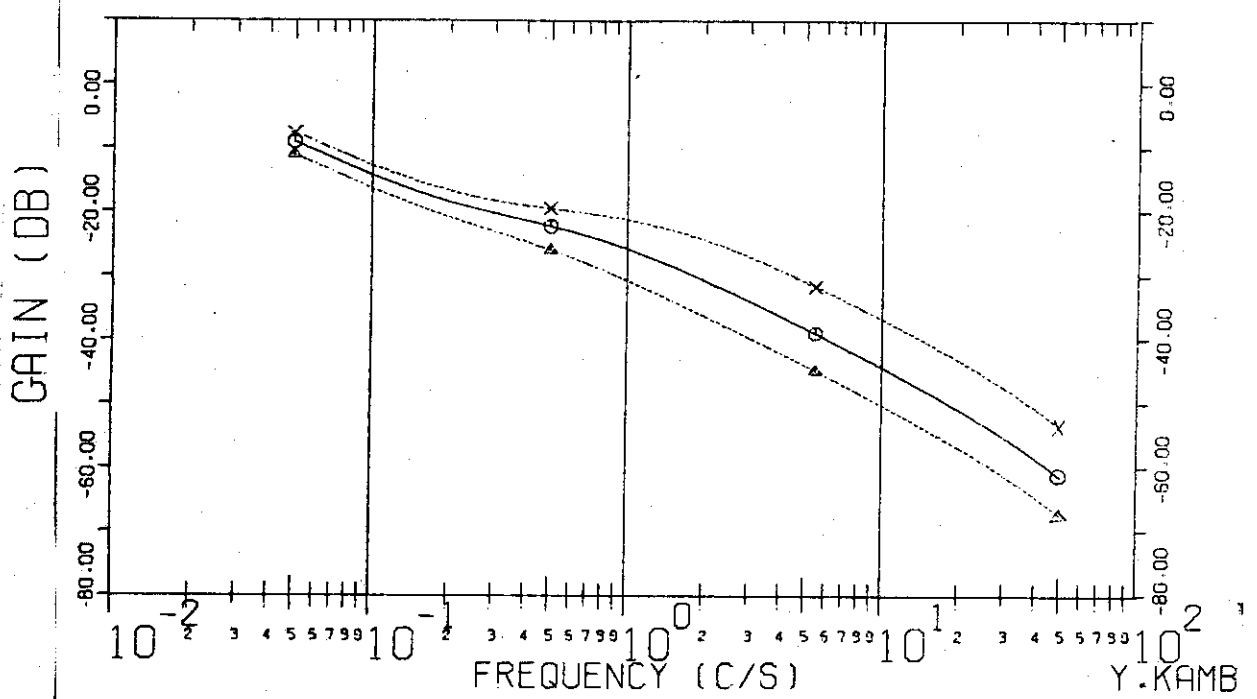


FIG. 5-18-B BODE DIAGRAM (PHASE)

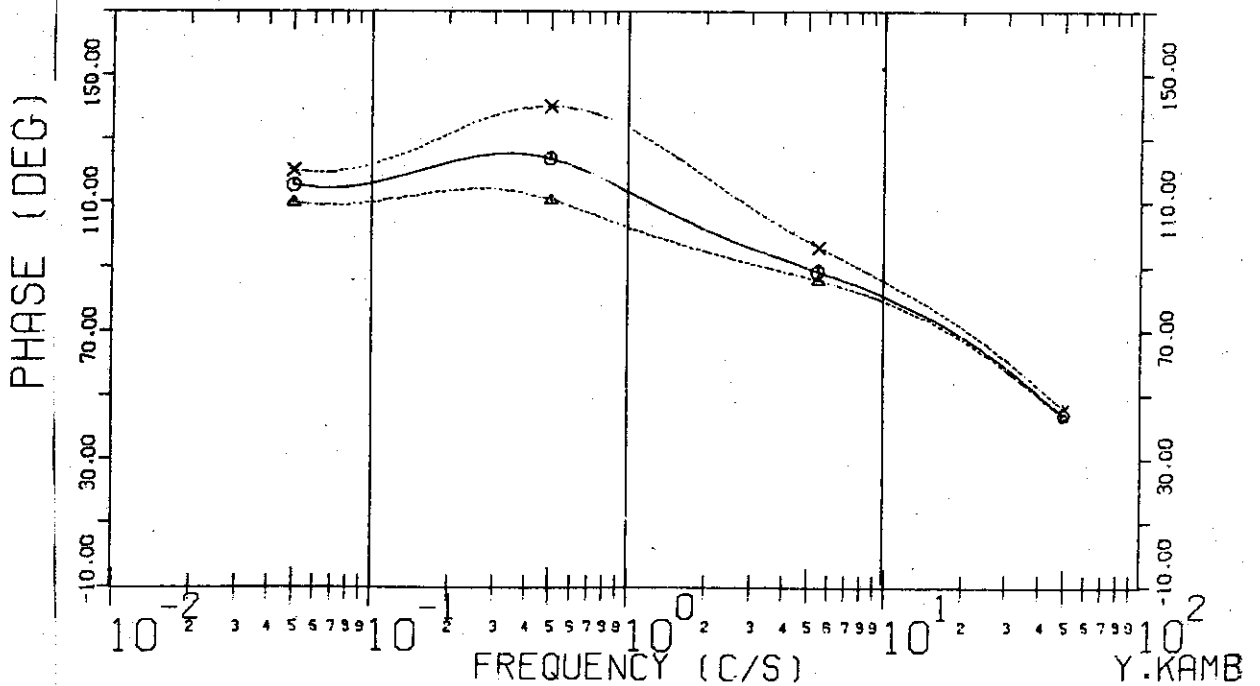
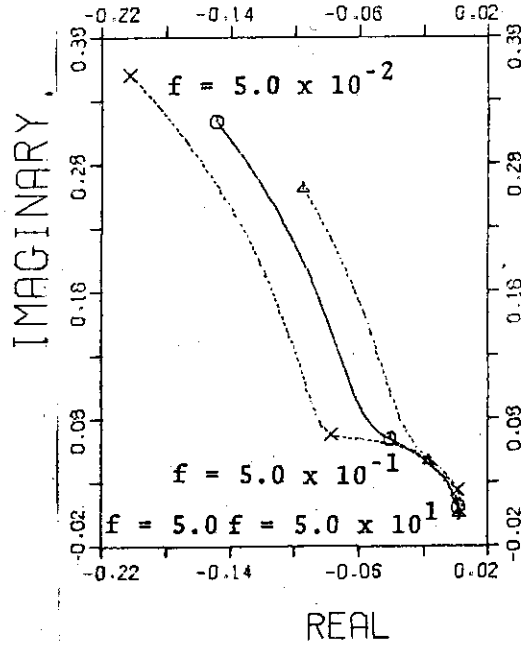


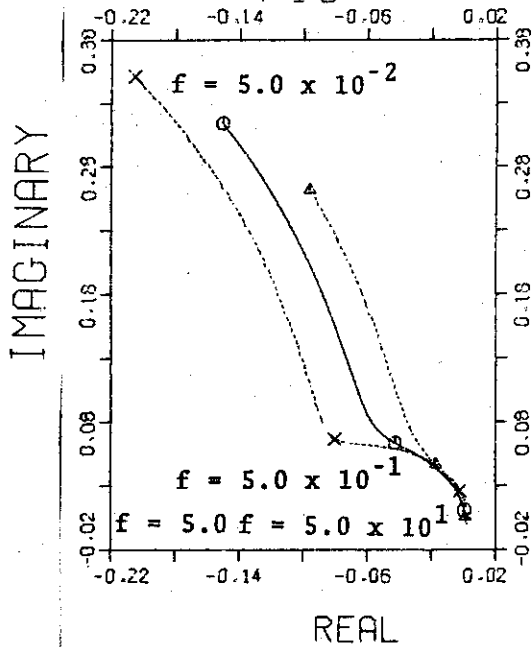
FIG. 5-17-C VECTOR DIAGRAM



7

Y.KAMB

FIG. 5-18-C VECTOR DIAGRAM



7

Y.KAMB

Fig. 5-19 Frequency Characteristics

Terminal Voltage ( $\delta V/V_0$ )  $\rightarrow$  Plasma Position ( $\delta R/R_0$ )

$\Gamma_0 = 2.2$	$\tau_l = 0.03$ --- $\Delta$ ---	$\tau_v = 1.0$	$\tau_t = 10.0$
$G = -0.8$	0.02 --- $\circ$ ---		
	0.01 --- $\times$ ---		

FIG. 5-19-A BODE DIAGRAM (GAIN)

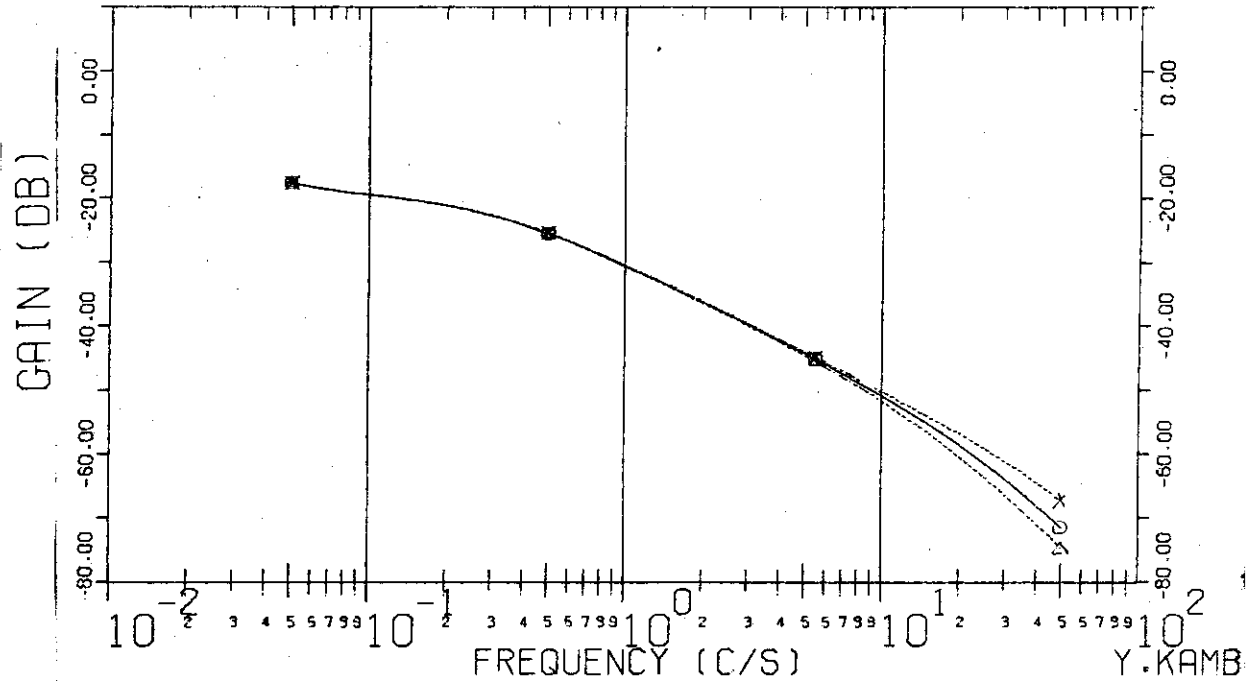


FIG. 5-19-B BODE DIAGRAM (PHASE)

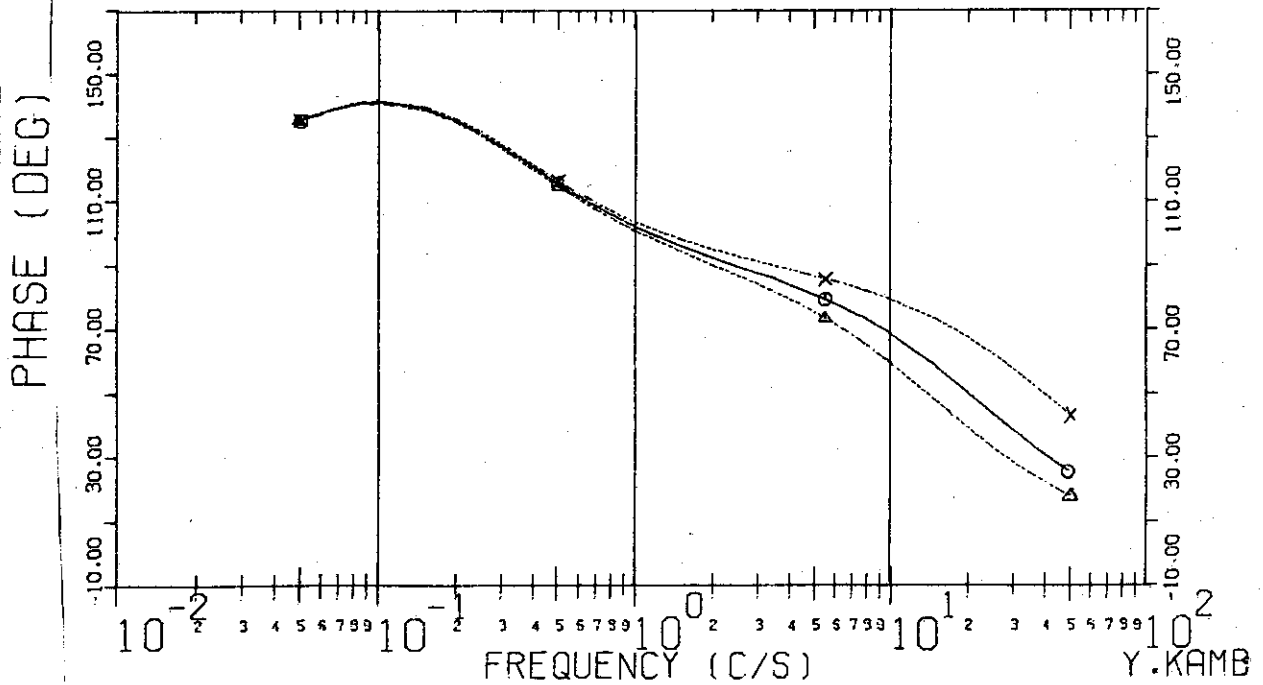


Fig.5-20 Frequency Characteristics

Terminal Voltage ( $\delta V/V_0$ )  $\rightarrow$  Plasma Position ( $\delta R/R_0$ )

$\Gamma_0 = 2.2$        $\tau_l = 0.03$  --- $\Delta$ ---       $\tau_v = 1.0$        $\tau_t = 5.0$   
 $G = -0.8$       0.02 --- $\circ$ ---       $\tau_v = 1.0$        $\tau_t = 5.0$   
                   0.01 --- $\times$ ---

FIG. 5-20-A BODE DIAGRAM (GAIN)

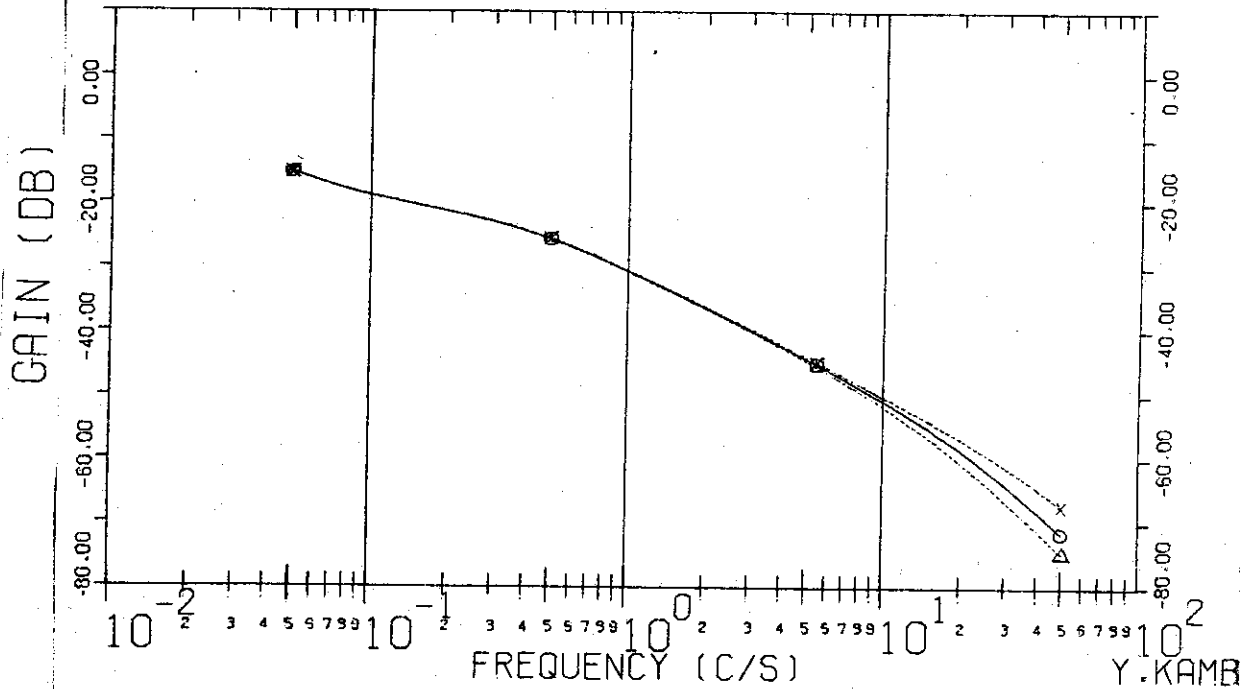


FIG. 5-20-B BODE DIAGRAM (PHASE)

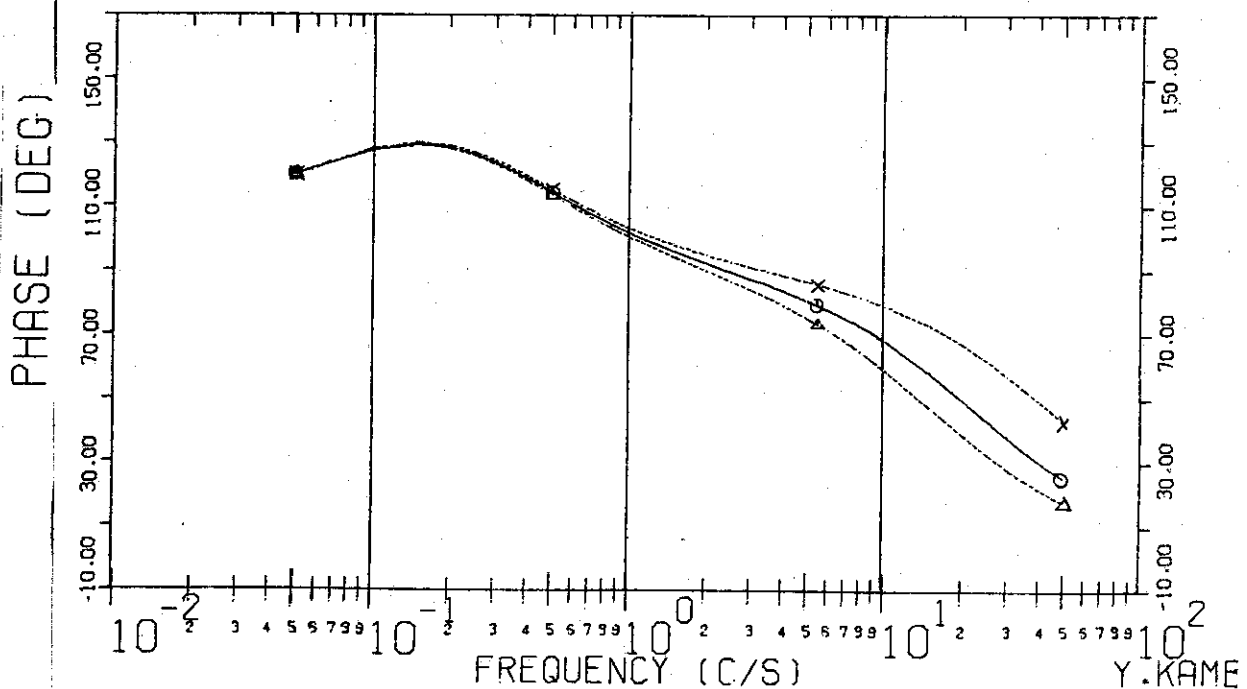
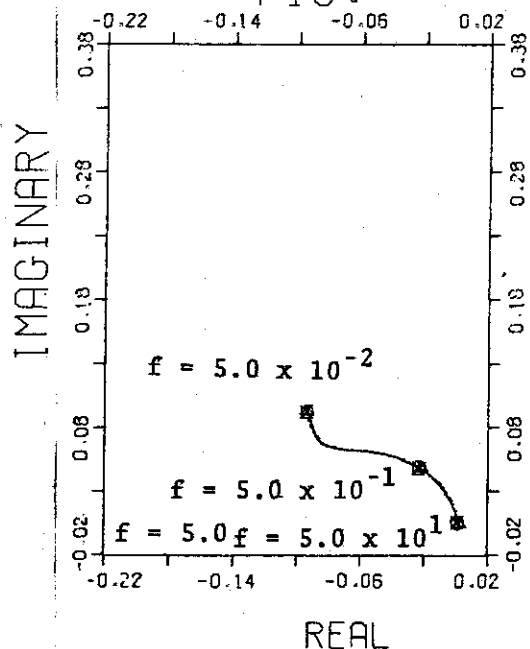


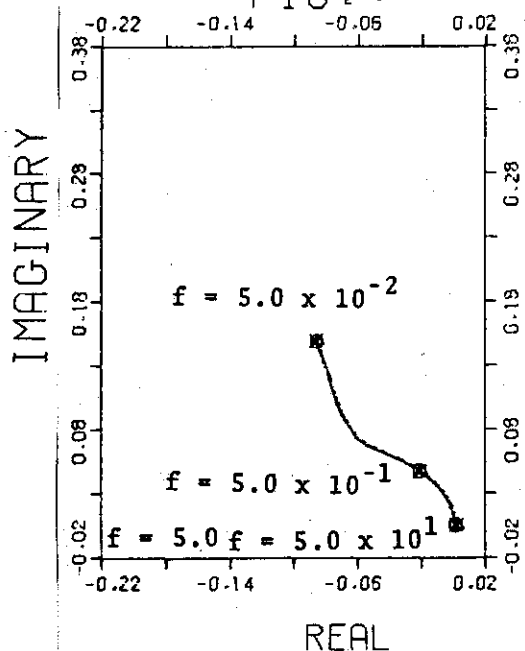
FIG. 5-19-C VECTOR DIAGRAM



7

Y.KAMB

FIG. 5-20-C VECTOR DIAGRAM



7

Y.KAMB

Fig. 5-21 Frequency Characteristics

Terminal Voltage ( $\delta V/V_0$ )  $\rightarrow$  Plasma Position ( $\delta R/R_0$ )

$\Gamma_0 = 2.2$	$\tau_L = 0.03$ --- $\Delta$ ---	$\tau_V = 1.0$	$\tau_t = 2.0$
$G = -0.8$	0.02 --- $\circ$ ---		
	0.01 --- $\times$ ---		

FIG. 5-21-A BODE DIAGRAM (GAIN)

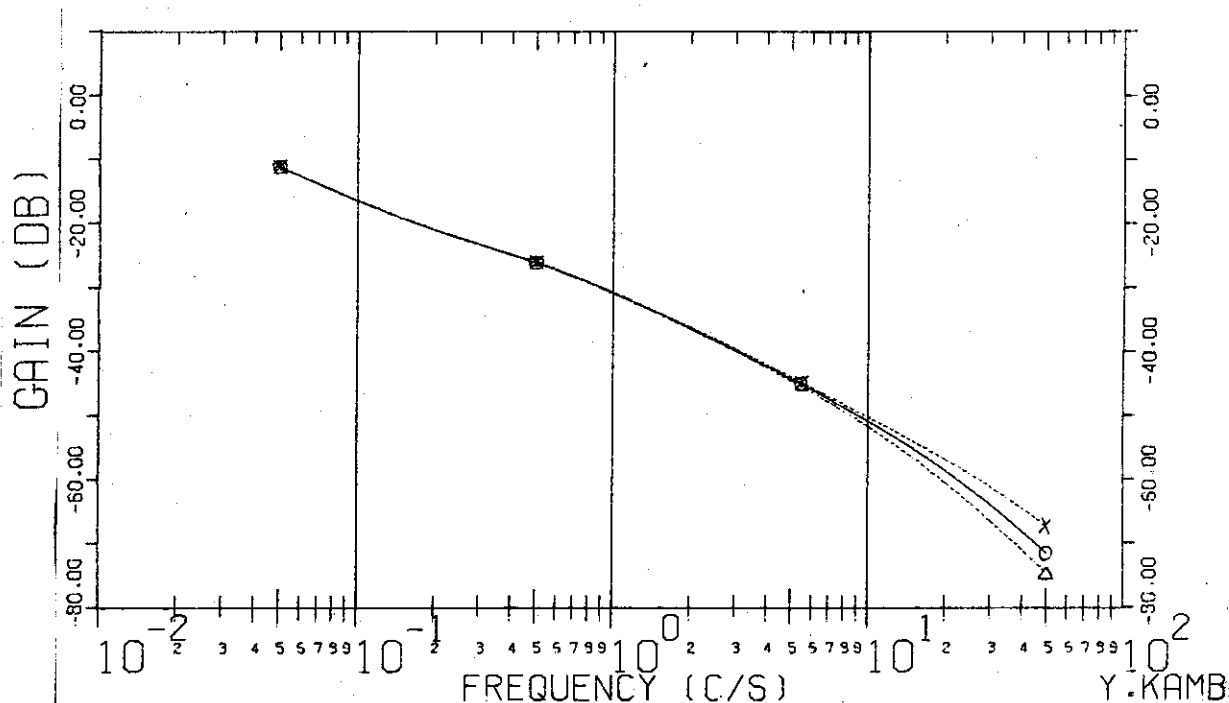


FIG. 5-21-B BODE DIAGRAM (PHASE)

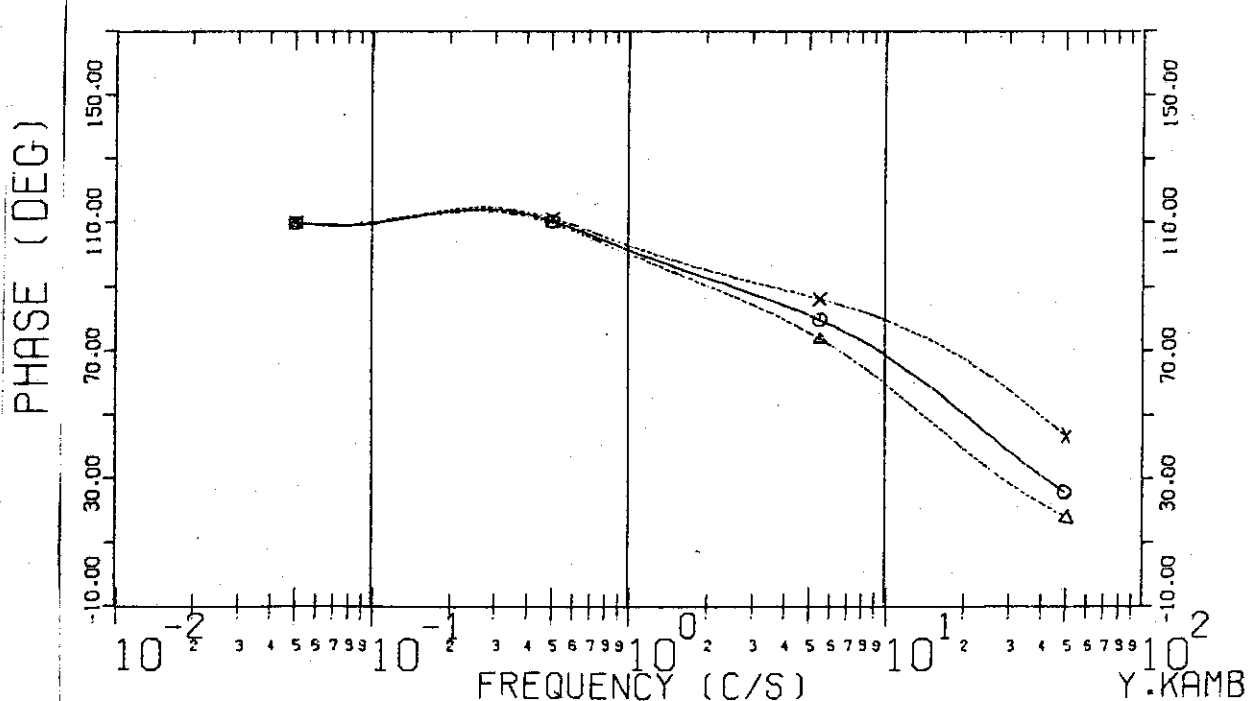


Fig.5-22 Frequency Characteristics  
 Terminal Voltage ( $\delta V/V_0$ )  $\rightarrow$  Plasma Position ( $\delta R/R_0$ )  
 $\Gamma_0 = 2.2$        $\tau_l = 0.03$     --- $\Delta$ ---     $\tau_V = 0.5$      $\tau_t = 10.0$   
 $G = -0.8$       0.02    --- $\circ$ ---  
 0.01    --- $\times$ ---

FIG. 5-22-A BODE DIAGRAM (GAIN)

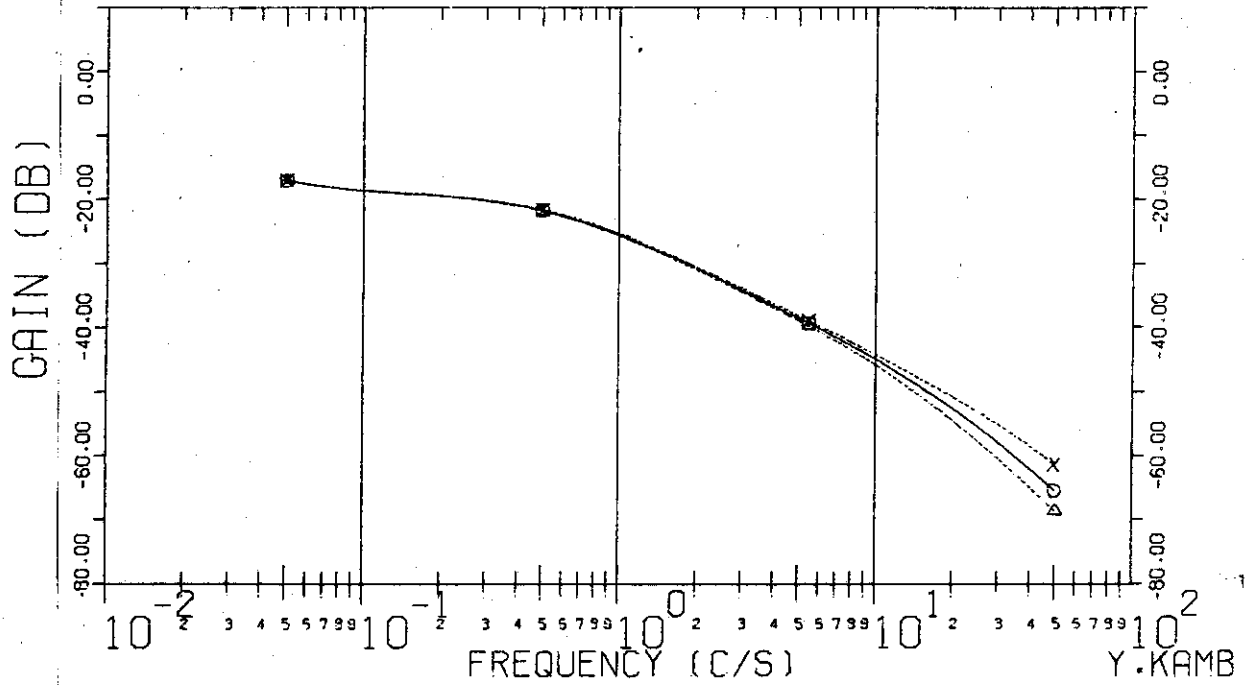


FIG. 5-22-B BODE DIAGRAM (PHASE)

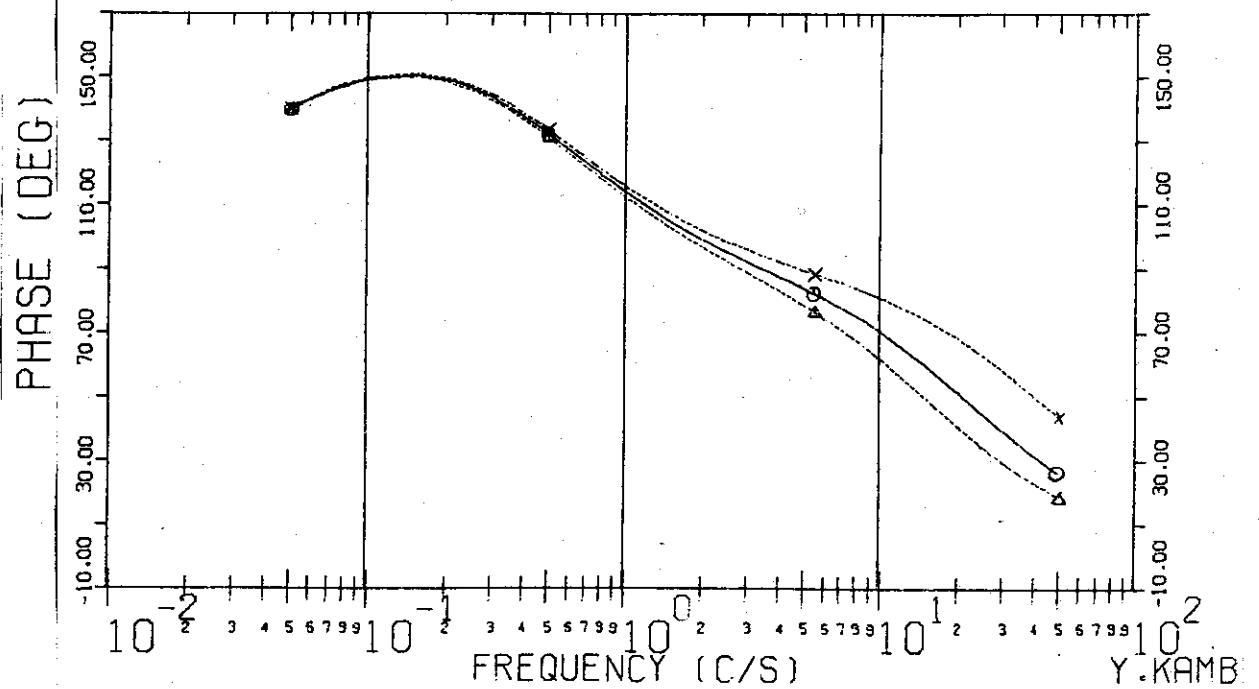
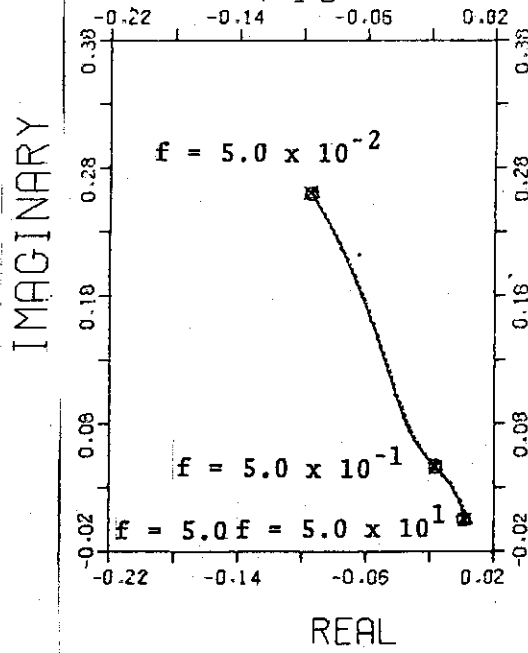


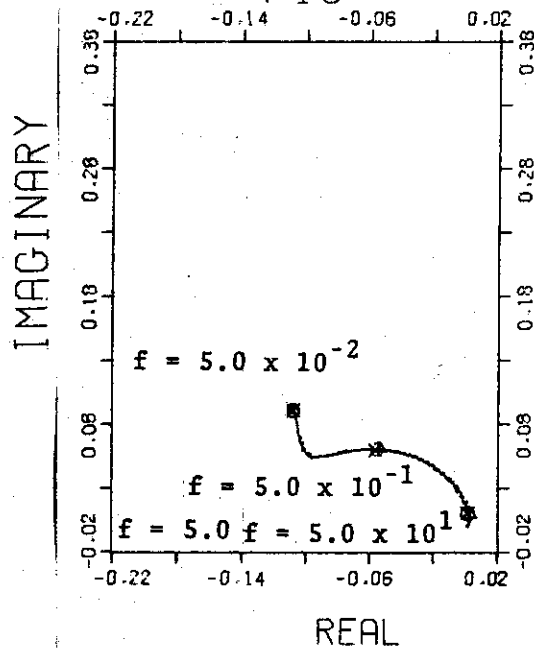
FIG. 5-21-C VECTOR DIAGRAM



7

Y.KAMB

FIG. 5-22-C VECTOR DIAGRAM



7

Y.KAMB



Fig. 5-23 Frequency Characteristics  
 Terminal Voltage ( $\delta V/V_0$ )  $\rightarrow$  Plasma Position ( $\delta R/R_0$ )  
 $\Gamma_0 = 2.2$        $\tau_l = 0.03$  --- $\Delta$ ---       $\tau_v = 0.5$        $\tau_t = 5.0$   
 $G = -0.8$       0.02 --- $\circ$ ---  
 0.01 --- $\times$ ---

FIG. 5-23-A BODE DIAGRAM (GAIN)

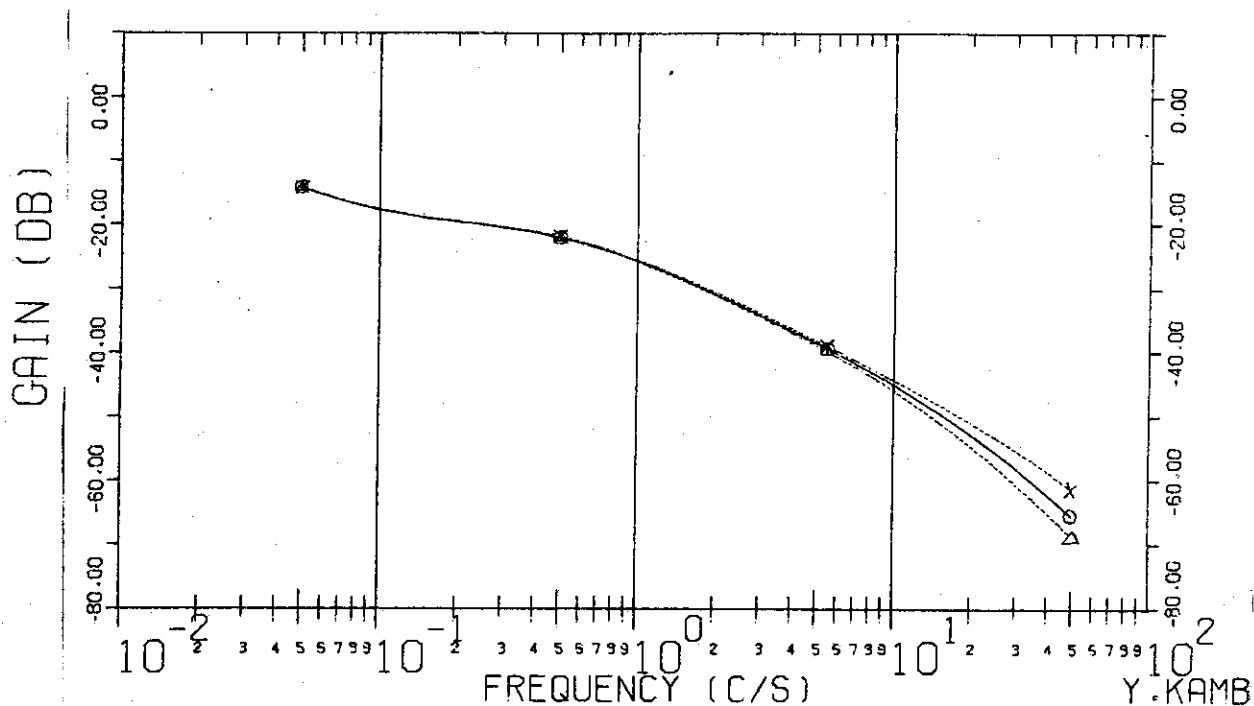


FIG. 5-23-B BODE DIAGRAM (PHASE)

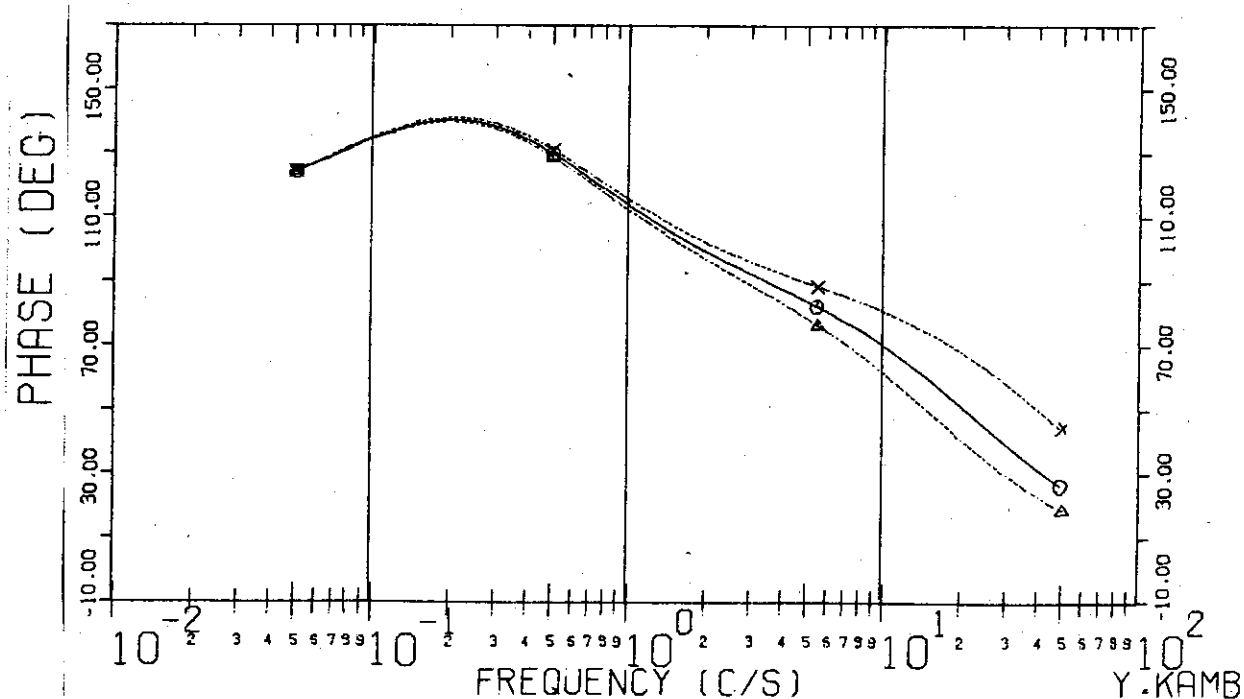


Fig. 5-24 Frequency Characteristics  
 Terminal Voltage ( $\delta V/V_0$ )  $\rightarrow$  Plasma Position ( $\delta R/R_0$ )  
 $\Gamma_0 = 2.2$      $\tau_l = 0.03$  --- $\Delta$ ---     $\tau_v = 0.5$      $\tau_t = 2.0$   
 $G = -0.8$     0.02 --- $\circ$ ---  
 0.01 --- $\times$ ---

FIG. 5-24-A BODE DIAGRAM (GAIN)

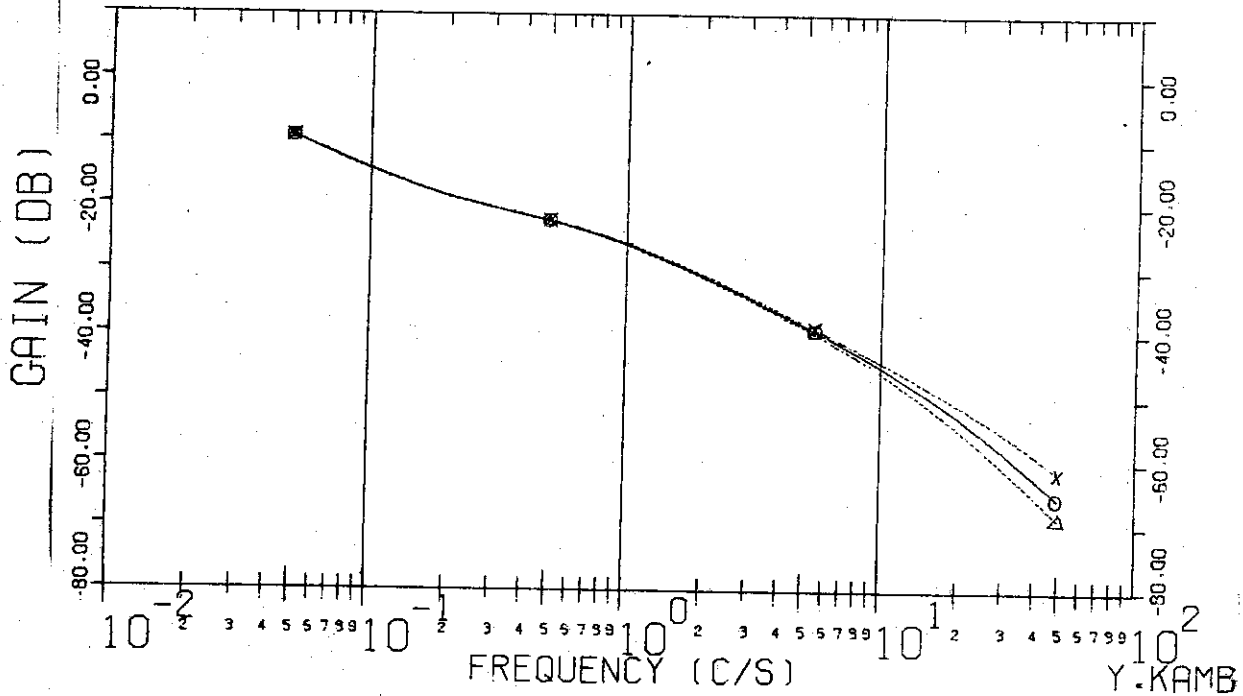
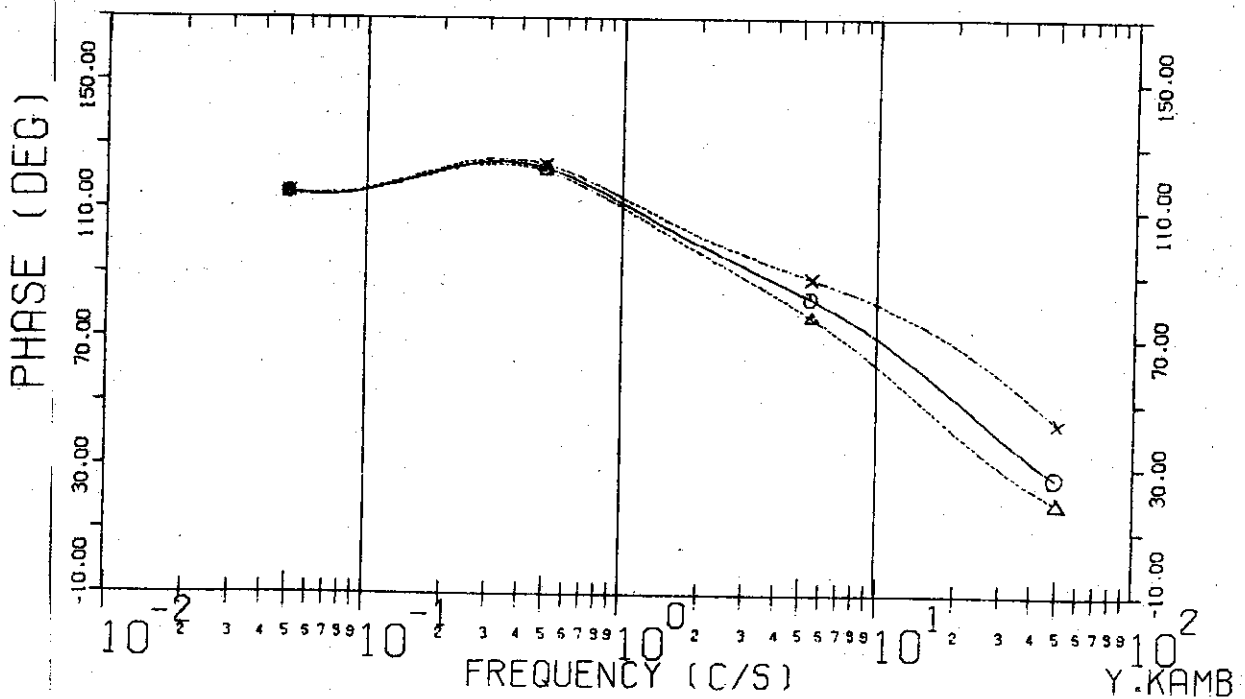


FIG. 5-24-B BODE DIAGRAM (PHASE)



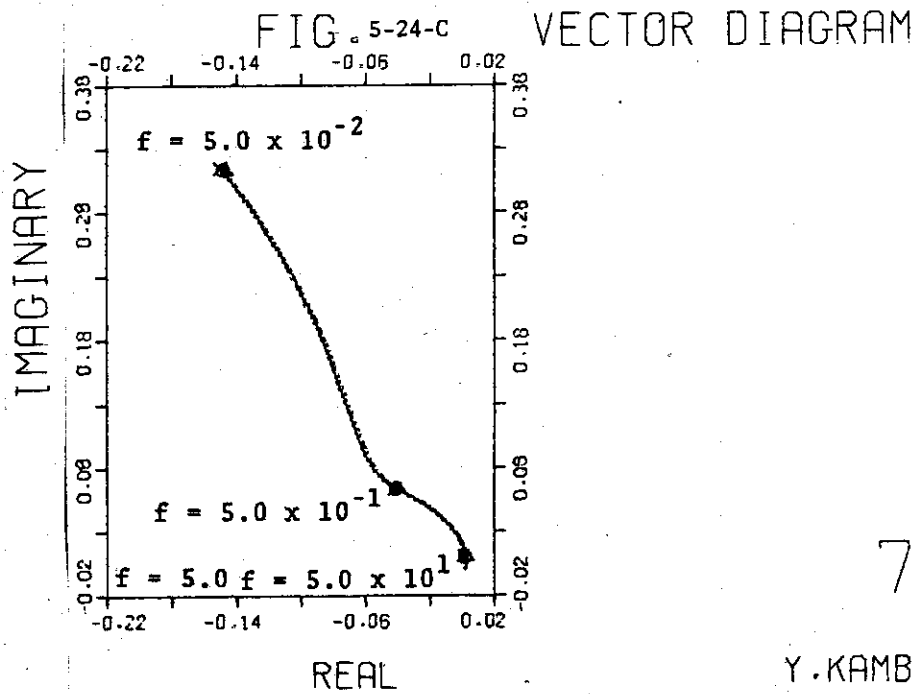
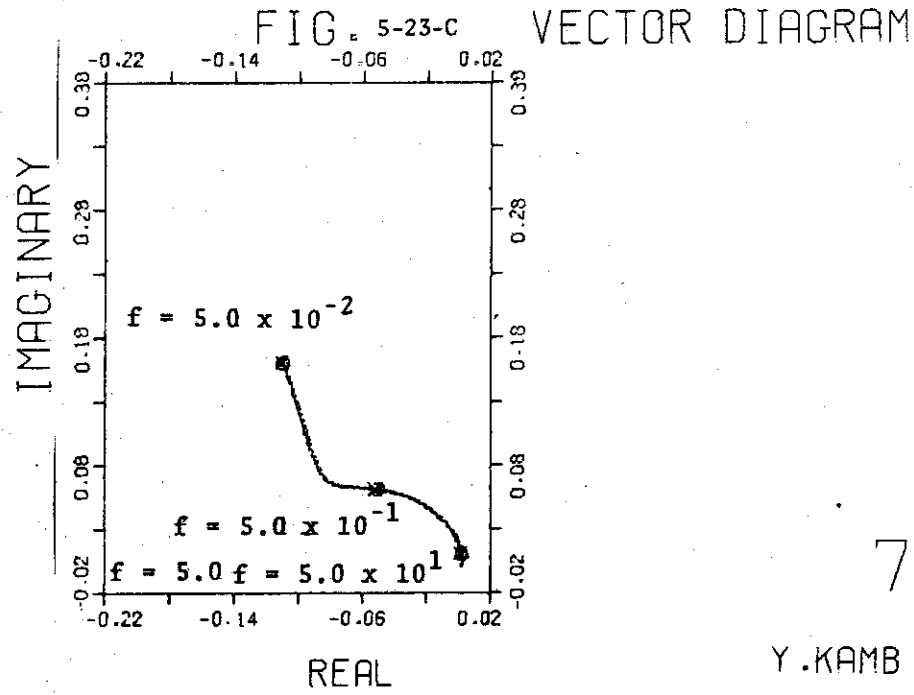


Fig.5-25 Frequency Characteristics

Terminal Voltage ( $\delta V/V_0$ )  $\rightarrow$  Plasma Position ( $\delta R/R_0$ )

$\Gamma_0 = 2.2$	$\tau_f = 0.03$	--- $\Delta$ ---	$\tau_v = 0.2$	$\tau_t = 10.0$
$G = -0.8$	0.02	— $\circ$ —		
	0.01	--- $\times$ ---		

FIG. 5-25-A BODE DIAGRAM (GAIN)

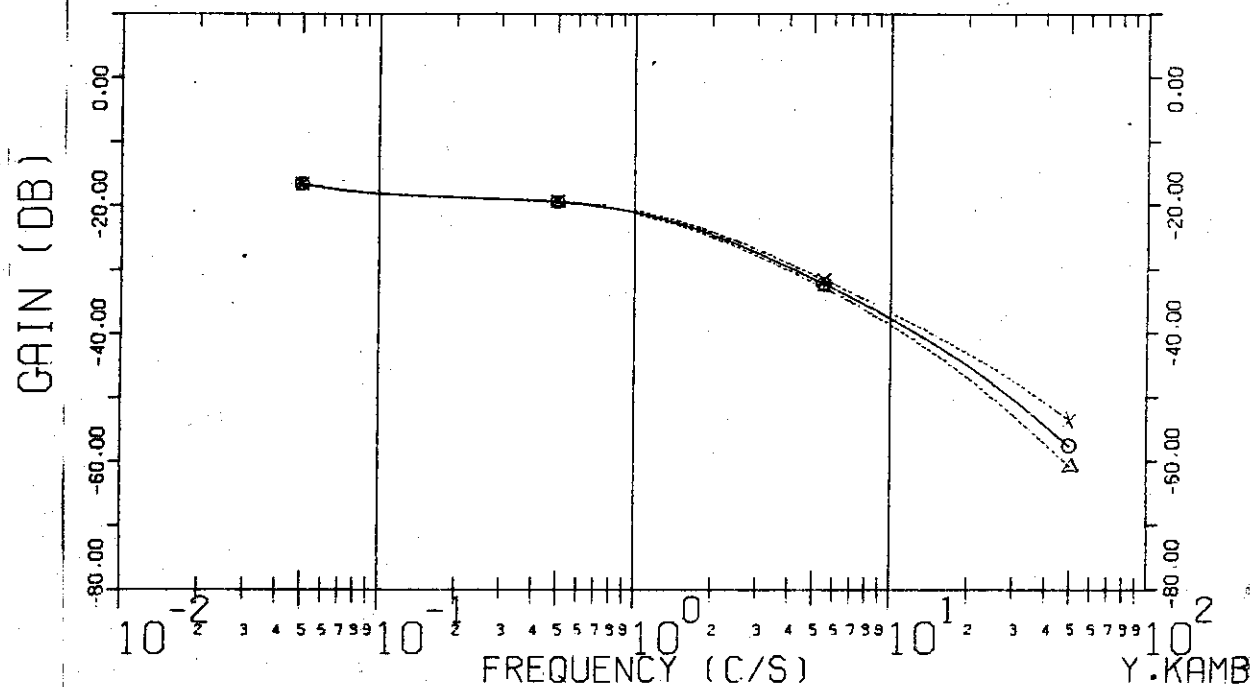


FIG. 5-25-B BODE DIAGRAM (PHASE)

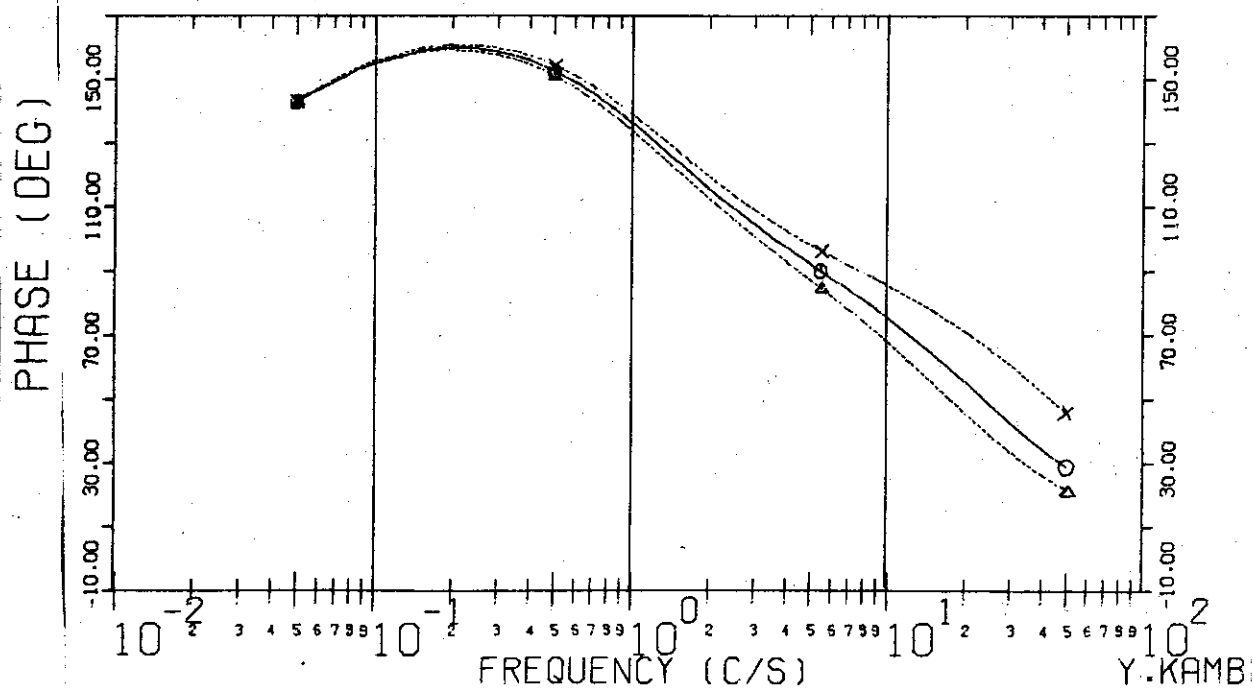


Fig. 5-26 Frequency Characteristics

Terminal Voltage ( $\delta V/V_0$ )  $\rightarrow$  Plasma Position ( $\delta R/R_0$ )

$\Gamma_0 = 2.2$	$\tau_l = 0.03$ --- $\Delta$ ---	$\tau_v = 0.2$	$\tau_t = 5.0$
$G = -0.8$	$0.02$ --- $\circ$ ---		
	$0.01$ --- $\times$ ---		

FIG. 5-26-A BODE DIAGRAM (GAIN)

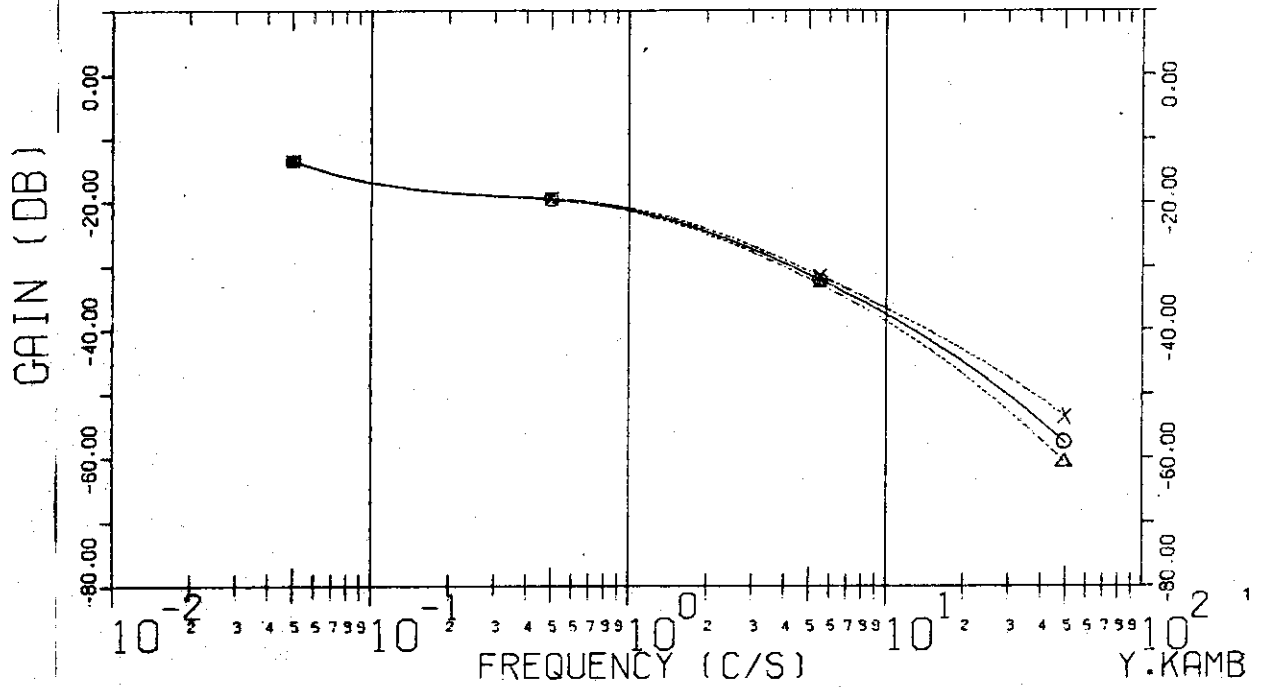


FIG. 5-26-B BODE DIAGRAM (PHASE)

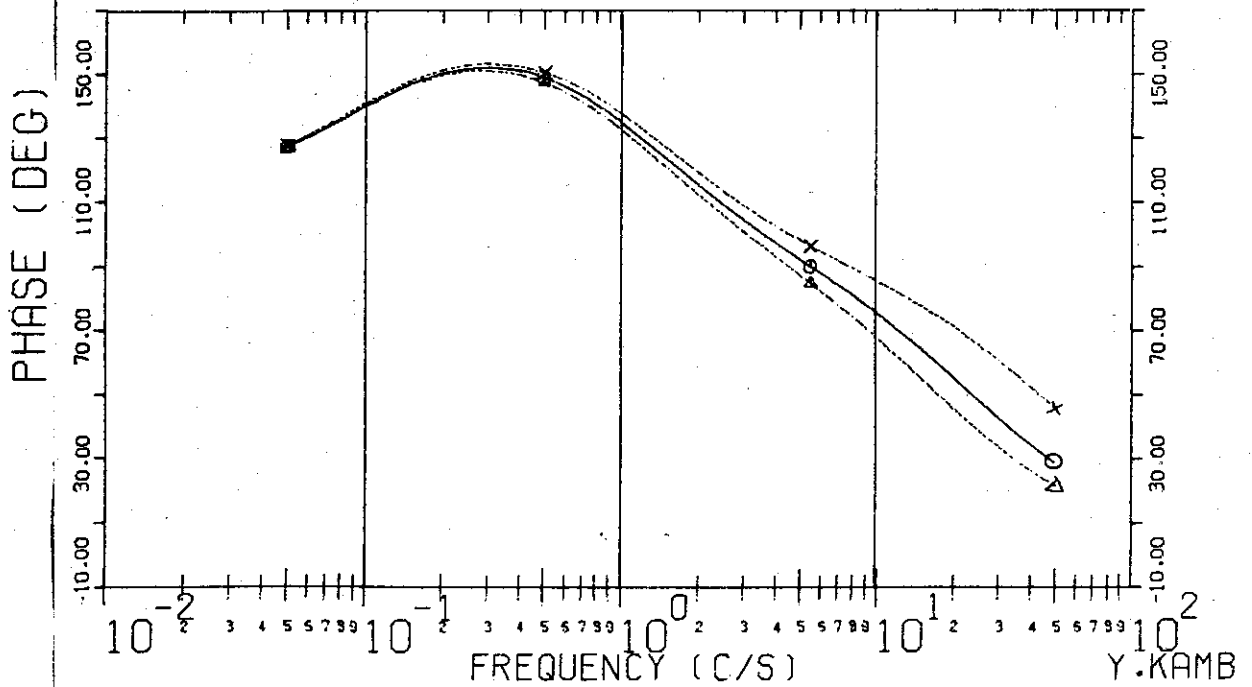
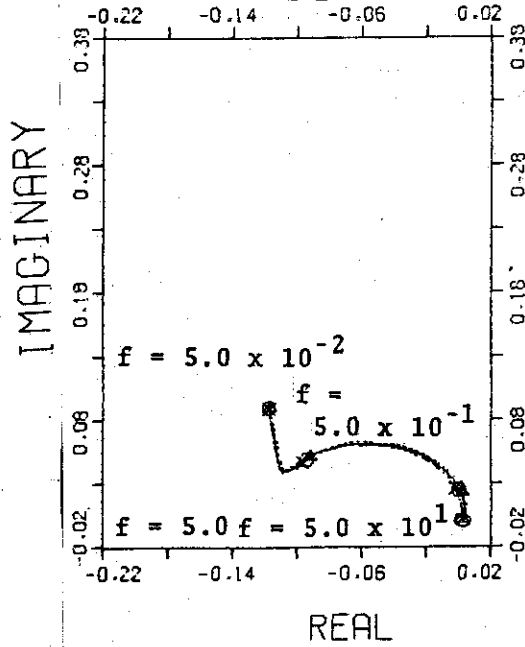


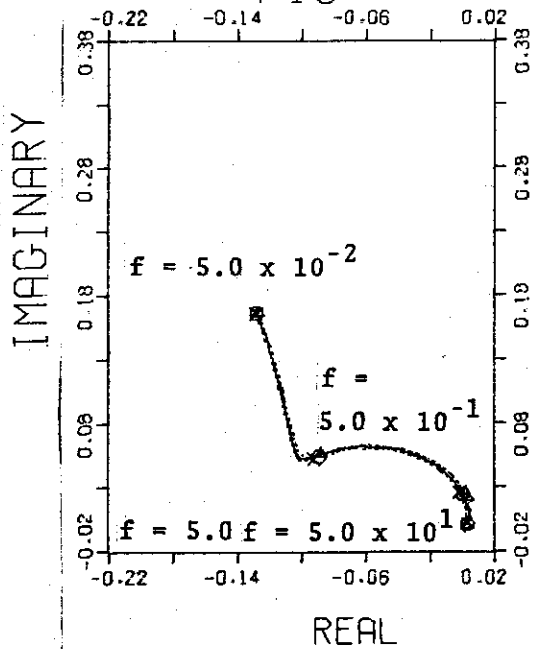
FIG. 5-25-C VECTOR DIAGRAM



8

Y.KAMB

FIG. 5-26-C VECTOR DIAGRAM



8

Y.KAMB

Fig. 5-27 Frequency Characteristics  
 Terminal Voltage ( $\delta V/V_0$ )  $\rightarrow$  Plasma Position ( $\delta R/R_0$ )  
 $\Gamma_0 = 2.2$      $\tau_l = 0.03$  ---  $\Delta$  ---  $\tau_v = 0.2$      $\tau_t = 2.0$   
 $G = -0.8$     0.02 ---  $\circ$  ---    0.01 --- x ---

FIG. 5-27-A BODE DIAGRAM (GAIN)

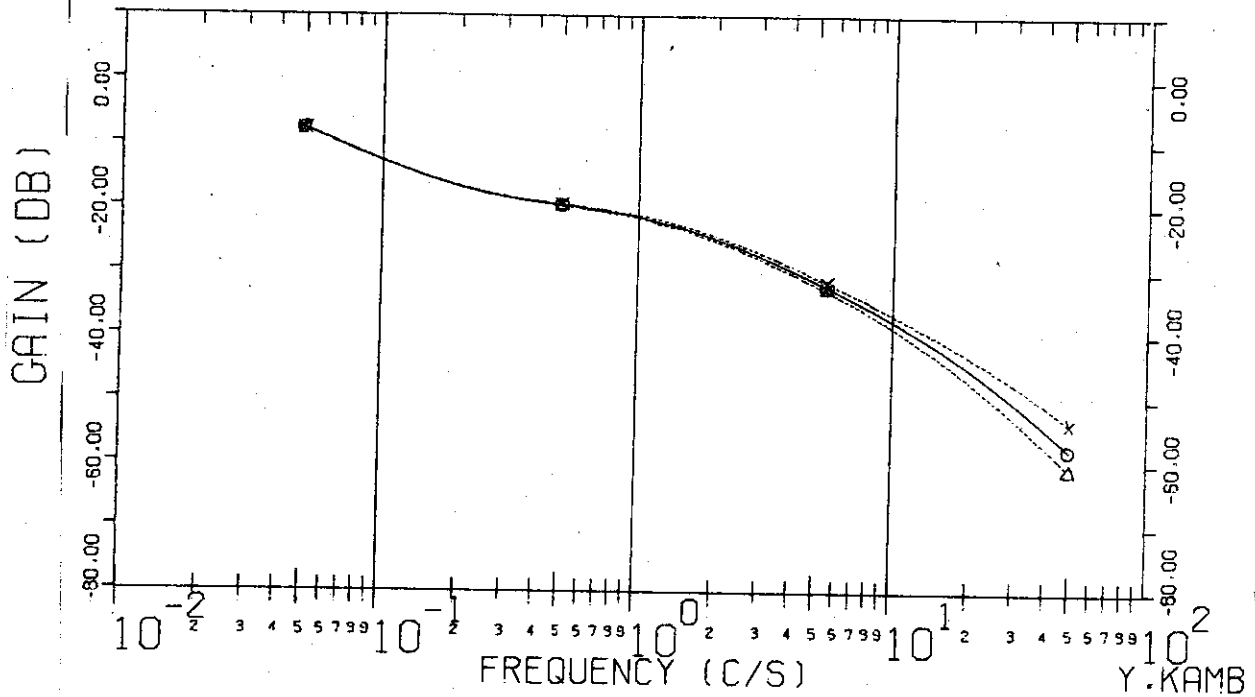


FIG. 5-27-B BODE DIAGRAM (PHASE)

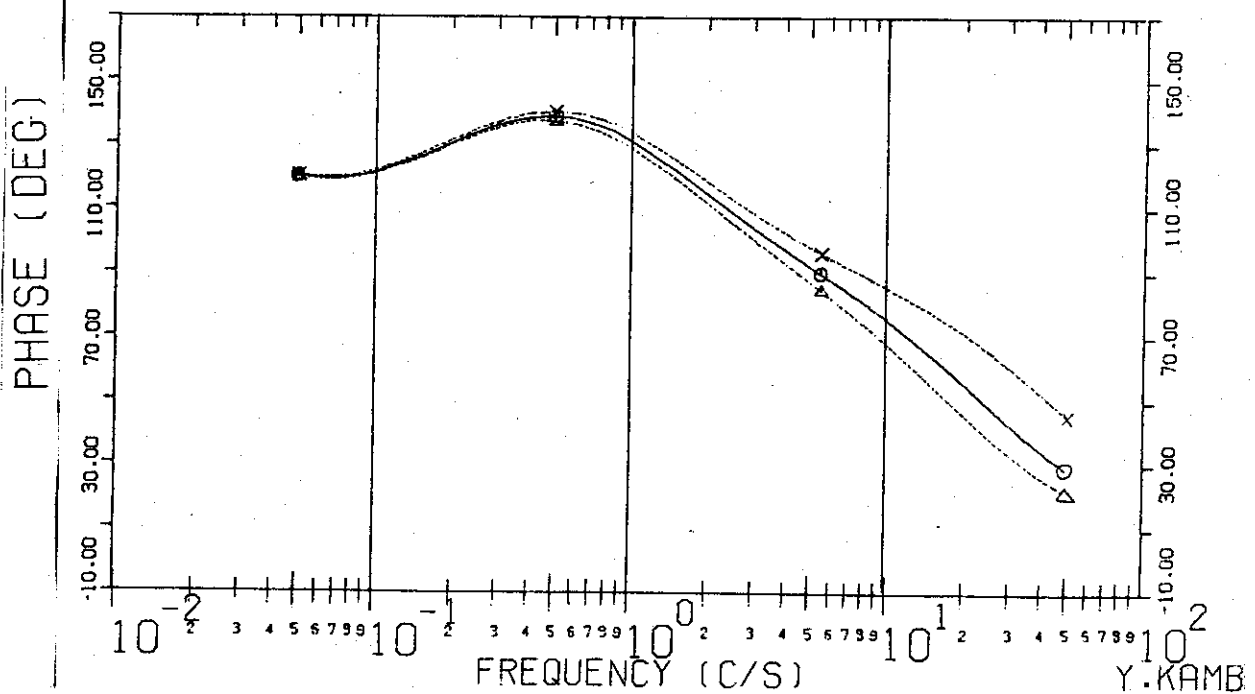
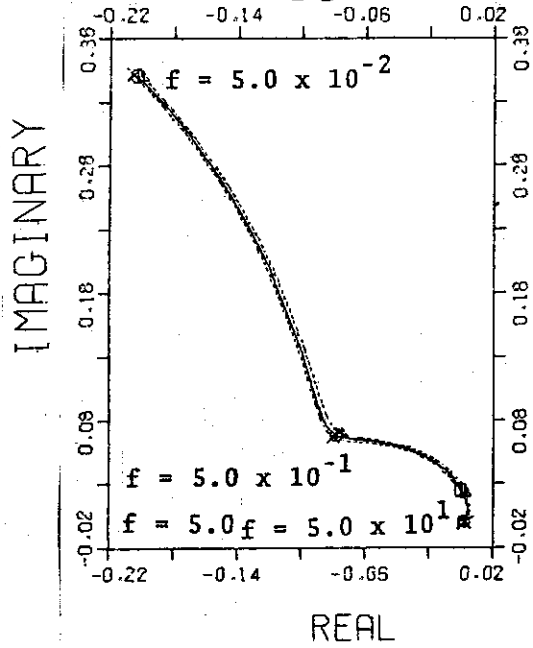


FIG. 5-27-C VECTOR DIAGRAM



Y. KAMB